Study of Screen-Printed Electroconductive Textile Materials

Studie van gezeefdrukte elektrisch geleidende textielmaterialen

Ilda Kazani

Promotoren: prof. dr. ir. L. Van Langenhove, prof. dr. ir. G. De Mey
Proefschrift ingediend tot het behalen van de graad van
Doctor in de Ingenieurswetenschappen: Textielkunde

Vakgroep Textielkunde
Voorzitter: prof. dr. P. Kiekens
Faculteit Ingenieurswetenschappen en Architectuur
Academiejaar 2011 - 2012

UNIVERSITEIT
GENT

ISBN 978-90-8578-517-0
NUR 971, 959
Wettelijk depot: D/2012/10.500/43

Legal Information

Supervisors

Prof. dr. ir. Lieva Van Langenhove
Department of Textiles
Faculty of Engineering and Architecture
Ghent University (UGent)

Prof. dr. ir. Gilbert De Mey
Department of Electronics & Information Systems
Faculty of Engineering and Architecture
Ghent University (UGent)

Members of the Examination Committee

Prof. dr. ir. Luc Taerwe (Chairman)	UGent – Belgium
Dr. ir. Carla Hertleer (Secretary)	UGent – Belgium
Prof. dr. ir. Lieva Van Langenhove (Supervisor)	UGent – Belgium
Prof. dr. ir. Gilbert De Mey (Supervisor)	UGent – Belgium
Prof. dr. ir. Genti Guxho	UPT– Albania
Prof. dr. Paul Kiekens	UGent – Belgium
Prof. dr. ir. Hendrik Rogier	UGent – Belgium
Dr. ir. Anne Schwarz	RWTH Aachen – Germany

Contact

Ilda Kazani
Ghent University - Department of Textiles
Technologiepark 907
9052 Zwijnaarde, Belgium
Tel: +32-9-264 5408
Fax: +32-9-264 5831

Funding

BASILEUS project [2008-1799/001 – 001 MUN ECW]
Ghent University's Special Research Fund (BOF)

Acknowledgement

At the end of my thesis, it is a pleasant task to express my thanks to all those who supported me in many ways to the success of this thesis. I could not have succeeded without the invaluable support of a several.

To this select group, I'd like to give special thanks, beginning with :

Prof. Lieva Van Langenhove

For giving me the opportunity to accomplish my PhD in the smart textile group

Prof. Gilbert De Mey

For his expert guidance, continuous and invaluable support during the entire period of my research

Dr. Carla Hertleer

for supervising my work, for providing me with encouraging and constructive feedback, for a good working relationship and the impetus for me to finish

Prof. Paul Kiekens and Prof. Genti Guxho

For giving me a possibility to embark on this research

The staff of the Department of Textile at Ghent University and the Textile & Fashion Department of Polytechnic University of Tirana

for providing me with a very pleasant and friendly working atmosphere

My colleague and friend Lina Rambausek

for many insightful discussions and suggestions, for her support and encouragement and for all the good times we shared together

My housemate Bella Murati

for sharing not only the place but also a very good time in Ghent. We have laughed, cooked and among others explored by bike the hidden beauties of Gent

All my international friends in Ghent

For making my stay here, in this remarkable city, a fantastic experience full of very good time and adventures, for providing me with some wonderful cultural insights

All my friends in Tirana

for supporting and believing in me

Nicole Hargarter and Erick Groothedde *from Epurex Films Company*
Peter Buttiens *from the European Specialist Printing Manufacturers Association (ESMA)*
Bob Smith and Frank Eirmbter *from Sun Chemical Company*
Jean Luc Derycke *from UTEXBEL*

for supporting me with materials for my experiments and providing links with specialist of screen printing

Lastly but most importantly a biggest THANK YOU goes to my parents Fatbardha and Agim Kazani and to my brother Marlen Kazani. I thank them for their understanding, endless patience and encouragement when it was most needed.

To my Parents,

Fatbardha & Agim

Table of Contents

Summary

During the last decade a lot of research is performed in screen printing with conductive silver-based inks on different woven and nonwoven textile fabrics. This method offers flexible and lightweight conductive textiles with excellent electroconductive properties. Furthermore, the printed textiles can find use in different applications such as textile antennas, feed lines or simple one-layer routing structures, electrodes and circuits. The only problem this method was facing is the maintenance of the printed textile in daily life.

In this dissertation, the screen printing technology was applied on different woven, nonwoven and foam substrates with four silver-based inks. Beside this, a solution was found to make these printed textiles washable/dry-cleanable for 60 cycles. To this end, a thermoplastic polyurethane (TPU) layer was put on top of the printed area to protect it during the frequent washing/dry-cleaning cycles.

The work is split up in 8 chapters. The first chapter introduces information about smart textiles and gives an overview of the current state-of-the-art on screen printing with conductive inks. Chapter 2 and 3 describe the characterisation of the screen-printed layers on different substrates such as foam, woven and nonwoven textiles. Whereas Chapter 4 and 5 focus on the anisotropic behaviour of the screen-printed woven textiles, Chapter 6 shows other electrical properties such as temperature coefficient of resistance and aging. In Chapter 7, two applications of the screen-printed textiles are addressed and preliminarily tested. Eventually, the research is concluded in Chapter 8.

In Chapter 1, first an overview of the specific terminology for smart textiles is given. It continues with a description of electroconductive textiles, the conductive inks available in the market and the printing technologies applied in the field of electronics. Most of the applications, especially on textiles, are limited to screen and inkjet printing, as they are very good for low volume and high-precision work. Although inkjet printing offers greater design versatility and production flexibility, still screen printing is chosen in this dissertation as it represents an inexpensive, flexible and fast way to obtain lightweight conductive coated textiles that can be integrated into smart textiles.

Furthermore, two methods are described that are used to measure the electrical properties of the conductive textiles: the four-point probe method and the Van Der Pauw method (VDP). The second method is used when it is impossible to use the four-point probe, for example, when the conductive surface is covered with a protective non-conductive layer. The first chapter ends with the outline of the dissertation work.

Chapter 2 describes the screen printing method with four silver-based inks on different woven textiles. The electrical properties of these textiles were investigated after screen-printing, before and after abrading and after washing. This chapter describes the covering of the screen printed textiles with a protective non-conductive layer, thermoplastic polyurethane (TPU). This is a solution to make the textiles long-term washable (60 washing cycles) since nearly half of the samples lost their conductivity after 20 washing cycles when not protected. It was found that the amount of ink, the solid content and the nominal sheet resistance of the printed samples influence the square resistance of the screen-printed samples.

Chapter 3 deals again with screen printing by means of four silver-based inks, but now on thicker substrates like foam and nonwoven polyester. Here the electrical properties were also measured after printing and before and after 60 dry-cleaning cycles. To preserve the electroconductive properties after dry-cleaning, here also a protective non-conductive layer, thermoplastic polyurethane (TPU), was used to cover the printed substrates.

In Chapter 4, two measurement methods were used to measure the electrical properties, the four-point probe and Van Der Pauw method (VDP). It was found that with the four-point probe method, it is not possible to detect anisotropy between the two directions of a fabric (warp and weft). This was also proved theoretically. However, Chapter 5 describes that screen-printed woven textiles do show an anisotropic behaviour. This is found by using the Van Der Pauw method (VDP) to measure the electrical resistance. Here a mathematical analysis of the measuring method was established aiming at a correct interpretation of the measurements.

In Chapter 6, the electrical properties such as temperature coefficient of resistance (TCR) and aging of the screen-printed woven textiles were investigated. The square resistance was evaluated as a function of temperature and time because it is very important to know what happens to the electrical properties when the temperature changes during operating time.

During the temperature coefficient of resistance (TCR) measurements, hysteresis was found both in weft and in warp direction. Also anisotropy was found in both tests (temperature coefficient of resistance and aging).

Chapter 7 is split up in two parts. The first part presents a potential application of the screen-printed textiles: electrodes. These electrodes can be used to measure biomedical parameters or as therapeutic treatments as they show a very good conductivity after 20 washing cycles. In this part, Electrochemical Impedance Spectroscopy (EIS) is used to learn more about the resistivity when the electrodes are in contact with human sweat. The results of the Electrochemical Impedance Spectroscopy test are promising.

The second part of Chapter 7 deals with screen-printed textile antennas for off-body communication. The pattern of the chosen antenna is a microstrip inset-fed patch antenna. For this application two woven textiles (Polyester and Cotton/Polyester) and two silver-based inks were used. The antennas were covered with a thermoplastic polyurethane layer (TPU) to protect them during the washing cycles. The influence of the five washing cycles on the antenna characterisation is described by evaluating the reflection coefficient and the radiation efficiency before and after five washing cycles, covered and non-covered with the thermoplastic polyurethane (TPU). It is observed that the screen-printed antennas after washing are quite stable due to the presence of the protective thermoplastic polyurethane layer (TPU) on top.

The work is concluded by Chapter 8, listing the main achievements presented in this dissertation. Based on the positive results obtained after their washing / dry-cleaning process, the screen-printed textile materials will hopefully find use in smart textile products.

Samenvatting

De laatste tien jaar werd veel onderzoek gedaan naar zeefdruk met geleidende zilverinkten op verschillende textielsubstraten zoals weefsels en vliesstoffen. Met deze methode kan licht en soepel geleidend textiel worden gemaakt met uitstekende, elektrisch geleidende eigenschappen. Bovendien kan het bedrukt textiel gebruikt worden in verschillende toepassingen zoals textielantennes, verbindingen tussen elektrische componenten, elektrodes en circuits. Het enige probleem waar deze methode mee kampt, is het onderhouden van het bedrukt textiel in het dagelijkse leven.

In deze dissertatie werd de zeefdruktechnologie toegepast op substraten zoals weefsels, vliesstoffen en schuimrubber met vier zilverinkten. Er werd tevens een oplossing gevonden om dit bedrukt textiel 60 cycli lang wasbaar/chemisch reinigbaar te maken. Hiervoor werd een thermoplastische polyurethaan (TPU)-laag bovenop het bedrukte gebied aangebracht om het te beschermen tijdens veelvuldige was- en droogkuiscycli.

Dit werk is opgedeeld in 8 hoofdstukken. Het eerste hoofdstuk is een inleiding tot intelligent textiel en biedt een overzicht van de huidige stand van zaken in het zeefdrukken met geleidende inkt. Hoofdstukken 1 en 2 behandelen de karakterisering van de gezeefdrukte lagen op verschillende substraten zoals schuimrubber, weefsels en vliesstoffen. Hoofdstukken 4 en 5 gaan in op het anisotropische gedrag van gezeefdrukt geweven textiel, terwijl hoofdstuk 6 over andere elektrische eigenschappen gaat zoals de temperatuurcoëfficiënt van de weerstand en het verouderingsgedrag. In hoofdstuk 7 worden er twee toepassingen van gezeefdrukt textiel beschreven en voorbereidend getest. Ten slotte wordt in hoofdstuk 8 een besluit gemaakt over het onderzoek.

In Hoofdstuk 1 wordt eerst een overzicht gegeven van de terminologie specifiek voor intelligent textiel. Verder wordt een beschrijving gegeven van elektrisch geleidend textiel, van de op de markt beschikbare geleidende inkten en van de in de elektronica toegepaste druktechnologieën. De meeste toepassingen, vooral in textiel, beperken zich tot zeef- en inktstraaldruk omdat die goed zijn voor kleine volumes en uiterst nauwkeurig werk opleveren. Hoewel het inktstraaldrukken meer flexibiliteit in design en productie biedt, werd in deze dissertatie toch voor zeefdruk gekozen omdat het een betaalbare, flexibele en snelle manier vormt om licht, geleidend, gecoat textiel te creëren dat in intelligent textieltoepassingen kan worden gebruikt.

Er worden eveneens twee methodes beschreven die worden gebruikt om de elektrische eigenschappen van geleidend textiel te meten: de vierpuntsmeting en de Van der Pauwmethode. De tweede methode wordt gebruikt wanneer het niet mogelijk is de vierpuntsmeting toe te passen, bijvoorbeeld als het geleidend oppervlak bedekt is met een niet-geleidende beschermlaag. Het eerste hoofdstuk eindigt met een overzicht van het onderzoekswerk.

Hoofdstuk 2 beschrijft de zeefdrukmethode met vier op zilver gebaseerde inkten op verschillende geweven stoffen. De elektrische eigenschappen van deze stoffen werden onderzocht na het zeefdrukken, voor en na abrasie en na het wassen. Er wordt ook ingegaan op het bedekken van het gezeefdrukte textiel met een niet-geleidende beschermlaag van thermoplastisch polyurethaan (TPU). Dit is een manier om het textiel wasbaar te maken op lange termijn (60 wascycli) aangezien vrijwel de helft van de stalen na 20 wasbeurten hun geleidbaarheid had verloren wanneer ze niet beschermd waren. Het blijkt dat de hoeveelheid inkt, het gehalte aan vaste stof en de nominale laagweerstand van de gedrukte stalen een invloed uitoefenen op de vierkantsweerstand van de gezeefdrukte stalen.

Hoofdstuk 3 behandelt eveneens het zeefdrukken met vier zilverinkten, maar nu op dikkere substraten zoals schuimrubber en polyestervliesstof. Ook hier werden de elektrische eigenschappen gemeten na het drukken en voor en na 60 droogkuisbeurten. Om de elektrisch geleidende eigenschappen na chemische reiniging te behouden, werd ook hier een niet-geleidende beschermlaag van thermoplastisch polyurethaan (TPU) gebruikt om de bedrukte substraten te beschermen.

In Hoofdstuk 4 werden twee meetmethodes gebruikt om de elektrische eigenschappen te meten: de vierpuntsmeting en de Van der Pauwmethode. De vierpuntsmeting bleek niet in staat anisotropie te detecteren tussen de twee richtingen van een weefsel (ketting en inslag). Dit werd ook theoretisch bewezen. Hoofdstuk 5 toont echter aan dat gezeefdrukt geweven textiel wel degelijk anisotropisch gedrag vertoont. Dit werd ontdekt door de Van Der Pauwmethode te gebruiken om de elektrische weerstand te meten. Er werd een wiskundige analyse van de meetmethode opgesteld om de metingen correct te kunnen interpreteren.

In Hoofdstuk 6 werden elektrische eigenschappen zoals de temperatuurcoëfficiënt van de weerstand en het verouderingsgedrag van het gezeefdrukte textiel onderzocht. De vierkantsweerstand werd geëvalueerd als

functie van de temperatuur en de tijd omdat het van belang is te weten wat er gebeurt met de elektrische eigenschappen als de temperatuur verandert tijdens de functioneringsduur. Tijdens de metingen en de temperatuurcoëfficiënt werd hysteresis ontdekt in zowel de ketting- als de inslagrichting. Ook anisotropie werd geobserveerd in de beide proeven (temperatuurcoëfficiënt en veroudering).

Hoofdstuk 7 is opgesplitst in twee delen. In het eerste deel wordt een potentiële toepassing van het gezeefdrukt textiel voorgesteld: elektrodes. Deze elektrodes kunnen worden gebruikt om biomedische parameters te meten of voor therapeutische behandelingen aangezien ze een goede geleidbaarheid vertonen na 20 wasbeurten. In dit deel wordt gebruik gemaakt van EIS (*Electrochemical Impedance Spectroscopy*) om inzicht te krijgen in het weerstandsvermogen als de elektrodes in contact komen met menselijk zweet. De resultaten van de EIS-proeven zien er veelbelovend uit.

Het tweede deel van Hoofdstuk 7 gaat over gezeefdrukte textielantennes voor *"off-body"* communicatie. Het patroon van de gekozen antenne is een *microstrip inset-fed patch antenne*. Voor deze toepassing werden twee geweven stoffen (polyester en katoen/polyester) en twee zilverinkten gebruikt. De antennes werden met een thermoplastische polyurethaan (TPU)-laag bedekt om hen te beschermen tijdens het wassen. De invloed van de vijf wasbeurten op de karakterisering van de antenne wordt beschreven door de reflectiecoëfficiënt en het stralingsrendement te beoordelen voor en na vijf wascycli, zowel met als zonder de thermoplastische polyurethaan (TPU)-beschermlaag. Het was duidelijk dat de gezeefdrukte antennes na het wassen nog steeds vrij stabiel waren dankzij de beschermende thermoplastische polyurethaanlaag.

In Hoofdstuk 8 wordt een besluit gemaakt van het onderzoekswerk met een overzicht van de belangrijkste resultaten. Op basis van de positieve resultaten na de was- en droogkuisbeurten, is er voor de gezeefdrukte textielmaterialen hopelijk een toepassing weggelegd in intelligent textiel.

List of Publications

A1 Publications

- *Van der Pauw method for measuring resistivities of anisotropic layers printed on textile substrates*

Ilda Kazani, Gilbert De Mey, Carla Hertleer, Jedrzej Banaszczyk, Anne Schwarz, Genti Guxho and Lieva Van Langenhove
Textile Research Journal, 2011, Vol. 81 (20), pp. 2117-2124

- *Electrical conductive textiles obtained by screen printing*

Ilda Kazani, Carla Hertleer, Gilbert De Mey, Anne Schwarz, Genti Guxho and Lieva Van Langenhove
Fibres & Textiles in Eastern Europe, 2012, Vol. 20, No.1 (90), pp. 57-63

- *Dry-cleaning of electroconductive layers screen-printed on flexible substrates*

Ilda Kazani, Carla Hertleer, Gilbert De Mey, Genti Guxho and Lieva Van Langenhove
On 9 March 2012 accepted to be published in Textile Research Journal

- *About the collinear 4-point probe technique´s inability to measure the resistivity of anisotropic electroconductive fabrics*

Ilda Kazani, Gilbert De Mey, Carla Hertleer, Jedrzej Banaszczyk, Anne Schwarz, Genti Guxho and Lieva Van Langenhove
On 25 April 2012 accepted to be published in Textile Research Journal

- *Electrical circuit model of elastic and conductive yarns produced by hollow spindle spinning*

Anne Schwarz, Laetitia Cuny, Carla Hertleer, Filipe Ghekiere, Ilda Kazani, Geert De Clercq, Gilbert De Mey and Lieva Van Langenhove
Materials Technology, 2011, Vol. 26, No. 3, pp. 121-127

- *Comparative study on the mechanical properties of elastic, electro-conductive hybrid yarns and their input materials*

Anne Schwarz, Ilda Kazani, Laetitia Cuny, Carla Hertleer, Filipe Ghekiere, Geert De Clercq and Lieva Van Langenhove
Textile Research Journal, 2011, Vol. 81 (16), pp. 1713-1723

- *Electro-conductive and elastic hybrid yarns - The effects of stretching, cyclic straining and washing on their electro-conductive properties*

Anne Schwarz, Ilda Kazani, Laetitia Cuny, Carla Hertleer, Filipe Ghekiere, Geert De Clercq, Gilbert De Mey and Lieva Van Langenhove
MATERIALS & DESIGN, 2011, Volume 32, No 8-9, p 4247-4256

- *Stability and efficiency of screen printed wearable and washable antennas*

Maria Lucia Scarpello, Ilda Kazani, Carla Hertleer, Hendrik Rogier, and Dries Vande Ginste
Submitted in the IEEE Antennas and Wireless Propagation Letters Journal on 13 February 2012

Conferences

- *Printed electroconductive textiles*

Ilda Kazani , Carla Hertleer , Gilbert De Mey, Anne Schwarz and Lieva Van Langenhove
4th International textile conference, 2010. Tirana, Albania

- *Elastic, electrically conductive textile structures for intelligent textiles*

Carla Hertleer, Anne Schwarz, Ilda Kazani, Lieva Van Langenhove and Geert De Clercq
2nd International scientific conference on Textiles of the Future (Futurotextiel 2008). Kortrijk, Belgium

- *Metal yarns spiraling around elastic cores*

Anne Schwarz, Laetitia Cuny, Ilda Kazani, Filipe Ghekiere, Carla Hertleer, Geert De Clercq and Lieva Van Langenhove
AUTEX 2010 Conference Vilnius, Lithuania.

- *A study on the lifetime behaviour of elastic and electro-conductive hybrid yarns*

Anne Schwarz, Ilda Kazani, Laetitia Cuny, Filipe Ghekiere, Carla Hertleer, Geert De Clercq, Gilbert De Mey and Lieva Van Langenhove
AUTEX 2011 Conference Mulhose, France.

- *Washable screen-printed textile antennas*

Ilda Kazani, Maria Lucia Scarpello, Carla Hertleer, Hendrik Rogier, Gilbert De Mey, Genti Guxho and Lieva Van Langenhove
Accepted to be presented in CIMTEC 2012, 4th Conference ``Smart Materials, Structures and systems``, Montecatini Terme, Tuscany, Italy. June 2012

- *Flexible screen-printed electroconductive textiles*

Ilda Kazani, Carla Hertleer, Gilbert De Mey, Genti Guxho and Lieva Van Langenhove
Accepted to be presented in CEC 2012, 7th Central European Conference on Fibre-Grade Polymers, Chemical Fibres and Special Textiles, Portorose, Slovenia. September 2012

Poster presentation

- *Electroconductive textiles*

Ilda Kazani, Carla Hertleer and Lieva Van Langenhove
12th FEA PhD Symposium of Gent University, 2010

- *Dry-cleaned electroconductive textiles*

Ilda Kazani, Carla Hertleer, Gilbert De Mey, Genti Guxho and Lieva Van Langenhove
AUTEX 2011 Conference Mulhose, France.

- *Flexible conductive textiles*

Ilda Kazani, Carla Hertleer, Gilbert De Mey, Genti Guxho and Lieva Van Langenhove
International Workshop on Flexible and Stretchable Electronics, Berlin 2011

List of Abbreviations

Abbreviations

AC	Alternating current
DC	Direct current
EIS	Electrochemical Impedance Spectroscopy
ECG	Electrocardiogram
FRA	Frequency Response Analyser
LED	Light emitting diode
PES	Polyester textile material
PCBs	Printed Circuit Boards
PPy	Polypyrrole
PERC	Perchloroethylene
PCE	Tetrachloroethylene
PVC	Polyvinyl chloride
RFID	Radio-frequency identification
RH	Relative Humidity
SEM	Scanning Electron Microscope
TPU	Thermoplastic polyurethane
VDP	Van Der Pauw

Greek symbols

π	Mathematical constant (3.14)
σ	Electric conductivity
$\emptyset$	Electrical potential
η	Radiation efficiency

Roman symbols

C	Capacitance
I	Electric current
J	Electric current density
$R_{□}$	Square resistance
t_s	Thickness
V	Voltage
Z	Electrical impedance
$\|S_{11}\|$	Reflection coefficient
T	Temperature
TCR	Temperature Coefficient of Resistivity

Units

%	Percentage
$Ω/□$	Ohm per square
°C	Degree Celsius
K	Kelvin
mA	Milliampère
mm	Millimetre
cm	Centimetre
g	Gram
g/m^2	Gram per square meter
g/cm^3	Gram per cub centimetre
$µm$	Micrometer
$Pa.s$	Pascal-second
$ppm/°C$	Parts per million per degree Celsius
mHz	Millihertz
MHz	Megahertz
KHz	Kilohertz

1

Introduction

This chapter introduces information about smart textiles, electroconductive textiles, conductive inks, printing technology and methods for measuring the electrical properties.

TABLE OF CONTENTS

1.1 Smart textiles

Textiles are among the oldest materials that are known to humankind. But evolution in technology has made it possible to apply different materials and to integrate electronic devices into these textiles in order to make them smart or intelligent [1]. The 1960s marked an era of innovations in materials with the discovery of shape memory materials. One decade later, in the 1970s, smart materials were introduced with the invention of polymeric gels. Later on in the 1990s, researchers started to integrate these smart materials into textiles, consequently creating smart textiles.

Regarding to their reaction a categorization of smart textiles was made dividing them in three groups:

•*Passive smart textiles*, which are just sensors, can only sense the environmental surroundings.

•*Active smart textiles*, which are sensors and actuators, can sense the stimuli from the environment and react to these stimuli.

•*Very smart textiles* can sense and react in such a way that they can adapt their performance to the environment [2, 3].

Today, terms such as ``Smart Textiles``, ``Intelligent Textiles`` and ``Wearable Electronics`` are commonly used in every textile environment. These terms refer to textiles that are able to sense stimuli from the environment around them and react and/or adapt to these stimuli [2, 4].

Smart textiles are systems composed with different materials and components such as sensors, processors, actuators, power supply and communication (Figure 1.1).

Sensors are able to measure parameters e.g. from the human body or the environment and collect data such as temperature, heart beat rate, electrical activity, humidity, pH. The information provided by them is in form of an electrical signal. Nowadays sensors can be found made out of textiles [2].

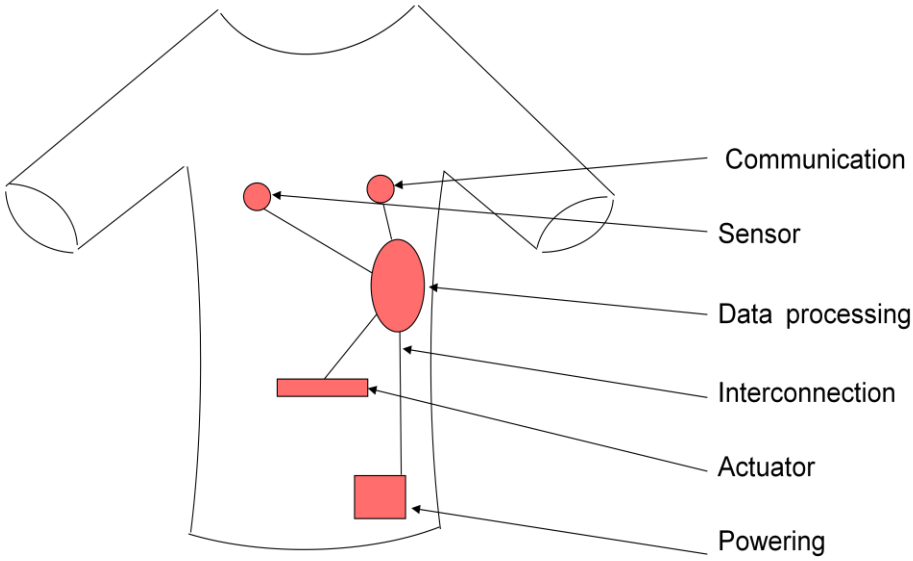

Figure 1.1 Components of a smart textile system, by UGent

Processors are used when active processing is required in order to process all the data collected from the sensors, which is done with electronic devices as a textile processor does not exist yet.

Actuators are able to respond or react to the signals coming from sensors or processors. They can react in form of a movement, in form of an auditive or a visual alarm or in form of substance release to warn the wearer when something goes wrong.

Power supply is required for the smart textile in order to make the system work. It should be combined with energy storage to be able to function as a stand-alone unit. One example of this is a battery. Nowadays batteries for smart textile applications can be found in a printed version, very thin, flexible and rechargeable [5, 6].

Communication for smart textiles can be:

- Between the wearer and the suit,
- From the suit to the environment.

Communication with the wearer has been realized by France Telecom with an Optical Fibre Flexible Display [7]. Another communication textile based on photonics is that from the Philips Lumalive [8].

For communication over longer distances wireless networks can be used. Now this communication is available through textile antennas which can easily be integrated into garments [9-11].

Interconnections are used to join the distinct components within the smart textile. They can be electroconductive yarns woven, knitted, sewn or embroidered in/onto the garment. Another way to achieve them is by screen printing with conductive inks onto the textile surface. Within the suit, communication can be realized by optical fibres or conductive yarns.

The first electronic textile introduced into the market was the ICD+ (Industrial Clothing Design Plus) jacket in 2000 by Levi Strauss & Co. and Philips Research Laboratories [12]. The jeans jacket could host an MP3 player and a mobile phone. Wires connecting these devices are incorporated into the garment. However, all devices and wires need to be removed when the jacket enters the washing machine for maintenance. Subsequently, several communication systems, such as mobile phones, MP3 players, computers and GPS were integrated into garments. In order to allow these devices to operate as 'wearable electronics', different conductive materials, wires and batteries were used [11, 13]. From a textile point of view, the challenge for researchers is to make as many components as possible out of textile materials. Therefore, it is necessary to develop electroconductive textiles, which can be obtained in several ways, for example by integrating conductive fibres or yarns, by applying conductive coatings, or by using conductive inks [14-16].

Research on smart textiles from different groups with different backgrounds was carried out (designers, engineers, chemists, doctors, etc) aiming at developing applications for the military, fire-fighters and first responders to medical garments and also casual garments. Most of this research is supported by projects and in the last decade the research in smart and wearable textiles is done through European projects like: All4Rest, Stella,

BIOTEX, CONTEX, OFSETH, MERMOTH, myHeart, ProeTEX, Leapfrog, Avalon, Clevertex and Lidwine [17-28].

Smart textiles can be used in a variety of applications such as heating, monitoring of human vital signs or illuminating textiles. In many of these products a special property is required, namely electroconductivity to transport electrical current.

1.2 Electroconductive textiles

Over the last years smart textiles have become popular as a concept. To manufacture these wearable textile systems, electroconductive textiles are needed. Electroconductive textiles are materials which can conduct an electrical current [29]. These textiles can be achieved by using conductive fibres, yarns, coatings, polymers or inks (Figure 1.2) [30-33].

Electroconductive fibres/yarns can be divided in two main groups:

- Fibres/yarns, which are conductive. They can be pure metals mainly silver, copper and stainless steel, produced by methods such as wire drawing, bundled wire drawing, cutting production, melt spinning and melt extraction.

- Fibres/yarns treated to be conductive. In the second group fibres/yarns are coated with metals, galvanic substances or metallic salts. The coating processes used are: electroless plating, evaporative deposition, sputtering and coating with conductive polymers.

There are several techniques that integrate conductive fibres/yarns into a textile structure such as knitting, weaving, embroidering, sewing and needle felting. Conductive textiles can be obtained also by treating the surface of the traditional textile. This can be achieved by coating with a conductive layer, by coating with polymers such as polypyrrole [33], deposited onto the surface of textile substrates or by printing with conductive inks (Figure 1.3). This last technology, which is the topic of the dissertation, is very flexible and shows therefore growing interest in the development of printed electronics, which expected to give rise to low-cost, flexible displays and disposable electronics [34].

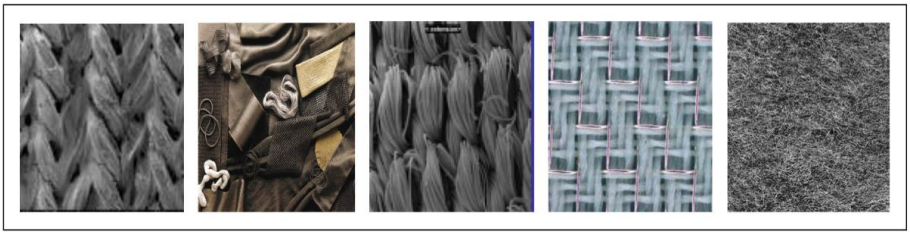

Figure 1.2 Conductive textiles: knitted, coated, woven and felted,

by Bekintex and Sefar

1.3 Conductive inks

There are many conductive inks available on the market for use in the field of electronics and produced by different companies such as DuPont, Acheson, SunChemical, ECKART, Xennia, Precisia, ClimaNanoTech, Parlex, Creative materials Incorporated and Motson Graphics. The conductive inks have different applications such as Printed Circuit Boards (PCBs), hybrid cirquits on ceramic substrates, wiring boards, antennas, transmission lines, electric circuits.

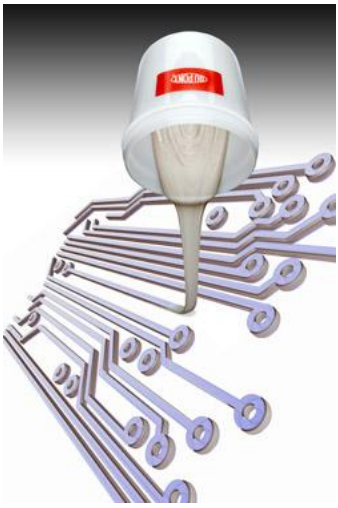

Figure 1.3 Conductive inks for electronic applications, by DuPont

There are different properties conductive inks should have for different printing technologies such as viscosity, surface tension, stability, metal content, drying rate, coverage and adhesion. The screen printing process e.g., requires inks that have a high viscosity to prevent in this case the ink to simply passing through the screen onto the substrate, while inkjet printers work by depositing small droplets of ink with low viscosity onto a substrate.

In screen printing technology the used ink consists of a dispersion of metal and suitable resins in an organic or inorganic solvent (see Chapter 1.4.3) [35]. While in the inkjet printing technology the substrate is first printed with the reducing ink and then with metal precursor ink (see Chapter 1.4.2). As follows, the contact of metal salt and reducing agent generates insoluble metallic particles.

With the intention of creating conductive textiles, metal particles such as copper, silver, gold, carbon and nickel are used in these conductive inks. Besides metal particles, one can also mention the conductive polymers and conductive silicones (which are screen-printed, produced by Dow Corning Company).

Generally, it is not so easy to work with copper ink because it is thermodynamically unstable in atmospheric conditions due to oxidation [36-38]. When copper metal is used, it is necessary to control the formation of copper oxide and this adds technical complexity to the process; it is likely that a nitrogen atmosphere is required.

Since gold ink is very expensive, silver-based ink is the best option for printing on textiles. In this study four silver-based inks are applied which are referred to as Ink 1, Ink 2, Ink 3 and Ink 4.

1.4 Printing with conductive inks on textile substrates

1.4.1 Printing technologies

Printing technology with conductive ink has found use in many applications such as electronics, computers and communication. Many techniques are involved in printed electronics, such as rotogravure, offset lithography, flexography, screen and inkjet printing technologies [1, 10].

The major high volume printing processes are rotogravure, offset lithography and flexographic where rotogravure and flexographic are used to fabricate conductors, resistors, while lithography is used to fabricate circuits, microwave integrated circuits etc. Most of the applications, especially on textiles, are limited to screen and inkjet printing as they are very good for low volume and high-precision work. Although inkjet printing offers greater design versatility and production flexibility, screen printing is more economic and covers a huge range of manufactured items, including key boards, plastic boxes, control panels, instruments faces, membrane switch overlays, fascias, vehicle graphics banners and textiles.

1.4.2 Inkjet printing

Inkjet printing with conductive inks was first used in electronics. This technology is divided in two categories; continuous and drop-on-demand method. In the continuous method (Figure 1.4) the ink is continuously shot out in tiny drops onto the substrate, while during the time when nothing is being printed, the ink is deflected into a gutter for recirculation, depending upon the imposed electric field. In the other classification, drop-on-demand (Figure 1.5), the drops are formed only when required.

In recent years many applications are done on different substrates such as glass, paper, textile and plastic with different conductive inks [36, 41 and 42].

In 2004, Redinger *et al.* used gold nanocrystals to print on plastic and polyester film surfaces. They investigated two ways how to create lines from discrete drops. The first way was placing drops only on top of dried surface.

The result was problematic. The second way was to create linear lines from drops by overlaid them. Through inkjet printing on these substrates passive devices for use in low frequency (radio frequency identification (RFID)) applications were achieved [43].

The following year Bidoki *et al.* inkjet printed with silver nitrate, copper sulphate and reducing agents. Different substrates such as paper, hydrophilic-coated polyester film and woven fabric were used. They first printed on the surface with the reducing ink and then with the metal precursor ink. During the process of inkjet deposition the presence of glut oxygen of copper oxide became a problem as it quickly converted some of the metallic copper formed in the printed area to copper oxide. Different applications like PCBs, wiring boards, antennas and electrodes were accomplished with this technology [37, 38].

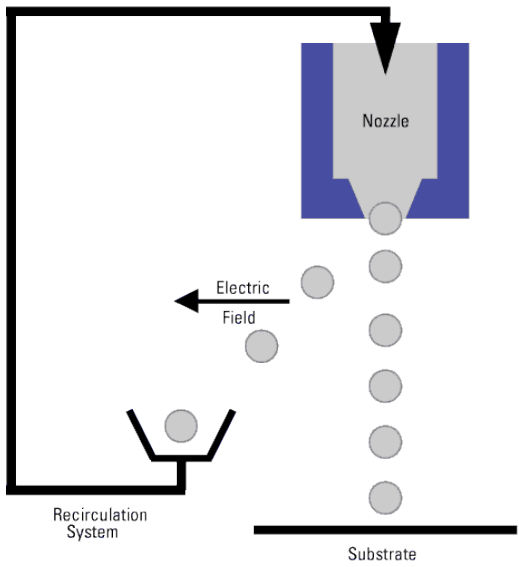

Figure 1.4 Schematic of continuous ink jet, by Ecotextiles

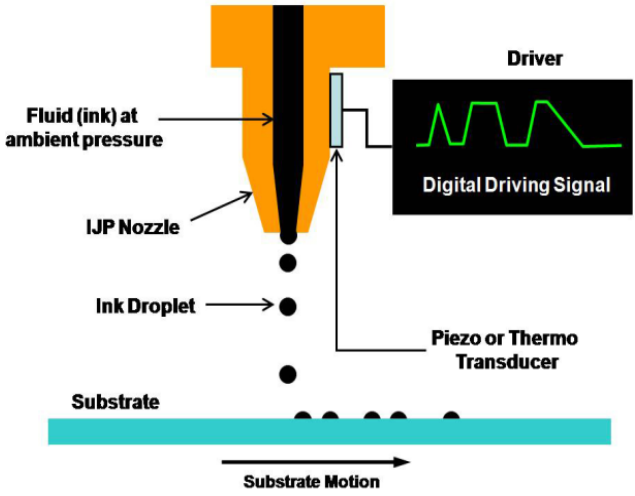

Figure 1.5 Schematic of drop-on-demand inkjet printing, by SPIE

In 2006 TNO, a research organisation from Netherlands, worked in the European project ConText [20]. The contribution of TNO in this project was inkjet printing copper and gold inks onto textile substrates for electrode applications. In the end of the project, an ECG shirt with printed electrodes was introduced. TNO concluded that the inkjet printing process was appropriate but expensive and limited the size and shape of the electrodes. This project was finished without trying to experiment the maintenance of the shirt by washing processes, which is however very important in the daily life [44].

In 2007, Calvert *et al.* inkjet printed piezoresistive sensors with silver nitrate and conductive polymers (PEDOT) on woven nylon fabric [45]. Using this technology, sensing lines of conducting polymer were deposit on fabric. To connect the sensors to the monitoring equipment, silver lines were printed. These printed sensors can be used for monitoring knee and wrist motion thus to collect information such as rehabilitation from joint damage.

With this technology it is necessary to repeat the printing sequence more than once in order to achieve connectivity between the metallic particles formed on the surface. Hence, the deposited layer is thicker and the conductivity is higher [37, 38].

1.4.3 Screen printing

Screen printing is a traditional way of printing that was introduced at the end of the 9th century. The technique is used on a whole range of materials such as textiles, ceramics, glass, polyethylene, polypropylene, paper, metal and wood. It is often preferred to other processes like hand block printing, engraved roller printing, heat transfer printing and inkjet printing, because it is a low-cost and easy process. With this printing technique, a design is imposed on a screen of fine mesh, containing blank areas coated with an impermeable substance. The ink is then forced through the mesh onto the printing substrate by moving a squeegee across the mesh (Figure 1.6).

Screen printing with conductive ink is a technique used first in the field of electronics. In the last decade many research groups started to screen print on different substrates such as paper, Polyimide, Polyethylene terephthalate, Polyvinylchloride, fabrics and glass [46-54].

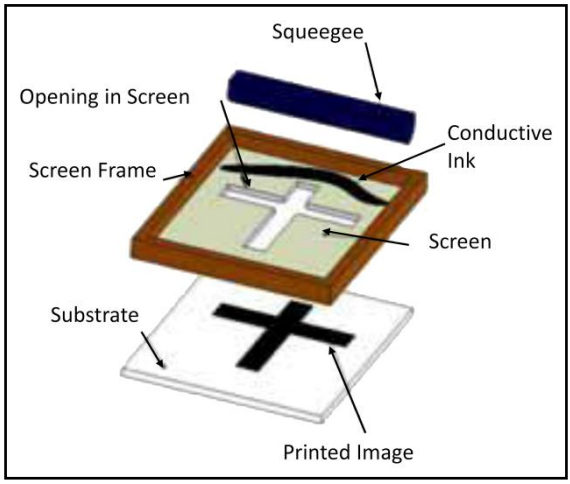

Figure 1.6 Screen printing process, by Gwent group

In 2005, a group of researchers from the National Textile Centre (NTC) in U.S started screen printing with conductive silver inks on different nonwoven

substrates in order to obtain printed coplanar waveguide transmission lines and electric circuits [46, 47]. They measured the printed transmission lines and specified their electrical parameters such as DC resistance and line impedance before and after washing. However, printed traces on most textiles failed after 25 washing cycles due to mechanical agitation. A durable and flexible lamination method has been developed by them, in order to protect the printed ink during the washing process.

Then in 2007, Locher *et al.* [48, 49] have screen-printed with silver conductive ink transmission lines on an acryl-cotton woven fabric. He concluded that the electrical resistance depends on the number of passes: the thicker the printed layer, the lower the resistance is. The sheet resistance of the printed transmission lines was about 0.15 Ω/□.

One year later, in 2008, proving that this technology was becoming successful, Hertleer *et al.* [50] screen-printed for the first time antennas on aramid fabrics with silver conductive ink. The obtained sheet resistance was 0.10 Ω/□ and she concluded that the patches screen-printed with conductive inks increased process ability.

Another study was done by Merilampi *et al.* [35] in 2009, about the mechanical and electrical properties of different silver conductive inks screen-printed on different flexible substrates such as paper, fabrics and plastics. The measured sheet resistance of the screen-printed patterns was in the range of 0.04 – 0.13 Ω/□.

During the same year, another research group from South Korea fabricated by screen printing of conducting epoxy and gold sputtering a planar fashionable circuit boards on woven textiles. In this way they deposited directly planar electrodes and planar circuits. Herein they compared the two methods concluding that the sputtering process was quite expensive and time-consuming [51]. In their case, the sheet resistance of the film printed on textile was of 0.23 Ω/□ [52].

Yang *et al.* [53] and Rius *et al.* [54] used a different kind of conductive ink in 2010. They preferred to use conductive carbon inks to screen print on different substrates. Yang *et al.* printed amperometric carbon electrodes on the elastic waistband of underwear, which is in direct contact with the skin. Also Rius *et al.* screen-printed with conductive carbon ink, but on plain and knitted fabrics that were coated before with polyurethane: they screen-printed

to electrically connect the power supply with the transceivers of the communication device [54].

In the research presented in this dissertation the screen printing method was specifically selected because it is an economical, flexible and fast way to obtain lightweight electroconductive textiles, to be used for different smart textile applications (Figure 1.7) such as electrodes for monitoring heart rate, textile-based antennas for off-body communication, which are described in Chapter 7. Furthermore, a solution is presented for making electroconductive flexible substrates that can be washed or dry-cleaned up to 60 times.

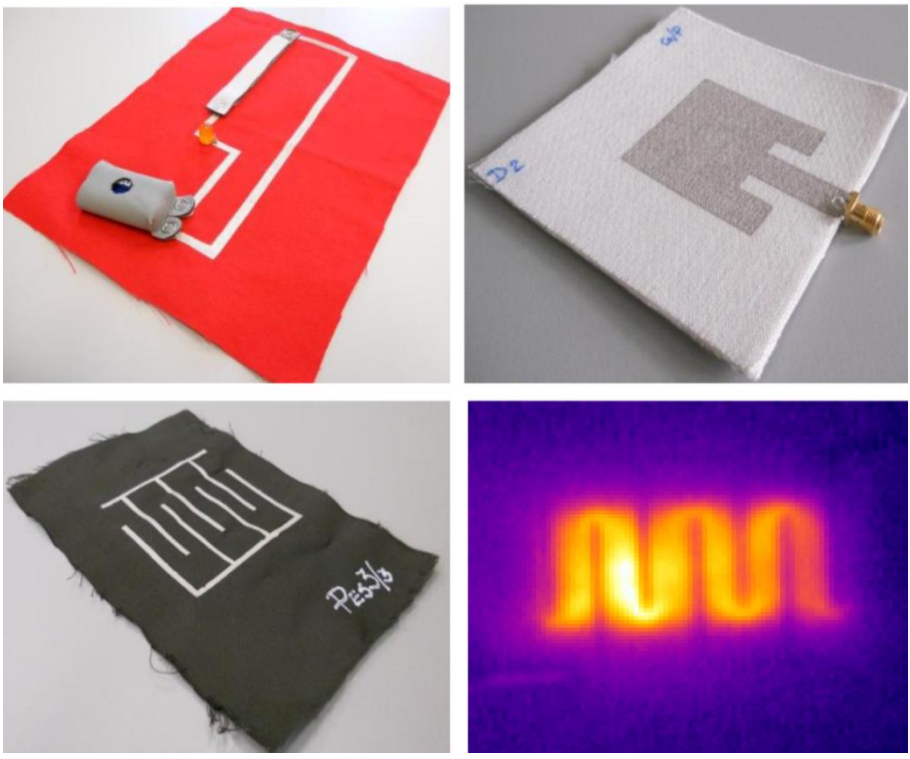

Figure 1.7 Screen printing with conductive silver inks on textile substrate for different applications, by UGent (*from left to right*): circuit with LED light and textile pressure sensor, microstrip inset-fed patch antenna, Polypyrrole-coated polyester fabric for heating element and thermo graphic image of the heating circuit

1.5 Methods used to measure electrical properties

In this dissertation the direct current (DC) resistance of the printed patterns was measured in order to evaluate four silver-based inks. Two methods were used to measure the electrical properties of the textiles that were screen-printed with these inks.

They are described in the following sections.

1.5.1 Four-point probe method

After printing, the square resistance of the screen-printed samples was measured with a four-point method, by means of an MR-1 instrument, manufactured by Schuetz Messtechnik [55]. To avoid any damage or burnouts of the printed square when the current is too high, the MR-1 instrument guarantees that the lowest possible current flow (100 mA) is used.

This technique uses separate pairs of current-carrying and voltage-sensing electrodes to improve the accuracy compared to a traditional two-point sensing method. The current *I* is fed through the outer contacts and the voltage *V* is measured across the inner electrodes, as shown in Figure 1.8.

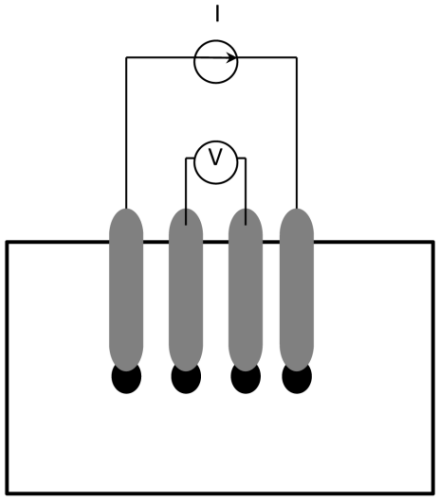

Figure 1.8 Four point-probe setup

The square resistance $R_{\square}$ was calculated by:

$$R_{\square} = \frac{\pi \cdot V}{\ln 2 \cdot I} \quad (1)$$

Where V is the voltage, I is the current and $\frac{\pi}{\ln 2}$ is the correction factor [56].

1.5.2 Van Der Pauw method

While the four-point probe method is applicable on textiles with a conductive surface, the VDP method [57] can be used for conductive textiles which are covered with a dielectric layer.

In order to measure the square resistance with this method, four contacts are required on the boundaries of the conductive sample. To this end, four stripes of copper foil were attached to the printed patch. In order to establish a good electroconductive contact between the copper foil (Cu) and the printed patch, electroconductive glue was applied.

According to the Van Der Pauw method, these contacts can be placed in various positions, such as in the centres of the sides, in the vertices, in the 1/3 or 1/4 of the length of the sides [58]. For this study, the contacts were made in the vertices of the printed squares (Figure 1.9) [59].

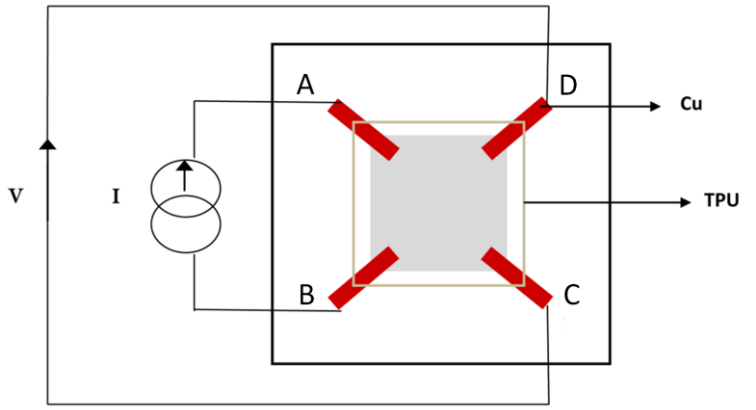

Figure 1.9 The printed sample with four contacts on the vertices and thermoplastic polyurethane foil on top.

The VDP method requires that two neighbouring contacts (A and B), as shown in Figure 1.9, are used to supply the current *I* while the other two contacts (C and D) are used to measure the voltage *V*. The currents applied in our study were 200, 400 and 1000 mA. From all these measurements, the average square resistance was calculated. The measurements were completed at room temperature.

1.6 Outline of the dissertation

The ***first chapter*** describes the printing process with conductive ink on textile substrates. The technologies, the material used for printing with conductive inks and the methods to measure the square resistance are presented. Taking into consideration that this area is in its early life, technologies and suitable conductive inks for textiles need to be identified.

In ***Chapter 2*** the combination of different woven textiles and four conductive inks through screen printing is examined. The electrical properties of these conductive woven textiles were evaluated after printing, abrading and washing. However, to make these conductive textiles resistant to 60 washing cycles the printed textiles were covered with a polyurethane (TPU) layer.

Chapter 3 continues with applying conductive inks but this time on thicker substrates such as Polyurethane foam (Urecom) and nonwoven Polyester (PES). As maintenance process these types of textiles are typically dry-cleaned. Therefore, the evaluation of the electrical properties was done after several dry-cleaning cycles.

In ***Chapter 4*** the possibility of using the four-point probe method to measure the anisotropic properties of the electrical conductivity of screen-printed woven textiles was investigated. Measurements in both directions (warp and weft) proved both theoretically and experimentally that no anisotropy could be detected. However, in ***Chapter 5*** anisotropic behaviour of these screen-printed textiles was found by using the Van Der Pauw method. With the intention of being able to interpret the measurements correctly a mathematical analysis of the measuring method was established.

Chapter 6 discusses the evaluation of the resistance changing with temperature and time. It is important to know what happens to the electrical properties with changing temperatures during operating time. During the measurements of the temperature coefficient of resistivity (TCR) and of aging, anisotropic behaviour was found again.

Chapter 7, dealing with applications, is split up in two parts: the first part explores the behaviour of screen-printed textiles as electrodes, while the second part describes the influence of 5 washings on the performance of screen-printed antennas.

1.7 References

1. Interactive Electronic textile development: A review of technologies. **D. Meoli, T. May-Plumlee.** 2, s.l. : Journal of Textile and Apparel Technology and Managment, 2002, Vol. 2.

2. *Functional Textile Materials.* **L. Van Langenhove.** 2010, Vols. Course scipt, ETEAM.

3. *Smart textiles (1): Passive smart.* **Z. X. Xiang, X. Ming.** s.l. : Textile Asia, 2001, pp. 28-29.

4. *Smart fibres , fabrics and clothing.* **X. Tao.** s.l. : Woodhead, 2001. 0-8493-1172-1.

5. Nec. *www.nec.co.jp/press/en/0512/0701.html,* visited in February 2012

6. *Rechargeable electronic textile battery.* **R. Bhattacharya, M. M. De Kok, and J. Zhou.** 22, 2009, Applied Physics Letters , Vol. 95.

7. *Communicating Clothes: Optical Fibre Fabric for a New Flexible Display.* **E. Deflin, A. Weill, V. Koncar.** 2002. AVANTEX.

8. Philips Lumalive. *http://www.lumalive.com/aboutus/press,* visited in February 2012

9. *The use of textile materials to design wearable microstrip patch antennas.* **C. Hertleer, A.Tronquo, H. Rogier, L. Van Langenhove.** s.l. : Textile Rersearch Journal, 2008, Vol. 78(8). pp. 651-658.

10. *Performance charachterisation of screen printed radio frequency indentification antennas with silver nanopaste.* **D. Y. Shin, Y. Lee, C. H. Kim.** s.l. : Thin Solid Films, 2009, Vol. 517, pp. 6112-6118.

11. *Wireless communication for firefighters using dual-polarized textile antennas integrated in their garment.* **L. Vallozzi, P. Van Torre, C. Hertleer, H. Rogier, M. Moeneclaey, J. Verhaevert.** s.l. : IEEE Transactions on Antennas ans Propagation, 2010, Vol. 58 (4). pp. 1357-1368.

12. *Interactive electronic textiles: technologies, applications, opportunities, and market potential.* **D. Meoli.** sl : North Carolina State University, Raleigh, 2002.

13. *The use of textile materials to design wearable microstrip patch antennas.* **C. Hertleer, A. Tronquo, H. Rogier, L. Van Langenhove.** s.l. : Textile Rersearch Journal, 2008, Vol. 78(8). pp. 651-658.

14. **P. Xue, X. Tao, M-Y. Leun, H. Zhang.** *Wearable electronics and photonics.* [red.] X.Tao. 2007. pp. 81-103.

15. *Electroconductive textile structures through electroless deposition of polypyrrole and copper at polyaramide surfaces.* **E. Gasana, P. Westbroek, J. Hakuzimana, K. De Clerck, G. Priniotakis, P. Kiekens, D. Tseles.** 2006, Surface & Coatings Technology, Vol. 201, pp. 3547-3551.

16. *"Current distribution modelling in electroconductive fabrics".* **J. Banaszczyk, G. De Mey, A. Schwarz and L. Van Langenhove.** 2009, Fibres and Textiles in Eastern Europe, Vol. 17, pp. 28-33.

17. *www.all4rest.aitex.net,* visited in February 2012

18. *www.stella-project.eu,* visited in February 2012

19. *www.biotex-eu.com,* visited in February 2012

20. *www.context-project.org,* visited in February 2012

21. *www.ofseth.org,* visited in February 2012

22. *www.mermoth.org,* visited in February 2012

23. *www.hitech-projects.com/euprojects/myheart/,* visited in February 2012

24. *www.proetex.org,* visited in February 2012

25. *www.leapfrog.com,* visited in February 2012

26. *www.avalon-eu.org,* visited in February 2012

27. *www.clevertex.net,* visited in February 2012

28. *www.cordis.europa.eu,* visited in February 2012

29. www.cen.eu, CEN/TC 248/WG 31 Technical Report, *Textiles and textile products-Smart textiles - Definitions, categorisation, applications and standardisation needs*

30. *Wearable electronics and photonics.* **P. Xue, X. Tao, M-Y. Leun, H. Zhang.** 2007. pp. 81-103.

31.*Gold coated para-aramid yarns through electroless deposition.* **A. Schwarz, J. Hakuzimana, A. Kaczynska, J. Banaszczyk, P. Westbroek, E. McAdams, G. Moody, Y. Chronis, G. Priniotakis, G. De Mey, D. Tseles, L. Van Langenhove.** 9-10, 2010, Surface & Coatings Technology, Vol. 204, pp. 1214-1418.

32. *Gold Coated Polyester Yarn.* **A. Schwarz, J. Hakuzimana, E. Gasana, P. Westbroek, L. Van Langenhove.** 2008, Advances in Science and Technology, Vol. 60, pp. 47-51.

33. *Current distribution modelling in electroconductive fabrics.***J. Banaszczyk, G. De Mey, A. Schwarz and L. Van Langenhove.** 2009, Fibres and Textiles in Eastern Europe, Vol. 17, pp. 28-33.

34. *Handbook of Conducting Polymers.* **N. D. Robinson, M. Berggren.** 4/1, s.l. : 2007, Vol. third.

35. *The characterisation of electrically conductive silver ink patterns on flexible substrates.* **S. Merilampi, T. Laine-Ma, P. Ruuskanen.** 2009, Microelectronics Reliability 49, pp. 782-790.

36. *Direct writing of copper conductive patterns by ink-jet printing.* **B. K. Parka, D. Kim, S. Jeong, J. Moon, J. S. Kim.** 19, 2007, Thin Solid Films, Vol. 515, pp. 7706-7711.

37. *Ink-jet fabrication of electronic components.* **S. M. Bidoki, D. M. Lewis, M. Clark, A. Vakorov, P. A. Millner, D. McGorman.** s.l. : Journal of Micromechanics and Microengineering, 2007, Vol. 17, pp. 967-974.

38. *Inkjet deposited circuit components.* **S. M. Bidoki, J. Nouri, A. A. Heidari.** s.l. : Journal of Micromechanics and Microengineering, 2010. Vol. 20.

39. produced by **DuPont.** *Data sheet of conductive ink 5025.* visited in February 2012

40. produced by **Acheson.** *Data sheet of conductive ink Electrodag PF 410.* visited in February 2012

41. *Inkjet printing of nanosized silver colloids.* **H. H. Lee, K. S. Chou, K. C. Huang.** s.l. : Nanotechnology, 2005, Vol. 16, pp. 2436-2441.

42. *Inkjet printing of conductive patterns on textile fabrics.* **S. M. Bidoki, D. McGorman, D. M. Lewis, M. Clark, G. Horler, R. E. Miles.** 2005, AATCC Rev. 5 (6), pp. 11–14.

43. *An ink-jet-deposited passive component process for RFID.* **D. Redinger, S. Molesa, S. Yin, R. Farschi, V. Subramanian.** s.l. : IEEE Transactions on Electron Devices, 2004, Vol. 51, pp. 1978-1983.

44.**TNO.** *Digital printing of conductive tracks,* visited in February 2012

http://www.tno.nl/downloads/TNO_Digital_printing_conductive_of_tracks1.pdf.

45. *Piezoresistive sensors for smart textiles.* **P. Calvert, P. Patra, T. C. Lo, C. H. Chen, A. Sawhney, A. Agrawal.** s.l. : Proc. SPIE, 2007. Vol. 6524.

46. *Electrical characterization of Transmission Lines on Nonwoven Textile substrates.* **C. R. Merritt, B. Karaguzel, T-H. Kang, J. M. Wilson, P. D. Franzon, H. T. Nagle, B. Poudeyhimi, E. Grant.** 2005, Material Research Society, Vol. 870E.

47. *Flexible, durable printed electrical circuits.* **B. Karaguzel, C. R. Merritt, T. Kang, J. M. Wilson, H. T. Nagle, E. Grant, B. Polurdeyhimi.** 1, s.l. : The Journal of the Textile Institute, 2009, Vol. 100, pp. 1-9. 1754-2340.

48. *Screen-printed textile transmission lines.* **I. Locher, G.Tröster.** 2007, Textile Research Jornal 77, pp. 837-842.

49. *Technologies for System-on-Textile.* **I. Locher.** 2006, Vol. 165. ISBN 3-86628-061-0.

50. *Printed Textile Antennas for Off-body Comunication.* **C. Hertleer, L. Van Langenhove, H. Rogier.** s.l. : Advances in Science and Technology, 2008, Vol. 60, pp. 64-66.

51. *A Wearable Fabric Computer by Planar-Fashionable Circuit Board Technique.* **H. Kim, Y. Kim, H. Y. Yoo.** s.l. : IEEE Compiuter Society, 2009, pp. 282-285. 978-0-7695-3644-6.

52. *Electrical charachterisation of screen–printed circuits on the fabric.* **Y. Kim, H. Kim, H. J. Yoo.** 2010, IEEE Transaction on Advanced Packaging, Vol. 33, No. 1.

53. *Thick-film textile-based amperometric sensors and biosensors.* **Y. L. Yang, M. C. Chuang, S. L. Lou, J. Wang.** 2010, Royal Society of Chemistry, pp. 135, 1230-1234.

54. *Electrical characterisation of conductive ink layers on textile fabrics: model and experimental results.* **J. Rius, S. Manich, R. Rodriguez, M. Ridao.** s.l. : http://dit.upc.es/lpdntt/rius/web/paper29.pdf. visited in February 2012

55. *MR-1 surface resistance meter.* visited in February 2012 http://www.schuetzmesstechnik.de/de/pdf/Ken-MR1.pdf.

56. *Accurate geometry factor estimation for the four point probe method using COMSOL multiphysics.* **A. Kalavagunta, R. A. Weller.** 2005, Excerpt from the proceedings of the COSMOL multiphysics user´s conference.

57. *A method of measuring specific resistivity and Hall effect of disc of arbitrary shape.* **L. J. Van Der Pauw.** 1958, Philips Research Reports, Vol. 13, pp. 1-9.

58. *The Van Der Pauw method for sheet resistance measurements of polypyrrole coated para aramide woven fabrics.* **J. Banaszczyk, G. De Mey, A. Schwarz, L. Van Langenhove.** 2010, Journal of Applied Polymer Science, Vol. 117, pp. 2553-2558.

59. *Van Der Pauw method for measuring resistivities of anisotropic layers printed on textile substrates.* **I. Kazani, G. De Mey, C. Hertleer, J. Banaszczyk, A. Schwarz, G. Guxho and L. Van Langenhove.** 20, 12 September 2011, Textile Research Journal, Vol. 81, pp. 2117-2124.

2

Electrical conductive textiles through screen printing

In this chapter the potential of screen printing on different textile substrates with silver-based inks is explained. In this study the conductivity is investigated by measuring the square resistance in different stages as after printing, abrading and after 60 washing cycles respectively.

This chapter is based on the publication
Electrical conductive textiles through screen printing
In Textile & Fibres in Easter Europe, Volume 2, No 1 (90), p 57-63, 2012

TABLE OF CONTENTS

2.1 Introduction

Conductive inks have found use in many applications, including electronics, computers and communication. More specifically, they have been used for Printed circuit boards (PCBs), Radio-frequency identification (RFID tags) or wiring boards [1]. To these rigid substrates, which are altogether different from textiles, diverse technologies have been applied, most notably screen printing.

In the last decade, electrodes, circuits, wearable computers and embedded systems for monitoring vital signs have been printed by screen printing conductive silver-based inks on different woven and nonwoven fabrics [2-6]. For textile applications, the technique is suitable for structures such as patch antennas, ground planes, feed lines or simple one-layer routing structures [7], resulting in flexible and lightweight components. However, when integrated in wearable textile systems, consumers will only accept them if they do not require any special maintenance other than regular washing processes, preferably without removing all devices.

In this chapter, it is present a method to obtain washable, screen-printed electroconductive textiles.

The screen printing method was specifically selected because it is an inexpensive, flexible and fast way to obtain lightweight conductive coated textiles that can be integrated into smart textiles. In order to examine the influence of different kinds of ink on textile materials, we screen-printed manually four silver-based conductive inks on different woven textiles.

The electrical properties were evaluated by measuring the square resistance of the printed textiles during different stages, such as after printing, abrading and washing. Since the electrical properties were not so good after washing, it was decided to put a protective layer on top of the conductive layers. Again, the electrical properties of the samples were assessed before and after washing.

2.2 Screen-printed woven textiles

2.2.1 Textile materials

In this study, 14 woven textile substrates were selected, made of different materials: natural, synthetic and also blended fibres: Cotton (100 % CO), Viscose (100% CV), Aramid (5% Kevlar / 95% Nomex), Polyamide (100% PA), Polyester (100% PES), Cotton/Polyester 1 (34.7% CO / 65.3% PES), Cotton/Polyester 2 (30.8% CO / 69.2% PES) and Polyester/Viscose (27.4% PES/ 72.6% CV).

The physical and mechanical properties were determined according to ISO standards and are listed in Table 2.1.

These materials were chosen in order to have a range of natural and synthetic fabrics that are commonly used in the clothing industry. We expect that the difference in properties will have an influence on the printing process and thus on the conductive properties of the wash/dry-cleaned printed samples.

A textile surface is not a flat uniform structure; moreover, it is an absorbing structure. From Table 2.1 we learn that our textiles cover ranges of surface roughness's and also have different absorption capacities. This will result in printed surfaces with different thickness. We expect that a thicker homogeneous printed layer on a smooth surface will result in a more conductive layer. Furthermore, our study involves washing tests in which a good adhesion of the printed layer to the textile surface is important. And we expect that the textiles with a higher surface roughness will show a better adhesion.

Table 2.1 Properties of applied woven textiles

Woven textile materials	Yarn Density of fabric[1]		The type of textile weave[2]	Thickness[3] (mm)	Basis weight[4] (g/m²)	Absorption capacity[5] (%)	Surface roughness[6] (µm)
	Warp (threads/cm)	Weft (threads/cm)					
Cotton 1	24	16	Twill 3/1	0.864	435	124	2.774
Cotton 2	52	24	Twill 2/2	0.390	238	98	2.426
Cotton 3	47	26	Twill 4/1	0.468	283	100	1.773
Viscose 1	18	11	Plain 1/1	0.488	254	101	11.398
Viscose 2	20	19	Plain 1/1	0.310	132	152	7.006
Aramid	32	20	Plain 1/1	0.378	191	88	6.316
Polyamide	45	32	Twill 2/2	0.198	99	135	2.028
Polyester 1	46	25	Plain 1/1	0.380	163	127	5.955
Polyester 2	55	48	Twill 1/2	0.140	101	64	1.105
Polyester 3	57	46	Twill 2/1	0.146	104	64	1.379
Polyester 4	21	22	Plain 1/1	0.478	177	162	6.298
Cotton/Polyester 1	46	26	Twill 3/1	0.296	113	161	2.584
Cotton/Polyester 2	42	29	Twill 3/1	0.414	233	77	2.878
Polyester/Viscose	45	25	Twill 3/1	0.246	108	153	2.970

[1] ISO 7211-2 ``*Textiles - Woven fabrics - Construction - Methods of analysis - Part 2: Determination of number of threads per unit length*``

[2] ISO 7211-1 ``*Textiles - Woven fabrics - Construction - Methods of analysis - Part 1: Methods for the presentation of a weave diagram and plans for drafting, denting and lifting*``

[3] ISO 5084 ``*Textiles - Determination of thickness of textiles and textile products*``

[4] ISO 3801 ``*Textiles - Woven fabrics - Determination of mass per unit length and mass per unit area*``

[5] EN ISO 9073-6:2003 E ``*Textiles - Test methods for nonwovens- Part 6: Absorption*``

[6] Determined by the author

2.2.2 Conductive inks

Four silver-based inks (Table 2.2) are applied in this study: Ink 1 from DuPont (5025) [8], ink 2 from Acheson (Electrodag PF 410) [9], ink 3 and 4 from SunChemical. These commercially available inks are mainly used in low voltage circuitry printed on flexible substrates such as polyester, polyamide, paper and epoxy glass. Furthermore, these inks are suitable for manual screen printing. As can be seen in Table 2.2, the inks have different properties. The solid content, cure conditions, the nominal sheet resistance and viscosity are indicated by the producers, and the resin is analyzed in our lab by Fourier Transform Infrared (FTIR) and Raman spectroscopy.

Silver particle sizes of the inks are: $\leq$ 2.5 µm for ink1, ≤ 3 µm for ink 2 and~7 µm for ink 3 and 4. For ink 1 and 2 the particle size was measured from the Scanning Electron Microscope (SEM) pictures whereas for ink 2 and 3 they were provided by the producer (Figure 2.1).

Table 2.2 Properties of applied silver-based conductive inks

Ink type	Ink 1	Ink 2	Ink 3	Ink 4
Solid content (%)	68 – 72	73.5 – 76	69-71	84 – 86
Cure conditions (120°C)	5-6 minutes	15 minutes	2-10 minutes	2-15 minutes
Sheet resistance (Ω/□ at 25µm)	0.012 – 0.015	<0.025	0.011	≤0.025
Viscosity (Pa.s)	20-30	10-25	2-3	7-9
Resin[7]	Epoxy	PES	PES	Epoxy

[7]Determined by the author

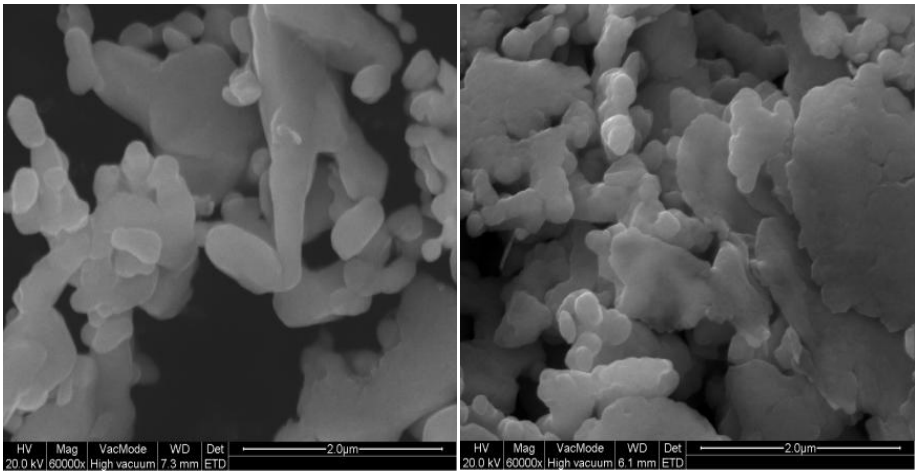

Figure 2.1 SEM pictures of ink 1 (left) and ink 2 (right)

2.2.3 Screen printing

In this study a polyester mesh was used, monofilament 90 T, with a sieve thickness of 110 µm and a sieve opening of 45%. The printing pattern was a square with dimensions of 6 by 6 cm.
For most of the samples, ten print passes were applied, which means that the squeegee was passed over the stencil ten times. However, for some samples, only five print passes were applied because the ink penetrated through the textile substrate as can be seen on the stereoscope images in Figure 2.2.

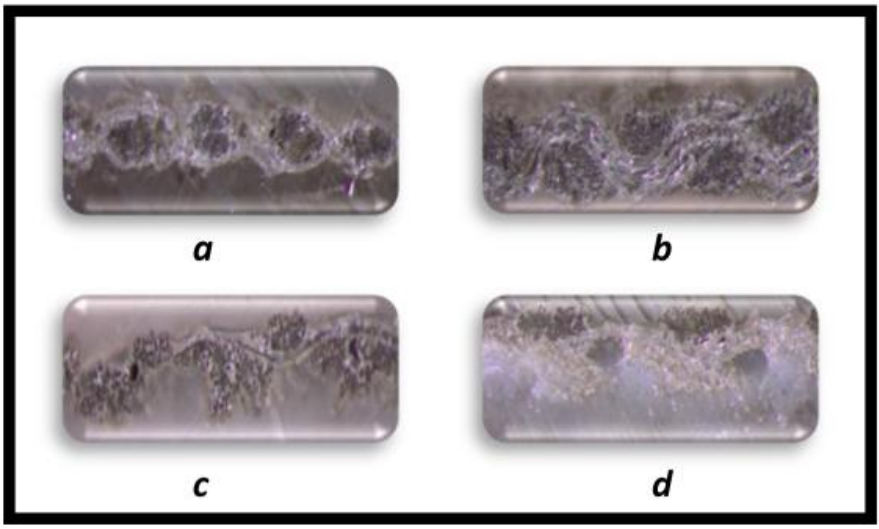

Figure 2.2 Stereoscope cross-section images of ink penetrating the textile substrates: a) Viscose 2, b) Polyester 4, c) Cotton/Polyester 1 and d) Cotton/Polyester 2 (printed with conductive ink 2)

Of each woven textile substrate, three samples were printed with four conductive inks (Figure 2.3 b).

In order to bond and fix the ink to the substrate, the samples were cured in an oven under conditions specified by the producers (Table 2.2). Next, the samples were placed in standard atmosphere for 24 hours (T=20 ± 2°C and RH=65 ± 2%) before their electrical properties were measured.

2.3 Electroconductive properties

2.3.1 The four-point probe measurements

The direct current (DC) resistance of the printed patterns was measured with a four-point probe method as it was explained in the Chapter 1.

At the first group of experiments of screen printing only ***ink 1*** and ***ink 2*** were used.

Square resistance measurements were performed before washing, after washing (5, 10, 15, 20 times) and after each number of abrading cycles.

Before measuring the square resistance, the samples were conditioned in a standard atmosphere for 24 hours. For each printed sample, five measurements of square resistance were made, each time on different spots on the sample, as shown in Figure 2.3. The average of these five measurements was taken as a value of the square resistance.

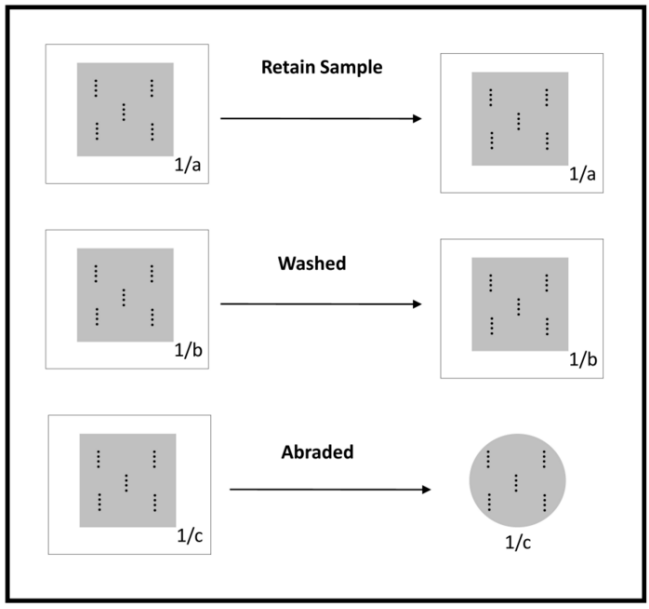

Figure 2.3 Square resistance measurements on five different spots on the sample

2.3.1.1 Square resistance after printing

The square resistance of the conductive layer on the 14 printed textile samples was measured after the samples were printed and cured in the oven. The obtained values are illustrated in Figures 2.4, 2.5.

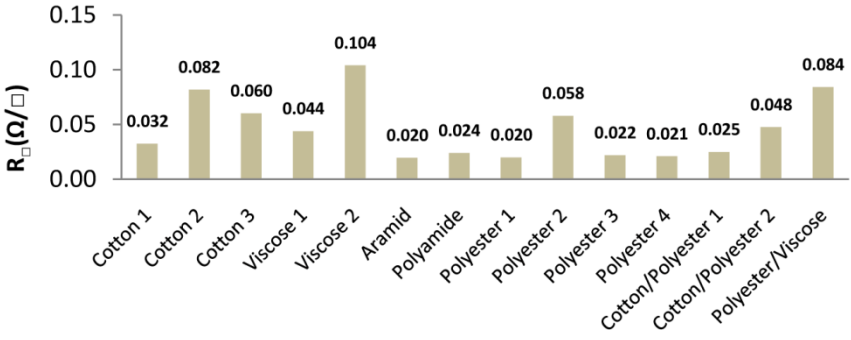

Figure 2.4 Square resistances of printed samples (printed with conductive **ink 1**)

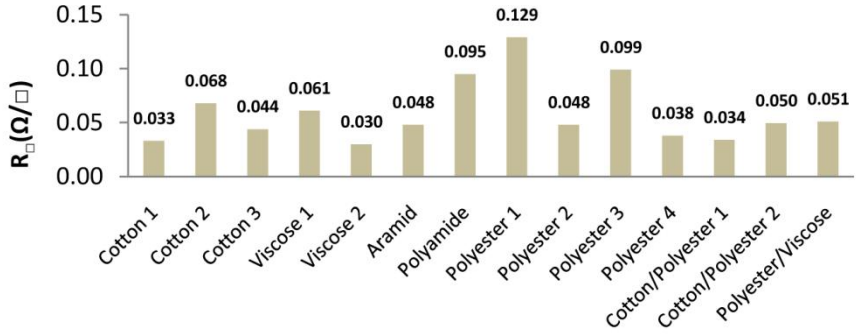

Figure 2.5 Square resistances of printed samples (printed with conductive **ink 2**)

Firstly, for the conductive layers of both inks, we observed that the resistance of the conductive layer obtained depended on the textile material that was

used. For ink 1 the resistance ranged from 0.020 to 0.104 Ω/□, while for ink 2 the data varied between 0.030 and 0.129 Ω/□.

We also noticed that the spreading of the inks on the textile surfaces was not the same for both inks: with ink 1 the lowest resistance values were reached on Aramid and Polyester 1 fabrics (0.020 Ω/□), but with ink 2, the lowest resistance was 0.030 Ω/□ on Viscose 2 fabric. Similarly the highest resistance levels were measured on conductive layers of different substrate materials: for Viscose 2 with ink 1 the square resistance was 0.104 Ω/□ and 0.129 Ω/□ for Polyester 1 with ink 2.

Secondly, we noted that resistance values for the conductive layers of ink 1 varied between 0.020 and 0.104 Ω/□, which is much higher than the resistivity as indicated by the producers (0.012 and 0.015 Ω/□). For conductive layers of ink 2, the obtained resistances on the textile substrates were also remarkably higher (0.030 and 0.129 Ω/□) than the value in the datasheet (< 0.025 Ω/□).

This can be explained by the fact that the textile material partly absorbs the ink, which does not happen on a rigid flat substrate used to determine the ink´s resistivity by the manufacturer.

According to the T test results the difference between the textiles printed with both inks and their square resistances $R_{\square}$ are not statistically significant, $p>0.05$.

2.3.1.2 Square resistance after washing

The ``smart textiles´´ that are now available on the market, like the O'Neil's NavJacket with an integrated GPS [10], require the removal of all electronic devices prior to washing. From a consumer point of view, this is not a desired situation because it complicates maintenance. Consequently, if these printed `conductive textiles` are intended to be used in smart textile applications, good washability properties are crucial.

In this study, the domestic washing behaviour of the printed textile samples was evaluated according to the International Standard ISO 6330:2000 [11]. Washing programme 6 A, which washes at a temperature of 40 ± 3°C, was chosen because it is relevant to the function of the printed samples. Each

sample was washed 5, 10, 15, 20 and 60 times, and in between the square resistance was measured, as described above.

After 20 washing cycles nearly half of the samples had lost their conductivity, and the remaining samples presented very high square resistances (see Tables 2.3). Therefore, no further washing cycles was conducted.

Of the samples that remained conductive after 20 washing cycles, the values of the square resistance appeared to be very high; values between 2 Ω/□ and 244 Ω/□ were measured. For ink 1, Polyester 4 had the highest value of 244 Ω/□ and Cotton/Polyester 1 had the lowest value of 4 Ω/□, while for ink 2 it was Cotton 3 that had the highest value of 71 Ω/□, whereas the lowest value of 2 Ω/□ was obtained for Cotton/Polyester 1.

Table 2.3 Square resistance of the samples before and after washing

Woven textile materials	Conductive layer - $R_{\square}$ Ω/□			
	Ink 1		**Ink 2**	
	Before washing	*20 times washed*	*Before washing*	*20 times washed*
Cotton 1	0.032	203	0.033	-
Cotton 2	0.082	-	0.068	-
Cotton 3	0.060	-	0.044	71
Viscose 1	0.044	26	0.061	-
Viscose 2	0.104	33	0.030	7
Aramid	0.020	11	0.048	36
Polyamide	0.024	45	0.095	-
Polyester 1	0.020	-	0.129	24
Polyester 2	0.058	-	0.048	-
Polyester 3	0.022	-	0.099	-
Polyester 4	0.021	244	0.038	8
Cotton/ Polyester 1	0.025	4	0.034	2
Cotton/ Polyester 2	0.048	-	0.050	40
Polyester/Viscose	0.084	78	0.051	5

The figure below shows how the resistance gradually increases after each 5 washing cycles, up to a maximum of 20 cycles.

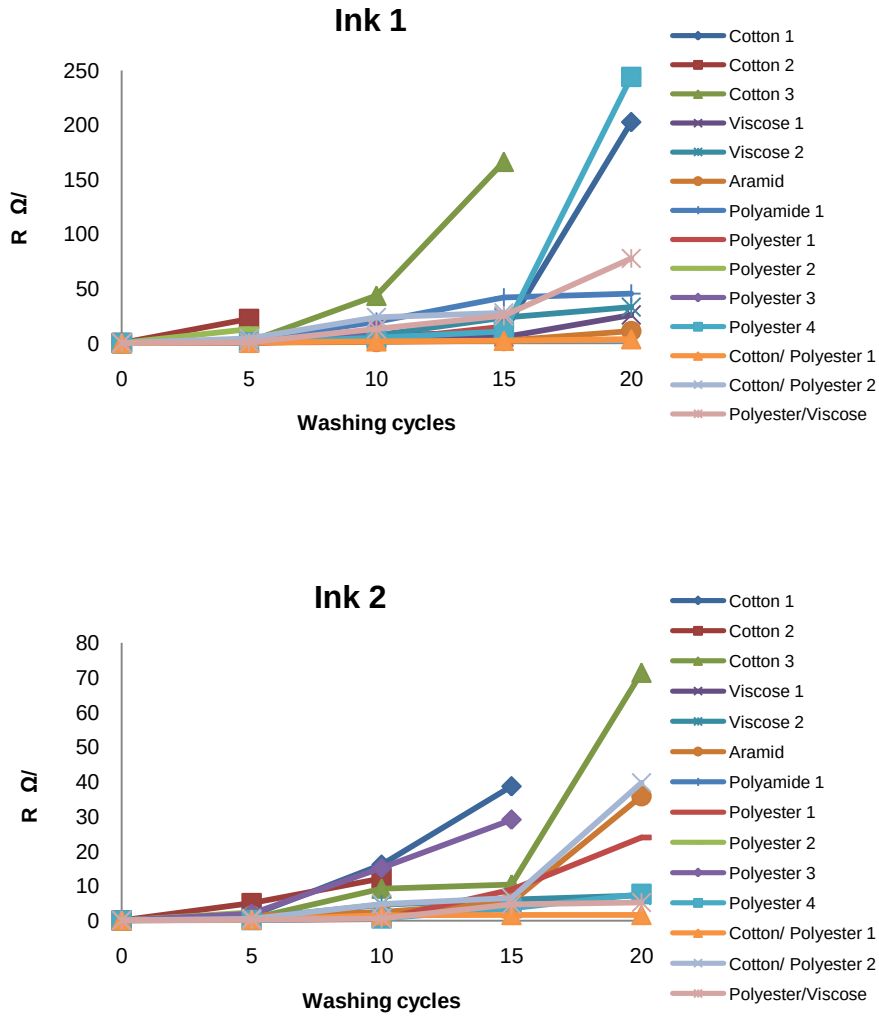

Figure 2.6 Square resistances of printed samples measured after every 5 washing cycles

As it can be seen from Table 2.3, conductive ink 2 showed a lower value of square resistance after washing than conductive ink 1, while it was the other way around before washing.

The values of the square resistance after washing for conductive ink 1 were very high in comparison with those before washing. They were also the highest compared to conductive ink 2.

After 20 washings cycles, nearly half of the samples, from each conductive ink used, had lost their conductivity (Figures 2.7 and 2.8).

The following pictures illustrate that the conductive layer had disappeared from the surface of the printed textiles.

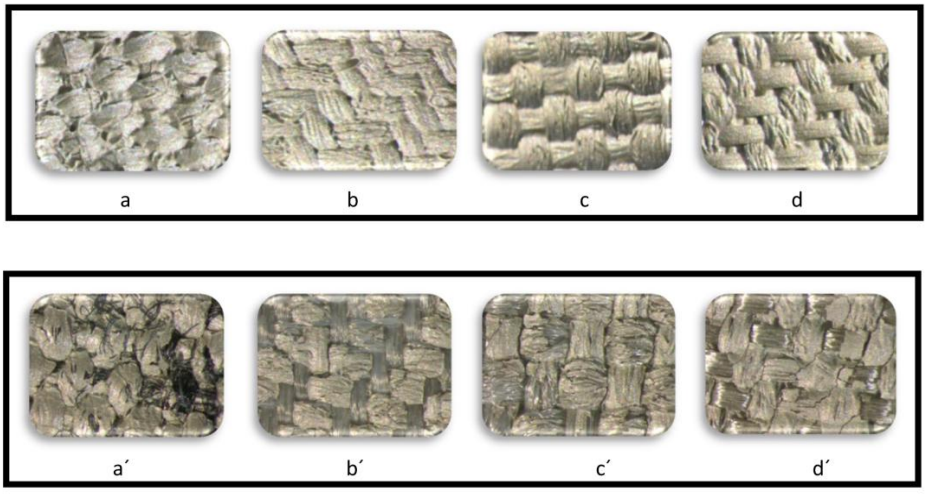

Figure 2.7 The samples before and after 20 washing cycles: a) Aramid, b) Polyamide 1, c) Polyester 1, d) Cotton/Polyester
(printed with conductive **ink 1**)

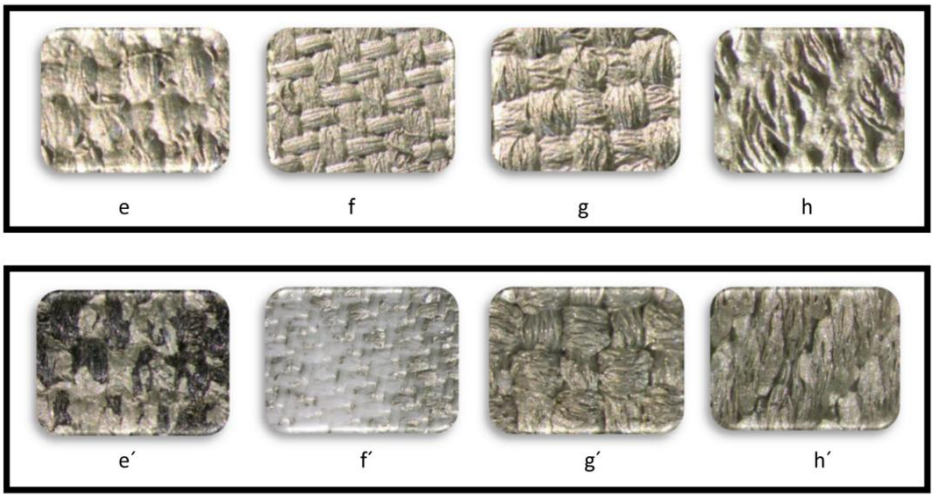

Figure 2.8 The samples before and after 20 washing cycles: e) Aramid, f) Polyamide 1, g) Polyester 1, h) Cotton/Polyester
(printed with conductive **ink 2**)

2.3.1.3 Square resistance after abrading

In this section the square resistance after abrading the textile substrates printed with ***four inks*** is discussed. The two other inks from Sun Chemical were used in ***the second group of experiments,*** when it was decided to find a solution for improving the washability. This discussion is inserted here as the measurements were done with the four-point probe method.

For the second group of experiments eight fabrics were selected according the evaluation of the electrical properties after washing tests described in 2.3.1.2: Viscose 2, Aramid, Polyamide, Polyester 3, Polyester 4, Cotton/Polyester 1, Cotton/Polyester 2 and Polyester/Viscose.

The abrasion resistance of the printed textile samples is an important property since these conductive textiles are meant to be used in clothes. As clothing is used on a daily basis, there will be abrasion between the fabric and the skin,

as well as between two different fabric layers, or between the fabric and the surfaces of the surrounding materials. Therefore it was necessary to examine the effect of abrasion on the square resistance of the printed textiles. This test was performed by means of the Martindale method (Figure 2.9), in compliance with the International Standard ISO 12947-2:1998 [12] for 500, 1000, 2000, 3000, 4000 and 5000 abrasion cycles.

Figure 2.9 Abrasion resistance apparatus

The principle of this test is that a circular specimen, which is mounted in a specimen holder with a load of 12 kPa, is rubbed against a 100% wool textile. The specimen holder is rotatable around its axis perpendicular to the plane of the specimen.

After the abrading test, the wool fabric showed a gray spot on the area where it had rubbed against the conductive layer, which indicates that much of the layer had come off. This resulted in a higher resistance. We expressed that as the increase of the square resistance $\Delta R_{\square}$, calculated as follows:

$$\Delta R_{\square} = \frac{R_M - R_O}{R_O} \cdot 100 \qquad (1)$$

R_M -square resistance after abrading

R_O -square resistance before abrading

Figures 2.10, 2.11, 2.12 and 2.13 confirm that a considerable increase of resistance was measured after 5000 abrading cycles.

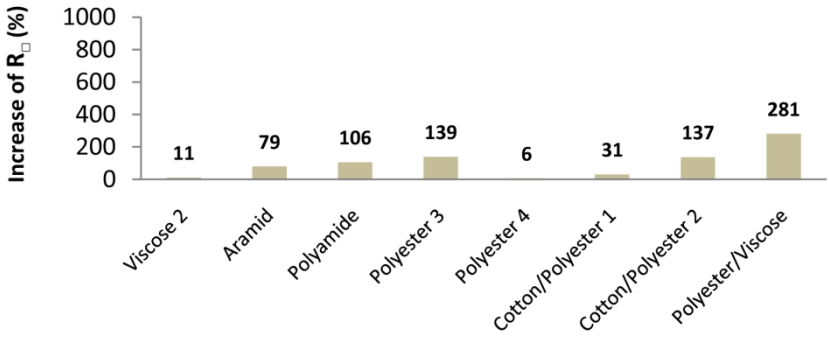

Figure 2.10 The increase of square resistance after 5000 abrasion cycles (printed with conductive **ink 1**)

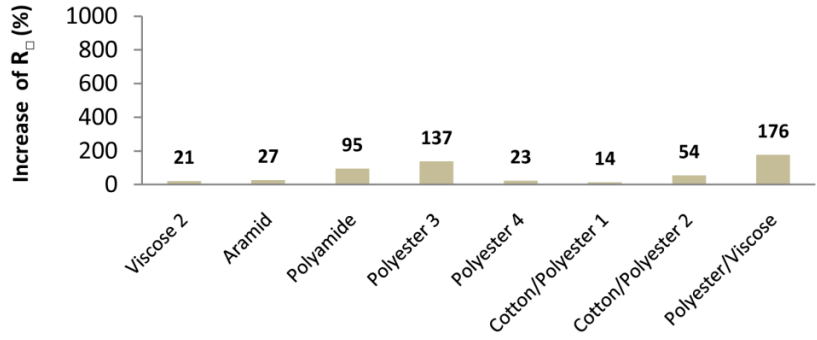

Figure 2.11 The increase of square resistance after 5000 abrasion cycles (printed with conductive **ink 2**)

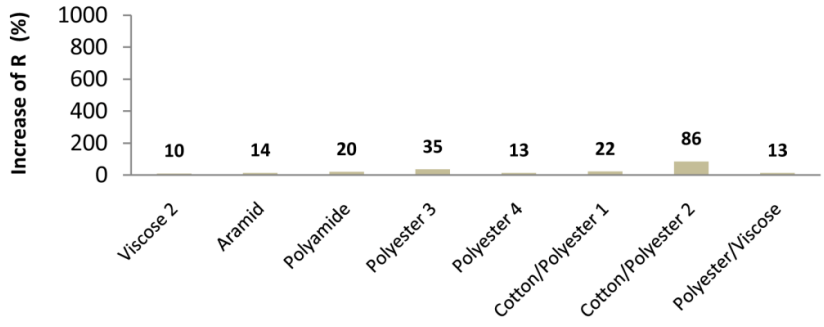

Figure 2.12 The increase of square resistance after 5000 abrasion cycles (printed with conductive **ink 3**)

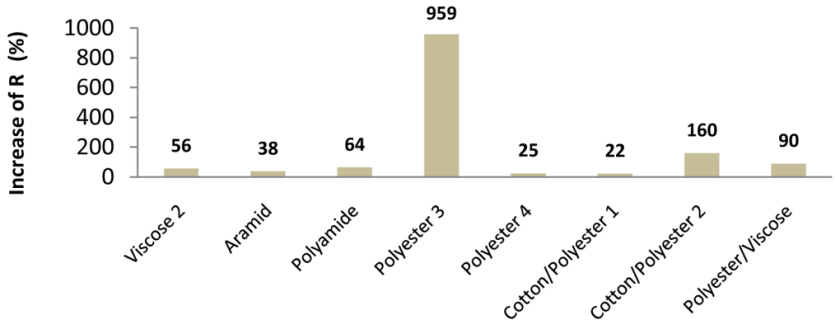

Figure 2.13 The increase of square resistance after 5000 abrasion cycles (printed with conductive **ink 4**)

When the four inks were compared after the abrading tests, the resistance of ink 4 was generally much higher, followed by ink 1. This can be explained by the epoxy resins that are used in these two inks, whereas ink 2 and 3 are based on a Polyester resin. Consequently, the adhesion between the textile substrates and the ink is not so good thus the ink abrades more easily and the resistance increases with additional abrading cycles.

We also observed that Polyester 3 shows pretty high resistance with ink 4). As is shown in Table 2.1, this material has a very low absorption capacity (64 %), which means that the textile material does not absorb the ink very well. In

addition, for Cotton/Polyester 1, which has a very high absorption capacity (161 %) the resistance of conductive layers increased only slightly (14 % for ink 2 up to 31 % for ink 1).

The absolute values of the square resistance after the abrading test for the conductive layers printed with ink 1 varied from 0.022 to 0.396 Ω/□, for ink 2 from 0.036 to 0.234 Ω/□, for ink 3 from 0.011 to 0.032 Ω/□ and for ink 4 from 0.007 to 0.111Ω/□.

2.3.1.4 Adhesion

Adhesion of the printed textile samples is an important property since these conductive textiles will be washed. This test was performed by means of method B, in compliance with the International Standard ISO D3359-09 [13]. This standard is used for assessing the adhesion of coating films to metallic substrates. Merilampi *et. al.* [3] used it on flexible substrates such as paper, polyimide, polyethylene terephthalate, fabrics, and polyvinylchloride. This method was chosen because it is applicable for film thicknesses lower than 125 µm.

The principle of this test is that a lattice pattern with six cuts in each direction is made in the printed layer to the substrate. Then a pressure-sensitive tape is applied over the lattice and then tape is pulled off rapidly under an angle of 180°. The scale in this standard is from 0B to 5B, where 5B denotes the best adhesion.

Table 2.4 The adhesion classification for all inks

Rate of adhesion	Viscose 2	Aramid	Polyamide	Polyester 3	Polyester 4	Cotton / Polyester 1	Cotton / Polyester 2	Polyester / Viscose
Ink 1	3B	2B	4B	2B	4B	3B	2B	4B
Ink 2	4B	3B	4B	0B	4B	3B	4B	3B
Ink 3	5B	4B	3B	3B	5B	5B	3B	3B
Ink 4	4B	3B	3B	3B	4B	4B	3B	3B

The adhesion for ink 3 and 4 was reasonably good ranging from 3-5B (Table 2.4). The variation in adhesion may occur because of the resin of each ink. Generally the surface roughness of the substrate effects on the adhesion as mechanical interlocking are formed easier on a rough surface than on a smooth surface [1]. Figure 2.14 shows that Polyester 3 has the smoothest surface, which corresponds with the lowest classification rate seen in Table 2.4.

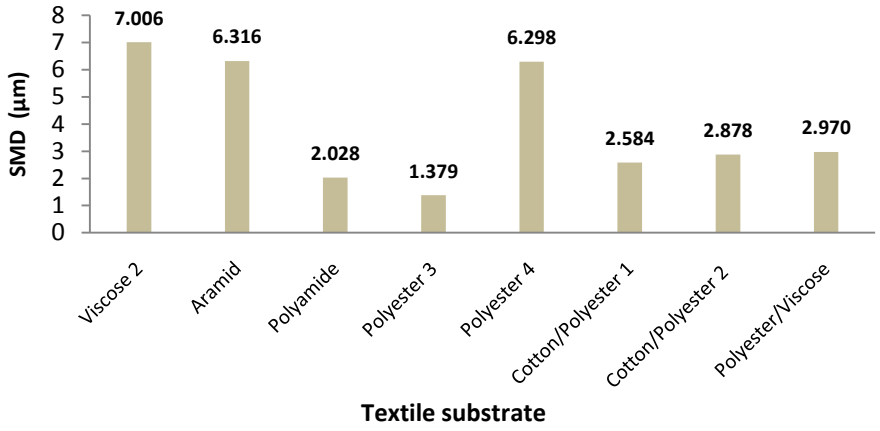

Figure 2.14 The surface roughness of textiles used for the screen-printed process

It needs to be mentioned that these inks are commercially available. Nevertheless their proprietary additives which have an effect on adhesion are kept secret to the customers.

2.3.2 Van Der Pauw measurements

In order to avoid cracks in the printed surface or ink to disappear after washing, some kind of pre-treatment may be conducted to the textiles; however, in this study it was chose to put a thermoplastic polyurethane (TPU) layer on top of the conductor. Consequently, the four-point method cannot be used anymore and we opted for the Van Der Pauw (VDP) method [14, 15] as describe in Chapter 1 (Section 1.5) as an alternative measurement method.

2.3.2.1 Square resistance after covering with TPU

The square resistance of the printed textile samples with four silver-based inks was measured after the samples were covered with the TPU layer.

The obtained values are shown in Figures 2.15, 2.16, 2.17 and 2.18.

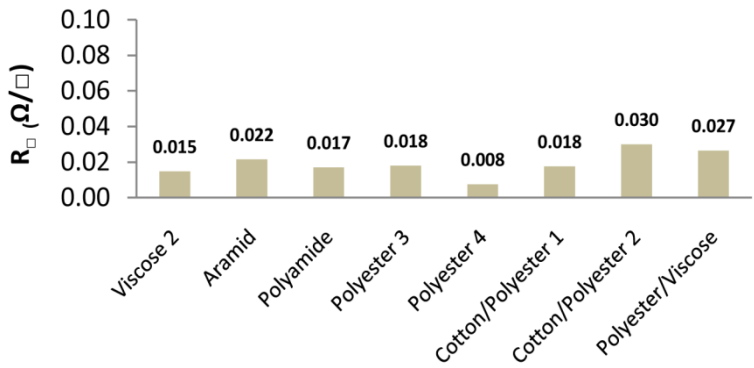

Figure 2.15 Square resistance of printed samples covered with TPU layer (printed with conductive **ink 1**)

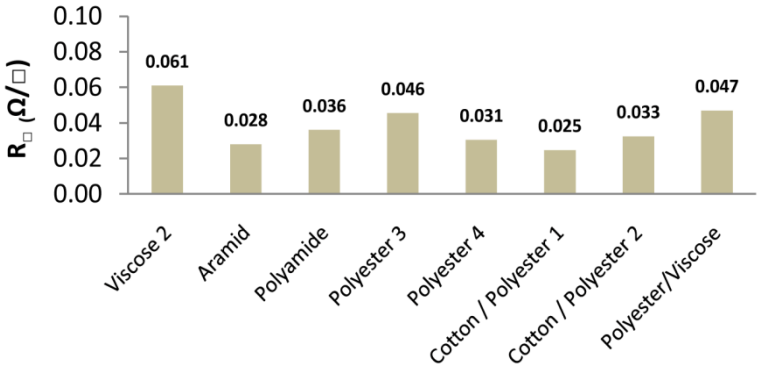

Figure 2.16 Square resistance of printed samples covered with TPU layer (printed with conductive **ink 2**)

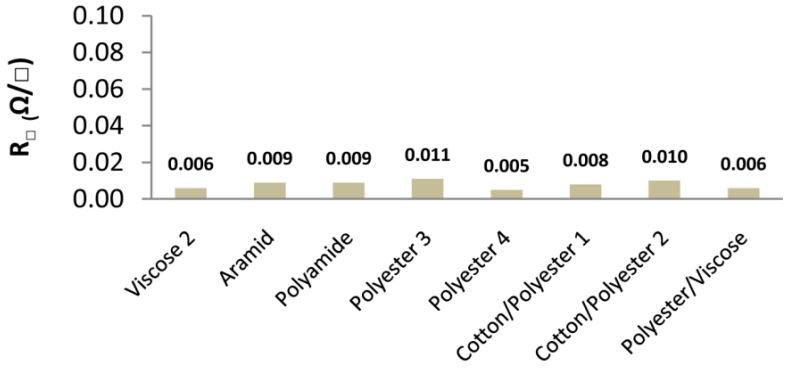

Figure 2.17 Square resistance of printed samples covered with TPU layer (printed with conductive **ink 3**)

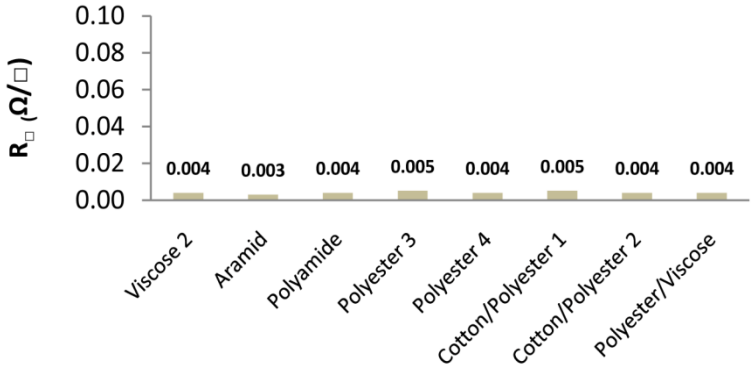

Figure 2.18 Square resistance of printed samples covered with TPU layer (printed with conductive **ink 4**)

We did not compare the absolute values of square resistance obtained with the four-point probe measurement and the VDP method, because our aim in this chapter was to focus on changes in square resistance when the fabrics were abraded or washed. However, this topic is addressed in Chapters 4 and 5.

Nevertheless, once again we observe that ink 2 generally leads to higher resistance values (between 0.025 and 0.061 Ω/□) and ink 4 to lower resistance values (between 0.003 and 0.005 Ω/□). According to the one-way ANOVA results, the differences between the mean square resistances $R_{□}$ of the four inks are statistically significant (Table 2.5). The Duncan post-hoc test (Table 2.6), $p<0.05$, reveals that ink 3 and ink 4 belong to the same subset and give the lowest $R_{□}$, followed by ink 1. Ink 2 gives the highest $R_{□}$.

Table 2.5 ANOVA table for four inks

	Sum of Squares	df	Mean Square	F	Sig.
Between Groups	,280	3	,093	28,455	,000
Within Groups	,617	188	,003		
Total	,897	191			

Table 2.6 ANOVA table of means for groups in homogeneous subset

Ducan[a]

		Subset for alpha = 0.05		
Ink	N	1	2	3
Ink 4	48	,008250		
Ink 3	48	,011344		
Ink 1	48		,044665	
Ink 2	48			,103229
Sig.		,792	1,000	1,000

2.3.2.2 Square resistance after washing

The washing test was repeated after the TPU layer was added on top of the printed samples. Here, according to the International Standard ISO 6330:2000 [11] the washing programme 8 A was chosen, which washes at a temperature of 30°C (± 3°C), as it is relevant to the function of the TPU layer on top of the printed samples. For each printed textile sample, 60 washing cycles were applied and the square resistance was measured (Figures 2.19, 2.20, 2.21 and 2.22).

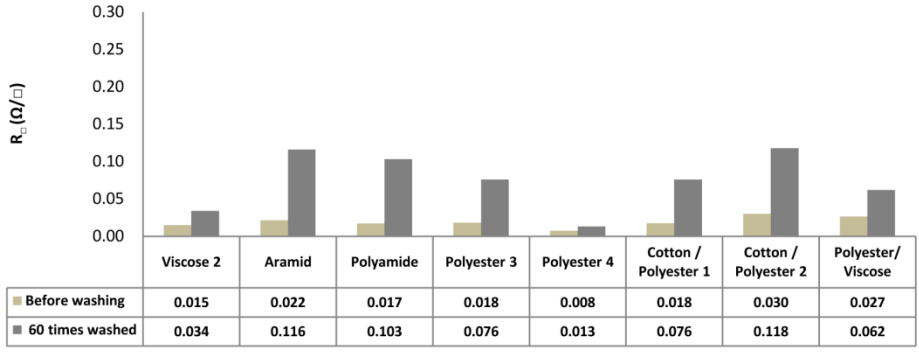

	Viscose 2	Aramid	Polyamide	Polyester 3	Polyester 4	Cotton / Polyester 1	Cotton / Polyester 2	Polyester/ Viscose
Before washing	0.015	0.022	0.017	0.018	0.008	0.018	0.030	0.027
60 times washed	0.034	0.116	0.103	0.076	0.013	0.076	0.118	0.062

Figure 2.19 Square resistance of washed samples covered with TPU layer (printed with conductive **ink 1**)

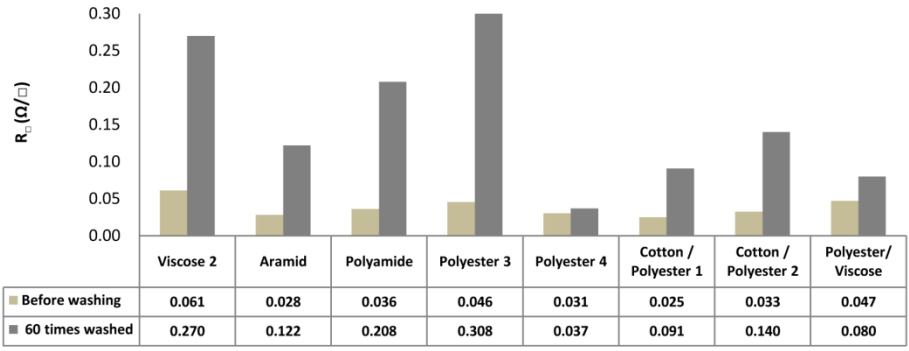

	Viscose 2	Aramid	Polyamide	Polyester 3	Polyester 4	Cotton / Polyester 1	Cotton / Polyester 2	Polyester/ Viscose
Before washing	0.061	0.028	0.036	0.046	0.031	0.025	0.033	0.047
60 times washed	0.270	0.122	0.208	0.308	0.037	0.091	0.140	0.080

Figure 2.20 Square resistance of washed samples covered with TPU layer (printed with conductive **ink 2**)

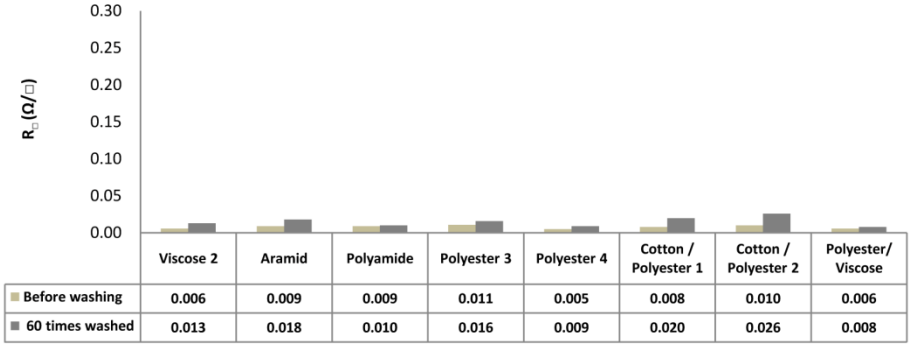

	Viscose 2	Aramid	Polyamide	Polyester 3	Polyester 4	Cotton / Polyester 1	Cotton / Polyester 2	Polyester/ Viscose
Before washing	0.006	0.009	0.009	0.011	0.005	0.008	0.010	0.006
60 times washed	0.013	0.018	0.010	0.016	0.009	0.020	0.026	0.008

Figure 2.21 Square resistance of washed samples covered with TPU layer (printed with conductive **ink 3**)

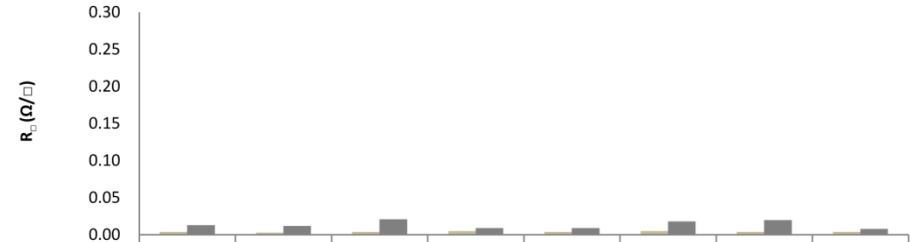

	Viscose 2	Aramid	Polyamide	Polyester 3	Polyester 4	Cotton / Polyester 1	Cotton / Polyester 2	Polyester/ Viscose
Before washing	0.004	0.003	0.004	0.005	0.004	0.005	0.004	0.004
60 times washed	0.013	0.012	0.021	0.009	0.009	0.018	0.020	0.008

Figure 2.22 Square resistance of washed samples covered with TPU layer (printed with conductive **ink 4**)

Again, we observed an increase in square resistance after 60 washings, but not as pronounced as without the TPU layer on top (Section 2.3.1.2). For several fabrics, there was nearly no change in resistance after washing, such as Polyester 4 printed with ink 1, 2, 3 and 4 (Figure 2.19, 2.20, 2.21 and 2.22), which is quite striking from a practical point of view because the square resistance remained stable after several washings. All resistances measured remained under 0.308 Ω/□.

Four polyester-based fabrics (Polyester 4, Polyester/Viscose and Cotton/Polyester 1 and 2) also showed very good electrical properties after washing. However, Polyester 3 behaves quite different with a higher increase of resistance after washing, which is due to the lower absorption capacity of the material compared to the other polyester-based fabrics. This results in a lower amount of ink after printing, which affects the conductivity level. The thicker the layer, the higher the conductivity level is [16, 17]. It is expected that the amount of conductive ink, weight, on the textile substrate relates to the resulting resistance and this trend can be observed in the Figure 2.23. One more reason here is the lower surface roughness of the Polyester 3 fabric which effect the mechanical interlocking because smother the surface is, lower the adhesion is. This supports our hypothesis from the beginning of this chapter that the surface roughness of the fabric is very important in order to have a good adhesion of the ink.

Ink 3 and 4 had the lowest square resistance before and after washing on eight textile substrates used.

A very important role here plays the inks´ parameters such as amount of ink, solid content and nominal sheet resistance. The amount of ink and the solid content for ink 1 and 3 were comparable but ink 3 had the lowest nominal sheet resistance, which makes it having a lower square resistance. Ink 4 has the highest amount of ink, the highest solid content and printed on textile surfaces made it the best conductive ink even after 60 washing cycles. This confirms our expectation at the beginning of the experiments, the higher the amount of ink the higher the conductivity is.

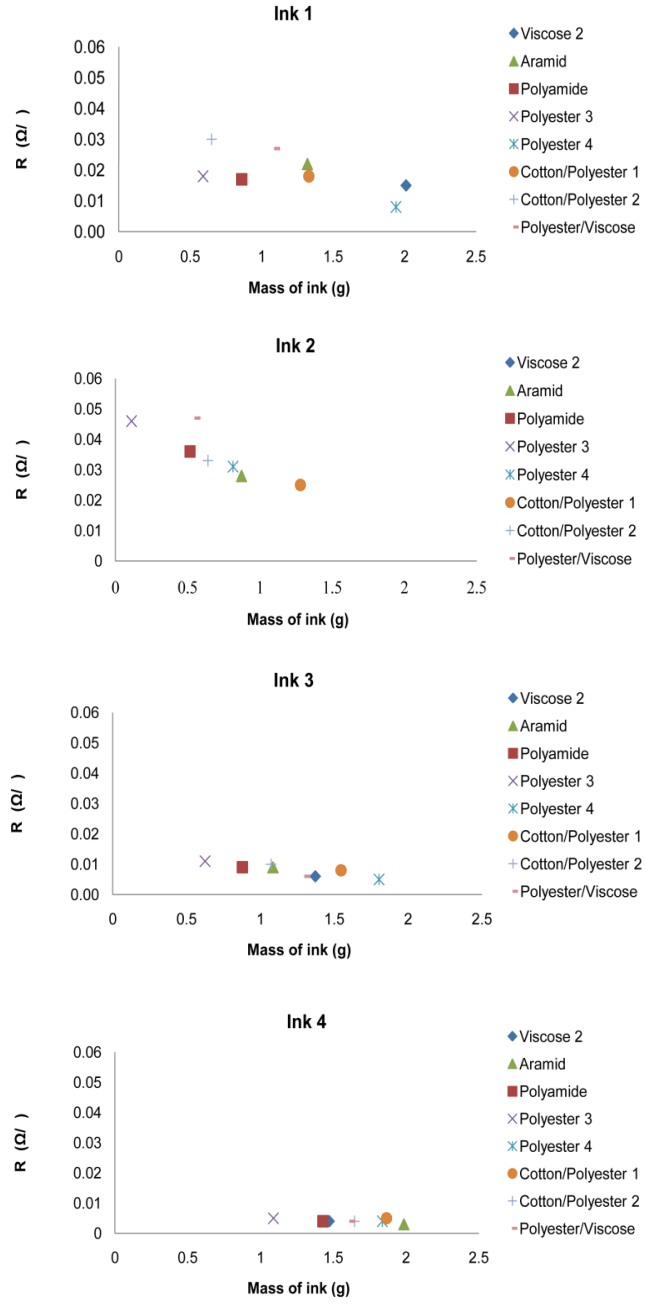

Figure 2.23 The amount of conductive inks related to the square resistance

2.4 Conclusions

The combination of textiles and conductive inks makes it possible to produce flexible, conductive, lightweight, practical and comfortable `smart textiles´.

The screen printing technique with conductive ink used in this research is not only a traditional but also an inexpensive method to make textiles conductive.

In this chapter, four silver-based electroconductive inks (ink 1, ink 2, ink 3 and ink 4) were applied to a selection of woven textile substrates. The electrical properties of the conductive layer on the printed samples were evaluated by means of the square resistance, measured after printing, after abrading and after washing.

The square resistance obtained with four inks used was influenced by the amount of ink, solid content and nominal sheet resistance of the printed samples.

The printed samples covered and not covered with a TPU layer were washed up to 20 and 60 times. The uncovered printed layer showed cracks after 20 times of washing and the conductive layer had disappeared during the washing cycles, resulting in a loss of conductivity. However, when the conductive layer was protected with a TPU layer, the conductivity was maintained after up to 60 washing cycles.

It was shown that electroconductive textiles obtained with screen printing of silver-based inks and protected with a TPU layer are suitable for washing.

2.5 References

1. *Electrical characterization of Transmission Lines on Nonwoven Textile substrates.* **C. R. Merritt, B. Karaguzel, T-H. Kang, J. M. Wilson, P. D. Franzon, H. T. Nagle, B. Poudeyhimi, E. Grant.** 2005, Material Research Society, Vol.870E.

2. *Interactive electronic textile development: A review of technologies.* **D. Meoli, T. May-Plumlee.** 2002, Journal of Textile and Apparel Technology and Management, Vol 2, Issue 2.

3. *The characterization of electrically conductive silver ink patterns on flexible substrates.* **S. Merilampi, T. Laine-Ma, P. Ruuskanen.** 2009, Microelectronics Reliability 49, pp. 782-790.

4. *Thick-film textile-based amperometric sensors and biosensors.* **Y. L. Yang, M. C. Chuang, S. L. Lou, J. Wang.** 2010, Royal Society of Chemistry, 135, pp.1230-1234.

5. *Electrical charachterisation of screen – printed circuits on the fabric.* **Y. Kim, H. Kim, H. J. Yoo.** 2010, IEEE Transaction on Advanced Packaging, Vol. 33 (1).

6. *Using conductive inks and nonwoven textiles for wearable computing.* North Carolina **B. Karaguzel.** sn. NTC Project: F04-NS17.

7. *Screen-printed textile transmission lines.* **I. Locher, G.Tröster.** 2007, Textile Research Journal , Vol. 77, pp. 837-842.

8. produced by **DuPont.** *Data sheet of conductive ink 5025.* visited in February 2012.

9. produced by **Acheson.** *Data sheet of conductive ink Electrodag PF 410.* visited in February 2012.

10.*http://gizmodo.com/334085/oneill-navjacket-shows-the-way-with-gps-integrated-audiovideo.* **NavJacket, O'Neil's.** sl: visited March 2012.

11. www.iso.org
Textiles - Domestic washing and drying procedures for textile testing: visited March 2012.

12. www.iso.org
*Textiles - Determination of the abrasion resistance of fabrics by the Martindale method - Part 2: Determination of specimen breakdown***:** visited March 2012.

13. http://enterprise.astm.org

Standard Test Methods for Measuring Adhesion by Tape Test: visited March 2012.

14. *A method of measuring specific resistivity and Hall effect of disc of arbitrary shape.* **L. J. Van Der Pauw.** 1958, Philips Research Reports, Vol. 13, pp. 1-9.

15. *The Van Der Pauw method for sheet resistance measurements of polypyrrole coated woven fabrics.* **J. Banaszczyk, G. De Mey, A. Schwarz, L. Van Langenhove.** 2010, Journal of Applied Polymer Science, Vol. 117, pp. 2553-2558.

16. *Inkjet printing of conductive patterns on textile fabrics.* **S. M. Bidoki, D. McGorman, D. M. Lewis, M. Clark, G. Horler, R. E. Miles.** 2005, AATCC Rev. 5 (6), pp. 11–14.

17. *Technologies for System-on-Textile.* **I. Locher.** 2006, Vol. 165. ISBN 3-86628-061-0.

3

Dry-cleaned electroconductive flexible substrates

In this chapter the screen printing process with four silver-based inks on flexible foam and nonwoven polyester is described. For the evaluation of the electrical properties the square resistance of the printed flexible substrates is measured before and after 60 dry-cleaning cycles.

This chapter is based on the publication
Dry-cleaning of electroconductive layers screen-printed on flexible substrates
On 9 March 2012 accepted to be published in Textile Research Journal

TABLE OF CONTENTS

3.1 Introduction

Textiles with electroconductive characteristics have found use in several fields of application, like military, electronics, medical and automotive [1-3]. Textiles are preferred when the end product needs to be flexible, lightweight and washable. One way to obtain these electroconductive textiles is by printing with conductive inks as described in Chapter 2. Several studies of screen printing with conductive inks on different woven and non-woven textiles have already been published [4-10]. However, textiles for clothing need to withstand a maintenance procedure: laundering or dry-cleaning. To our knowledge, this is the first time to report on the dry-cleaning durability of screen-printed electroconductive flexible substrates. The substrates used in this study are flexible foam and nonwoven polyester. Karaguzel et al. [7] have already proved that laundering printed electroconductive textiles in a washing machine results in a loss of conductivity.

This study, therefore, concentrates on dry-cleaning. A further motivation is the fact that dry-cleaning is the preferred maintenance method for garments in which these substrate materials will be integrated, e.g. protective clothing such as fire-fighting suits or casual jackets and outdoor sportswear. The procedure comprised the dry-cleaning of printed samples 5, 10, 15, 20 and 60 times. At first, the samples were measured after every single dry-cleaning cycle. But since the differences between the values after each cycle were negligible, the frequency of measuring was decreased to every 5 cycles.

In this chapter, we discuss about electroconductive flexible substrates screen-printed with four different silver-based inks on foam and nonwoven polyester. The direct current (DC) resistance of the printed patterns was measured before and after dry-cleaning in order to evaluate these four inks.

To preserve electroconductive properties after dry-cleaning, a protective non-conductive layer was put on top of the printed patterns. The final result was that the values of square resistance $R_{\square}$ only slightly increased after 60 dry-cleaning cycles, varying between 0.025 and 2.263 Ω/□.

3.2 Materials and methods

3.2.1 Flexible substrate materials

For this study two flexible substrates were selected: a polyurethane flexible foam (***Urecom***) and a nonwoven polyester (***nonwoven PES***) (Table 3.1). These particular two substrates were chosen, firstly, because they are clearly different, making it possible to observe potentially different interaction with the conductive inks, and secondly, because they both have the thickness (>2 mm) required by some applications, such as planar antennas for wireless off-body communication [11].

Table 3.1 Properties of applied foam and nonwoven PES

Printed flexible substrate	Thickness[1] (mm)	Basis weight [2] (g/m^2)	Density[3] (g/cm^3)
Urecom	3.43	225.18	0.15
PES	3.71	526.36	1.38

3.2.2 Conductive inks

Four silver-based inks are applied in this study, as mention in Chapter 2 (Section 2.2.2).

[1] ISO 9073-2 ``*Textiles - Test methods for nonwovens - Part 2: Determination of thickness*``

[2] ISO 9073-1 ``*Textiles - Test methods for nonwovens - Part 1: Determination of mass per unit area*``

[3] The density (g/cm^3) is indicated from the producers.

3.2.3 Screen printing

The screen-printing in this study was performed by a semi-automatic screen printing machine, Johannes Zimmer Klagenfurt - type Mini MDF 482. In order to achieve an even coverage of the ink over the entire pattern (square of 6 cm by 6 cm) a polyester mesh was used, monofilament 90 T, with a sieve thickness of 110 µm and a sieve opening of 45%.

Of each flexible substrate, three samples were printed with all four inks, resulting in a total of 24 printed samples.

In order to bond and fix the ink onto the substrate, the samples were cured in an oven at the temperature recommended by the ink producers (see Table 2.2).

3.2.4 Dry-cleaning

Dry-cleaning was chosen over laundering because the electroconductive materials examined in this study are meant for integration into garments that are normally dry-cleaned. Foam material, for example, is integrated in the shoulder pads of fire-fighter outer jackets to support the weight of the compressed air bottle. Nonwovens are commonly used as inlayers in collars and labels for jackets. In addition, a laundering study is already available: Karaguzel *et al.* [7] printed transmission lines on nonwoven substrates and reported that after 25 washing cycles in a home laundry machine conforming to the ISO 6330 standard, the printed inks began to degrade and showed lower conductivity.

The dry-cleaning machine used was a UNION XL 835 E, the capacity of whose drum is 15 kg. As cleaning agent the solvent Perchloroethylene (PERC), also known as Tetrachloroethylene (PCE) is used. This is a synthetically produced organic compound.

The dry-cleaning process lasts 45 minutes and consists of three steps: washing, extracting and drying. At the beginning of the washing process, the chamber is automatically filled with solvent to approximately one-third full and

is heated to a temperature of 30°C. The drum is agitated, in order to allow the solvent to clean the substrate material. The machine has two solvent tanks: one tank contains pure solvent and the other contains used solvent. Generally, clothes are first dry-cleaned with filtrated solvent and then rinsed with pure solvent.

Following washing, the extraction cycle begins by draining the solvent from the drum, causing much of the solvent to spin free of the fabric. The used solvent is passed through a filtration chamber and part of the filtered solvent is returned to the second tank to be used in another washing cycle. The residual solvent is then distilled to remove impurities (like oils, fats or grease) and is returned to the pure solvent tank. The filter often needs to be cleaned of impurities. After washing and extracting, the drying process starts. The printed samples tumbled in a warm air flow of around 60°C [12-14].

The printed samples were dry-cleaned 60 times in total.

3.3 Electrical characterization

3.3.1 Determination of amount of ink

The amount of ink on the flexible substrates screen-printed with the four inks was determined by weighing the samples before and after screen-printing (Table 3.2).

Table 3.2 Amount of ink for screen-printed flexible substrates

Flexible substrates	Ink 1 (DuPont) (g)	Ink 2 (Acheson) (g)	Ink 3 (Sun Chemical) (g)	Ink 4 (Sun Chemical) (g)
Urecom	2.67	2.62	2.22	3.87
PES	1.26	4.13	1.18	4.12

3.3.2 Resistance measured with four-point method

The electroconductive properties of the printed flexible substrates were studied by measuring their DC resistance. At the first stage of the study (before lamination), a four-point method by means of an MR-1 Instrument [15] was used before and after dry-cleaning (5, 10, 15 and 20 times).

The values of the square resistance for Urecom before dry-cleaning were between 0.005 - 0.030 Ω/□ and after 20 dry-cleaning cycles they increased to 0.135 - 0.280 Ω/□. However, the samples with inks 1 and 4 lost their conductivity completely, as can be seen from Figure 3.1. Regarding the nonwoven PES, the values of square resistance $R_{\square}$ before dry-cleaning varied from 0.002 to 0.020 Ω/□, slightly lower than those of Urecom. After 20 dry-cleaning cycles, the values increased to 0.050 - 0.122 Ω/□, still lower than with Urecom. Again though, as with Urecom, the sample with ink 1 entirely lost its conductivity.

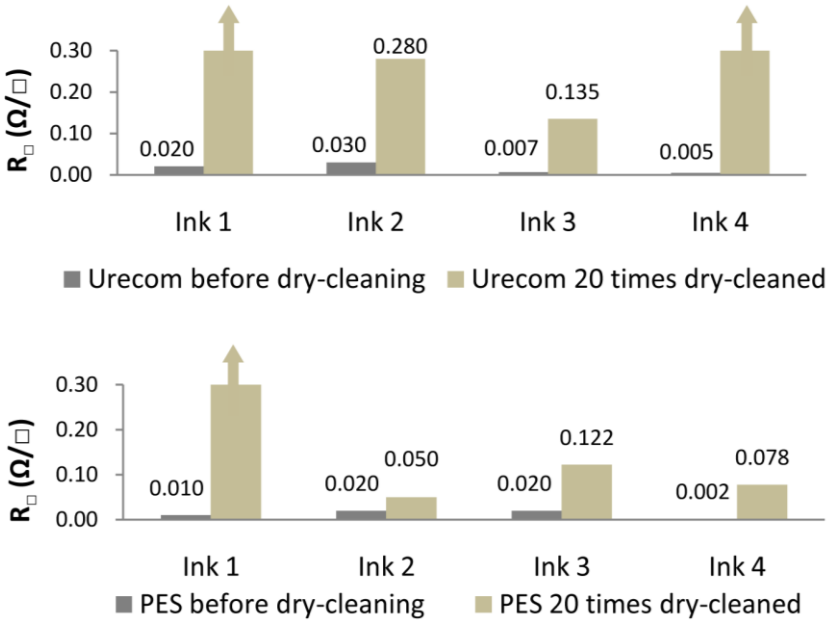

Figure 3.1 Square resistances of printed samples (before and after 20 times dry-cleaning)

Thus, the values of the square resistance after 20 dry-cleaning cycles were very high compared to those before dry-cleaning and some samples lost their conductivity entirely (Urecom samples printed with ink 1 and 4 and PES samples printed with ink 1, Figure 1 and 2).

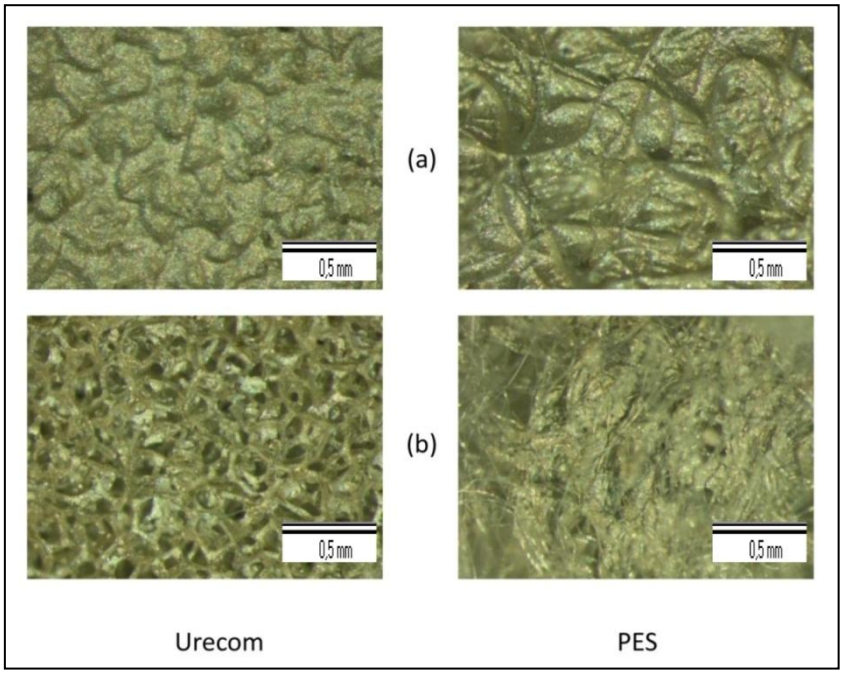

Figure 3.2 Printed samples (a) before and (b) after 20 dry-cleaning cycles (printed with ink 2)

Figure 3.2 illustrates that the conductive layer has disappeared from the surface of both printed flexible substrates.

3.3.3 Resistance measured with Van Der Pauw method

In order to avoid the ink to disappear, it was chosen to put a thermoplastic polyurethane (TPU) layer on top of the printed square. However, covering the printed square with this non-conductive layer meant that the four-point probe method was no longer suitable for evaluating the resistance. Therefore, the DC resistance was measured with the Van Der Pauw (VDP) method [16] as explained in the Chapter 1, Section 2.5.2

The square resistance of the printed textile samples before and after dry-cleaning, with four inks and covered with TPU layer, is shown in Figure 3.3.

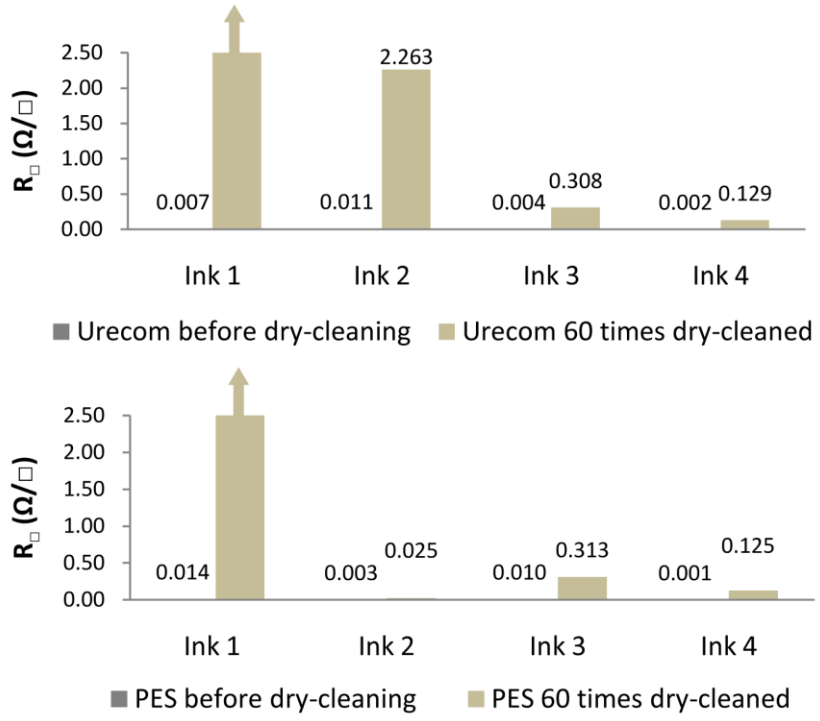

Figure 3.3 Square resistance of printed samples covered with TPU layer (before and after dry-cleaning)

Figure 3.4 shows how the resistance gradually increases after 5 dry-cleaning cycles, up to a maximum of 60 cycles. 60 dry-cleaning cycles is a worst case scenario, because that would mean cleaning the garment every two months during a life cycle of 10 years. A paper by Kalliala *et al.* [17] also fixes on a maximum of 60 laundries for cotton/polyester bed sheets, and it was this paper which inspired us to take dry-cleaning to the same lengths in our research.

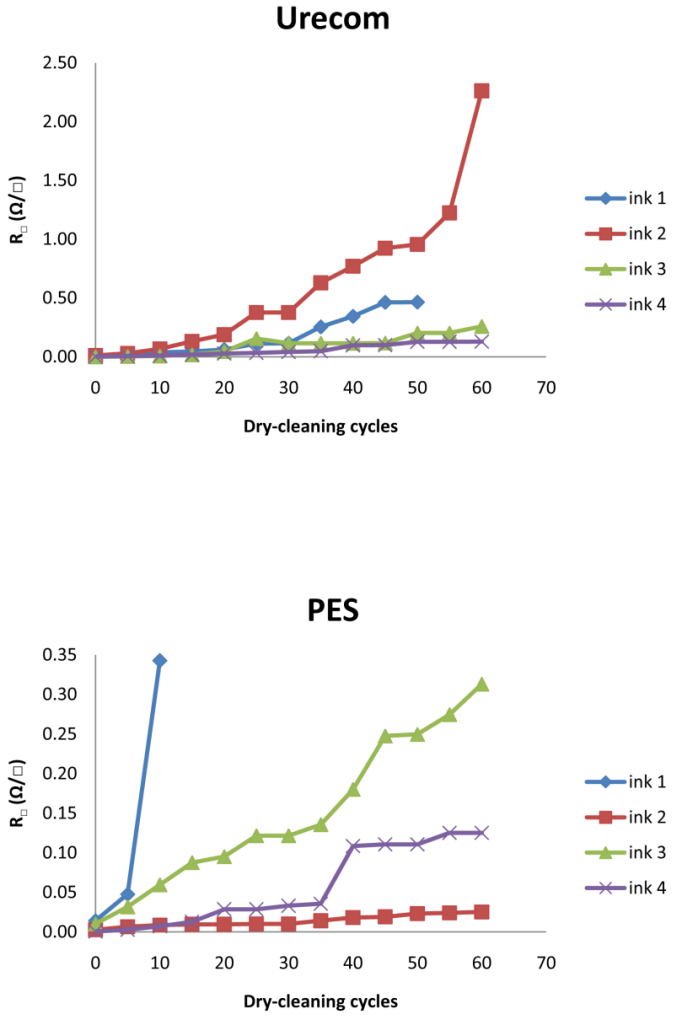

Figure 3.4 Square resistance of printed samples measured after every 5 dry-cleaning cycles

Again we observe that both substrates printed with ink 1 completely lost their conductivity after dry-cleaning. For nonwoven PES this trend was observed after as few as 10 dry-cleaning cycles. Figure 3.5 clearly shows what is happening: the conductive surface has several troughs, as seen from the cross-section. These discontinuities in the conductive layer prevent the electrical current from passing through. They are caused by creases in the fabric during the mechanical movements in the drum, in combination with a low amount of ink on the substrate and bad adhesion of the epoxy resin on the polyester substrate. For this reason, this ink cannot be recommended for use in combination with these substrate materials.

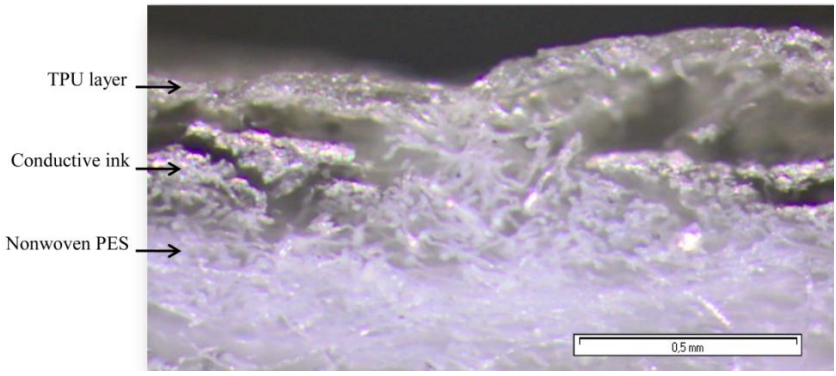

Figure 3.5 Crack of conductive printed layer on non-woven PES (printed with **ink 1**)

Ink 2 gives better values of square resistance $R_{\square}$ in combination with nonwoven PES than with polyurethane foam. The other two inks, 3 and 4, give the best results for both substrate materials. Furthermore, after dry-cleaning the values show almost no difference whether printed on polyurethane foam or on nonwoven PES.

After 60 dry-cleaning cycles, Urecom shows the lowest square resistance $R_{\square}$, 0.129 Ω/□ when printed with ink 4 (with epoxy resin - Table 2.2) and nonwoven PES shows the lowest square resistance $R_{\square}$, 0.025 Ω/□ when printed with ink 2 (with PES resin). Hence, for these substrates the inks have better adhesion after 60 cycles.

Conductive ink 4 generally (before and after dry-cleaning) shows lower square resistance $R_{\square}$ than the other inks. This can be explained by the amount of ink (Figure 3.6) and the value of solid content (84-86% - see Table 2.2), which is the highest for this ink.

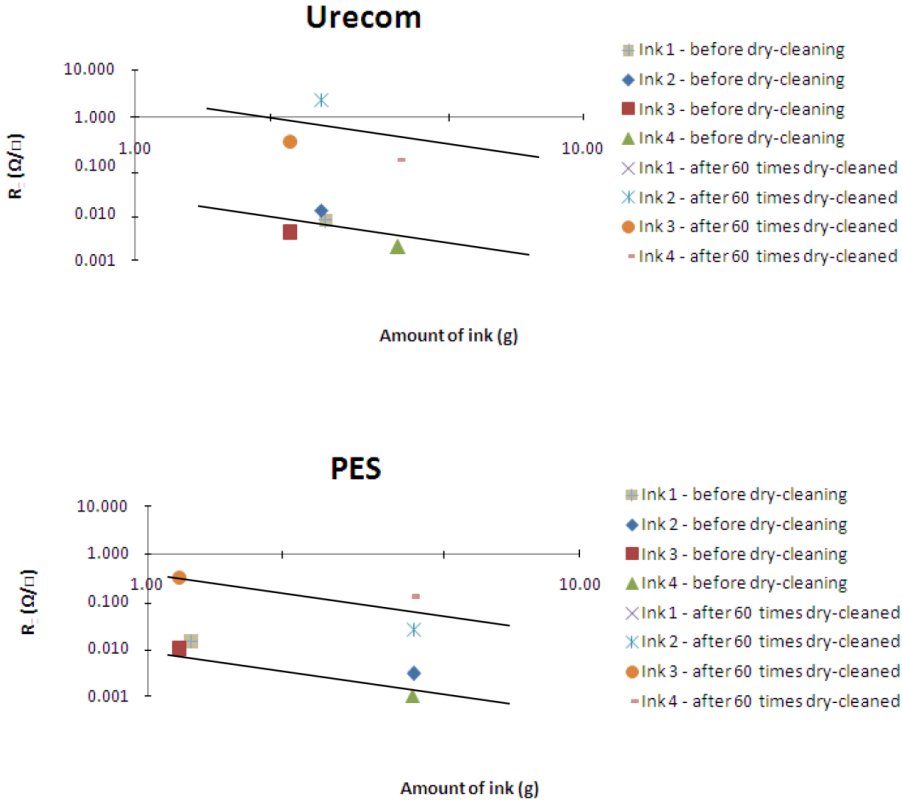

Figure 3.6 Square resistances versus the amount of ink before and after dry-cleaning on double logarithmic scale

In Figure 3.6 trendlines with a negative slope -1 have been added representing the relation $R_{\square}$ ~ 1/amount of ink, for physical reasons. For Urecom and PES (before and after dry-cleaning) the experimental data follow the trendlines.

Before dry-cleaning, it was observed that the amount of ink deposited on the substrate surface and the solid content of the ink (Table 2.2) play an important role in the conductivity: the higher these values, the lower the

square resistance $R_{\square}$ is. This can be seen for ***Urecom*** printed with ink 4 (Figure 7), which has the largest amount of ink (3.87 g) and the ink has the highest percentage of solid content (84-86% - Table 2.2), resulting in the lowest square resistance $R_{\square}$. However, the amount of ink and solid content are not enough to explain the conductivity of ink 1, 2 and 3 because the percentage of solid content of these three inks is very similar (around 70 %). It is possible, therefore, that the nominal sheet resistance of the inks may affect the resistance of the conductive flexible surfaces. The nominal sheet resistances of the inks as indicated by the producers are different: 0.012-0.015 Ω/□ for ink 1, <0.025 Ω/□ for ink 2, ink 4 and 0.011 Ω/□ for ink 3 at 25 µm dry coating thickness. In the case of ink 3, the smallest amount resulting in the lowest square resistance $R_{\square}$ can be explained by the lowest nominal sheet resistance. A closer look at inks 2 and 3 reveals that they have different amounts of ink (2.62 g and 2.22 g respectively) which should make it more likely that ink 2 has lower square resistance $R_{\square}$ but this does not turn out to be the case. Thus, this can only be assigned to the difference in nominal sheet resistance of ink 2 and 3.

The same situation pertains for nonwoven PES, where inks 2 and 4 have almost the same amount of ink (4.13 g for ink 2 and 4.12 g for ink 4) and almost the same nominal sheet resistance as indicated by the producer (<0.025 Ω/□ for both inks at 25 µm dry coating thickness). However, the square resistance $R_{\square}$ before dry-cleaning is different: 0.003 Ω/□ for ink 2 and 0.001 Ω/□ for ink 4. Here, the properties of the inks are different. The solid content is 73.5-76% for ink 2 and 84-86% for ink 4 and the resins are PES for ink 2 and epoxy for ink 4. So, higher the solid content is, the lower the square resistance $R_{\square}$ will be.

PES printed with ink 3, same as Urecom printed with ink 3, has the lowest amount of ink (1.18 g), before dry-cleaning, compared with ink 1 and (1.26 g) and the lowest square resistance $R_{\square}$ (before dry cleaning). The percentage of solid content here is approximately the same (around 70%) but the nominal sheet resistance indicated by the producer, 0.012-0.015 Ω/□ for ink 1 and 0.011 Ω/□ for ink 3 at 25 µm dry coating thickness are different.

So as it was discussed above the amount of ink, the solid content and the sheet resistance are very important and affect the conductivity level: the thicker the layer, the lower the square resistance [18, 19].

After dry-cleaning through the 60 cycles, it was observed that the type of resin also has a significant effect on electroconductive flexible substrate. ***Urecom*** printed with ink 4, which has epoxy resin, proved to have the lowest square resistance $R_{\square}$.

This also explains the behaviour of the ***nonwoven PES*** substrate printed with inks 2 (PES resin) and 4 (epoxy resin). Before dry-cleaning, the flexible substrate printed with ink 4 (epoxy resin) showed the lower resistance (0.001 Ω/□ versus 0.010 Ω/□ for ink 2). After 60 dry-cleaning cycles, however, the lower resistance was shown by the sample printed with ink 2 (PES resin - 0.025 Ω/□ versus 0.125 Ω/□ for ink 4). Before dry-cleaning, the amount of ink was approximately the same (4.12 g for ink 4 and 4.13 g for ink 2), and the nominal sheet resistance indicated by the producer was the same (≤0.025 Ω/□ at 25μm dry coating thickness). It is thus clear that, as well as the amount of ink and properties of the ink such as solid content and sheet resistance, the type of resin influences the resistance after dry cleaning.

3.4 Conclusions

In this study, we screen-printed with four different silver-based inks (two with PES resin and two with Epoxy resin) on polyurethane foam and nonwoven PES. The square resistance $R_{\square}$ was measured after each 5 cycles of dry-cleaning up to 60 cycles in order to provide an evaluation of the conductivity of the four inks with respect to each substrate. The values of the square resistance $R_{\square}$ ranged from 0.025 to 2.263 Ω/□.

We can conclude that the silver conductive inks available on the market for electronic applications give rise to square resistance $R_{\square}$ values comparable to the nominal values mentioned by the suppliers. However, it is necessary to cover them with a protective layer (e.g. a polyurethane layer) to maintain electrical properties after dry-cleaning. PES based inks combine best with PES substrates, whereas epoxy based inks give better results with polyurethane foam, so a good combination between ink and substrate needs to be found in order to obtain a high quality electroconductive substrate which can be integrated into garments and easily maintained.

3.5 References

1. *Interactive Electronic textile development: A review of technologies.* **D. Meoli, T. May-Plumlee.** 2, s.l. : Journal of Textile and Apparel Technology and Managment, 2002, Vol. 2.

2. *A smart sensor for induced stress measurement in automotive textiles .* **E. Drean, L. Schacher, F. Bauer, D. Adolphe.** 6, 2007, Journal of the Textile Institute, Vol. 98, pp. 523-531.

3. *Electroactive polymer-based devices for e-textiles in biomedicine.* **F. Carpi, D. De Rossi.** 3, 2005, IEEE Transactions on Information Technology in Biomedicine, Vol. 9, pp. 295-318.

4. *Electrical characterization of Transmission Lines on Nonwoven Textile substrates.* **C. R. Merritt, B. Karaguzel, T-H. Kang, J. M. Wilson, P. D. Franzon, H. T. Nagle, B. Poudeyhimi, E.Grant.** 2005, Material Research Society, Vol.870E.

5. *Thick-film textile-based amperometric sensors and biosensors.* **Y. L. Yang, M. C. Chuang, S. L. Lou, J. Wang.** 2010, Royal Society of Chemistry, pp. 135, 1230-1234.

6.*Electrical charachterisation of screen – printed circuits on the fabric.* **Y. Kim, H. Kim, H.J. Yoo,.** 2010, IEEE Transaction on Advanced Packaging, Vol. 33, No. 1.

7. *Flexible, durable printed electrical circuits.* **B. Karaguzel, C. R. Merritt, T. Kang, J. M. Wilson, H. T. Nagle, E. Grant, B. Polurdeyhimi.** 1, sl : The Journal of the Textile Institute, 2009, Vol. 100, pp. 1-9. 1754-2340.

8. *The characterization of electrically conductive silver ink patterns on flexible substrates.* **S. Merilampi, T. Laine-Ma, P. Ruuskanen.** 2009, Microelectronics Reliability 49, pp. 782-790.

9. *Screen-printed textile transmission lines.* **I. Locher, G.Tröster.** 2007, Textile Research Jornal 77, pp. 837-842.

10. Electrical charachterisation of conductive ink layers on textile fabrics: model and experimental results. **J. Rius, S. Manich, R. Rodriguez, M. Ridao.** s.l. : http://dit.upc.es/lpdntt/rius/web/paper29.pdf. visited in February 2012.

11. Printed Textile Antennas for Off-body Comunication. **C. Hertleer, L. V. Langenhoven, H. Rogier.** sl : Advances in Science and Technology, 2008, Vol. 60, pp. 64-66.

12. *A control technology evaluation of state-of-the art, perchloroethylene dry-cleaning machines.* **G. S. Earnest.** 5, 2002, Applied Occupational and Environmental Hygiene, Vol. 17, pp. 352-359.

13. *http://www.tsa-uk.org/.* **TSA.**

14. *A history of dry cleaners and sources of solvent releases from dry cleaning equipment.* **J. H. Lohman.** 2002: sn, Environmental Forensics, Vol. 3, pp. 35-58.

15. *MR-1 surface resistance meter.* visited in February 2012 http://www.schuetzmesstechnik.de/de/pdf/Ken-MR1.pdf.

16. *A method of measuring specific resistivity and Hall effect of disc of arbitrary shape.* **L. J. Van Der Pauw.** 1958, Philips Research Reports, Vol. 13, pp. 1-9.

17. Life Cycle Assessment Environmental profile of cotton and polyester-cotton fabrics. **E. M. Kalliala, P. Nousiainen.** *AUTEX Research Journal* 1999; 1: 8-20.

18. Inkjet printing of conductive patterns on textile fabrics. **S. M. Bidoki, D. McGorman, D. M. Lewis, M. Clark, G. Horler, R. E. Miles.** *AATCC Rev*. 2005; 5: 11.

19. Technologies for System-on-Textile. **I. Locher** 2006; 165: ISBN 3-86628-061-0.

4

The inability of four-point method to measure anisotropy of printed textile substrates

This chapter describes the four-point probe and the Van Der Pauw method to measure the anisotropic properties of the electroconductive textiles. In the end it was proved both theoretically and experimentally that no anisotropy can be detected with the collinear contacts of the four-point probe.

This chapter is based on the publication
About the collinear 4-point probe technique´s inability to measure the resistivity of anisotropic electroconductive fabrics
On 25 April 2012 accepted to be published in Textile Research Journal

TABLE OF CONTENTS

4.1 Introduction

The four-point probe method is an easy method to measure the sheet conductivity of conducting layers [1]. The most common configuration is to have four collinear contacts. The outer two contacts are used for the electric current supply whereas the remaining contacts are used to detect the voltage drop. Using four contacts instead of just two eliminates the influence of parasitic contact resistances caused by surface oxidation or moisture because almost no current flows through the voltage sensing contacts. An possible contact resistance will not cause any additional voltage drop so that the correct sheet resistance will be measured.

Nowadays four-point probe equipment is commercially available. The probe contains the four contacts and has to be pressed on the conducting layer to measure. The sheet resistance is then displayed. The measurement can be repeated on several points of the sheet so that possible non homogeneities can be detected. The only condition for a correct measurement is that the conducting layer may not be covered by an insulating protective layer.

A minor drawback is that the four-contact probe should not be too close to the boundaries of the sheet, because an error will be introduced. As a rule of thumb, the distance between the probe and the boundary should be at least three times the distance between the outer contacts. It must be remarked that the error is purely geometrical and one is able to calculate this error exactly by solving the potential equation in the sheet. This problem has been tackled in several papers a long time ago [2, 3].

In this chapter we investigate the possibility of using the four-point probe method to measure the anisotropic properties of the electric conductivity. Intuitively, one expects to measure something different if the probe is oriented in different directions on an anisotropic conducting sheet. It will be proved both theoretically and experimentally that no anisotropy can be detected with the four-point probe with the collinear contacts.

In order to have a reference value the Van Der Pauw method was used to measure the resistivities on thin conducting sheets [4]. This method was originally developed for thin conducting layers frequently used in electronics and microelectronics [5]. The method was then extended to investigate

anisotropic layers [6, 7]. Recently the Van Der Pauw method has been used to investigate electroconductive textile layers [8-11].

Only a few papers could be found in literature dealing with this topic. A mathematical analysis was published a long time ago [12]. Experimental work was published more recently buy Kanagawa et. al. [13]. An anisotropic surface state conductivity was created artificially by depositing In atom chains on a Si substrate. In this way a high anisotropic ratio of about 60 could be obtained.

For the experimental part of this chapter electroconductive layers have been screen-printed on textile substrates. The type of weave gives rise to different structures in the warp and weft directions, leading to anisotropy electric conductivities in the layer deposited on the fabric [11]. Anisotropic phenomena in textiles have been reported in several papers but limited to mechanical and optical properties [14-20]. Only a single paper was found related to anisotropic electric properties [21].

4.2 The four-point probe method for isotropic layers

Consider and infinite conducting sheet with a uniform thickness t_s and an electric conductivity σ. For practical purposes, it is more convenient to use the so called square or sheet resistance $R_{\square}$ defined by:

$$R_{\square} = 1 / (\sigma t_s) \quad (1)$$

$R_{\square}$ is the resistance value one should measure on a square shaped sample foreseen with two contacts along the opposite sides.

The four contacts of the probe labelled *A, B, C* and *D* are collinear and at an intermediate distance a (as shown in Figure 4.1). The contacts *A* and *D* are used to supply the current *I* whereas the voltage drop *V* will be sensed between *B* and *C*. If a current *I* is fed into the contact *A*, the potential distribution in the sheet will be given by:

$$\emptyset(x,y) = -\frac{R_{\square}I}{2\pi}\ln\sqrt{x^2 + (y - \frac{3a}{2})^2} \quad (2)$$

A similar expression can be written down for the current *I* extracted from the contact *D*. The potential is then found by superposition:

$$\emptyset(x,y) = \frac{R_{\square}I}{2\pi}[-\ln\sqrt{x^2 + (y - \frac{3a}{2})^2} + \ln\sqrt{x^2 + (y + \frac{3a}{2})^2}] \quad (3)$$

The voltage drop *V* is then obviously:

$$V = \emptyset\left(0, \frac{a}{2}\right) - \emptyset(0, -\frac{a}{2}) = \frac{R_{\square}I}{2\pi}[-\ln a + \ln 2a + \ln 2a - \ln a] = \frac{R_{\square}I}{\pi}\ln 2 \quad (4)$$

Hence:

$$R_{\square} = \frac{V}{I}\frac{\pi}{\ln 2} = 4.532\ \frac{V}{I} \quad (5)$$

π/ln 2 = 4.532 is the so called correction factor. Most of equipments take this correction automatically into account [22].

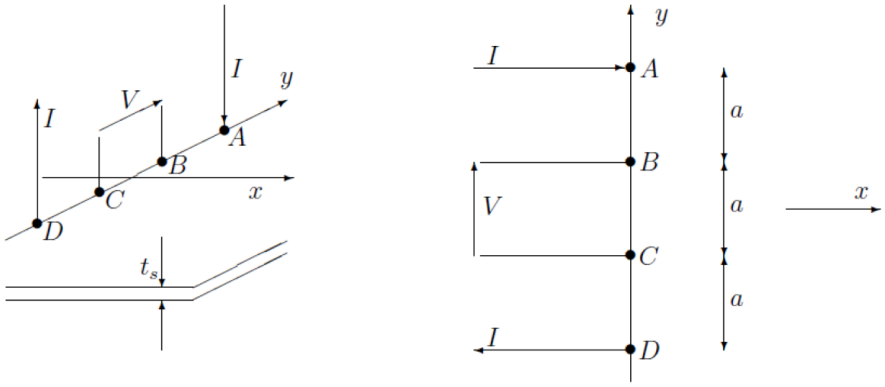

Figure 4.1 Collinear configuration of the four contact probe.

If the probes are too close to the boundary (5) is not valid any more. The potential distribution can still be found numerically for an arbitrary geometry. For a straight boundary an analytical approach is still possible by introducing image sources [5]. The equation for the potential distribution is then more complicated than (3) and different correction factors are obtained.

4.3 The four-point probe method for anisotropic layers

Anisotropy means that different resistances are measured in the *x* and the *y* direction:

$$R_{xx,\square} \text{ and } R_{yy,\square}$$

Without loss of generality we can assume that the major axes of the resistivity tensor are along the *x* and *y* axes. Hence, the non diagonal coefficient $R_{xy\square}$ is then zero. For woven textile substrates the main axes usually coincide with the weft (*x*) and warp (*y*) directions because the physical properties differ in both directions due to the fabrication process (for example the number of yarns/cm).

Imagine the same layout as shown in Figure 4.1. For an isotropic layer, the potential ∅ satisfies the Laplace equation:

$$\nabla^2 \emptyset = \frac{\partial^2 \emptyset}{\partial x^2} + \frac{\partial^2 \emptyset}{\partial y^2} = 0 \tag{6}$$

Needless to say that (2) and (3) are solutions of (6). In case anisotropy exists, the Laplace equation is not more valid and must be replaced by:

$$\frac{1}{R_{xx,\square}} \frac{\partial^2 \emptyset}{\partial x^2} + \frac{1}{R_{yy,\square}} \frac{\partial^2 \emptyset}{\partial y^2} = 0 \tag{7}$$

In order to solve equation (7), an affine transformation has to be used to map the (*x, y*) plane into the (*x', y'*) one:

$$x' = x \qquad y' = y\sqrt{\frac{R_{yy,\square}}{R_{xx,\square}}} \tag{8}$$

For the particular case that $R_{yy,\square} = 4R_{xx,\square}$ one gets *x'* = *x* and *y'* = 2*y*. Hence the four contacts will be now at a distance 2*a* from each other in the (*x',y'*) plane.

Using the affine transformation (8) for the equation (7), one gets:

$$\frac{\partial^2 \emptyset}{\partial x'^2} + \frac{\partial^2 \emptyset}{\partial y'^2} = 0 \tag{9}$$

which is the Laplace equation, only valid in the (x', y') plane. Due to the transformation (8), the layer in the (*x', y'*) plane has a uniform resistivity $R_{xx,\square}$.

A current *I* is fed through the contacts *A* and *D* in the (*x, y*) plane. This current has to be transformed into a current *I′* in the (*x′, y′*). There is no a priori reason why *I′* = *I*.

In order to find the exact relation between *I* and *I′*, one has to start with the potential distribution due to a current *I′* in the (*x′, y′*) plane:

$$\emptyset(x', y') = \frac{R_{xx,\square} I'}{2\pi} \ln\left[\sqrt{x'^2 + y'^2}\right] \tag{10}$$

Without loss of generality, it was assumed in the above equation (10) that the current *I′* was fed into the origin *x′* = *y′* = 0. After transforming back to the (*x, y*) plane, one gets for the potential distribution:

$$\emptyset(x, y) = \frac{R_{xx,\square} I'}{2\pi} \ln\left[\sqrt{x^2 + \frac{R_{yy,\square}}{R_{xx,\square}} y^2}\right] \tag{11}$$

In order to find the value of the current *I′*, we need to know the current densities in the *x* and *y* direction:

$$J_x = -\frac{1}{R_{xx,\square}} \frac{\partial \emptyset}{\partial x} = \frac{I'}{2\pi} \frac{x}{x^2 + \frac{R_{yy,\square}}{R_{xx,\square}} y^2} \tag{12}$$

$$J_y = -\frac{1}{R_{yy,\square}} \frac{\partial \emptyset}{\partial y} = \frac{I'}{2\pi} \frac{y}{x^2 + \frac{R_{yy,\square}}{R_{xx,\square}} y^2} \tag{13}$$

We consider now a square shaped region around the origin. The total current through the boundary of this square must be obviously equal to *I*, which can also be found by integrating the current densities (12) and (13). Due to symmetry it is sufficient to consider only one quarter of this region indicated by *EFG* in Figure 4.2. We first integrate the current density J_x along *EF* in order to obtain the partial current I_x:

$$I_x = t_s \int_E^F J_x dy = \frac{I'}{2\pi} \int_0^{\varepsilon} \frac{\varepsilon dy}{\varepsilon^2 + \frac{R_{yy,\square}}{R_{xx,\square}} y^2} = \frac{I'}{2\pi} \sqrt{\frac{R_{xx,\square}}{R_{yy,\square}}} \int_0^{\frac{R_{yy,\square}}{R_{xx,\square}}} \frac{dv}{1+v^2} = \frac{I'}{2\pi} \sqrt{\frac{R_{xx,\square}}{R_{yy,\square}}} \arctan\left(\sqrt{\frac{R_{yy,\square}}{R_{xx,\square}}}\right)$$

(14)

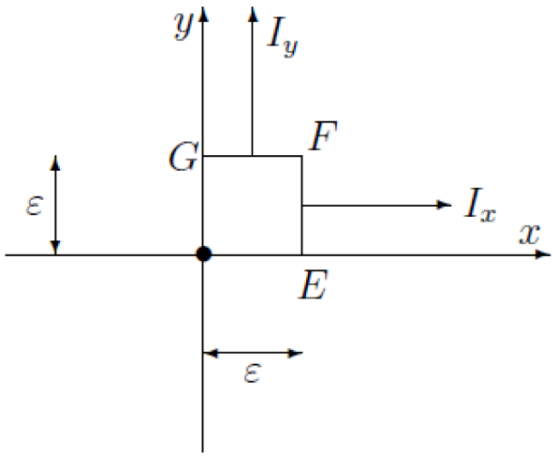

Figure 4.2 Diagram to calculate the partial current I_x and I_y.

In a similar way the partial current I_y flowing through *GF* is evaluated as:

$$I_y = t_s \int_G^F J_y dx = \frac{I'}{2\pi} \int_0^{\varepsilon} \frac{\varepsilon dx}{x^2 + \frac{R_{yy,\square}}{R_{xx,\square}} \varepsilon^2} = \frac{I'}{2\pi} \sqrt{\frac{R_{xx,\square}}{R_{yy,\square}}} \arctan\left(\sqrt{\frac{R_{xx,\square}}{R_{yy,\square}}}\right) \quad (15)$$

Taking into account that:

$$\arctan \alpha + \arctan 1/\alpha = \pi/2 \quad (16)$$

The sum of the two partial currents I_x and I_y is given by:

$$I_x + I_y = \frac{I'}{2\pi} \sqrt{\frac{R_{xx,\square}}{R_{yy,\square}}} \left[\arctan\left(\sqrt{\frac{R_{yy,\square}}{R_{xx,\square}}}\right) + \arctan\left(\sqrt{\frac{R_{xx,\square}}{R_{yy,\square}}}\right)\right] = \frac{I'}{4} \sqrt{\frac{R_{xx,\square}}{R_{yy,\square}}} \quad 17)$$

Taking into account that $I = 4(I_x + I_y)$, we finally obtain the relation between I and I':

$$I = I' \sqrt{\frac{R_{xx,\square}}{R_{yy,\square}}} \tag{18}$$

The potential distribution (11) is then:

$$\emptyset(x,y) = -\frac{I}{2\pi}\sqrt{R_{xx,\square}R_{yy,\square}}\ln\left[\sqrt{\mathrm{x}^2 + \frac{R_{yy,\square}}{R_{xx,\square}}\,\mathrm{y}^2}\,\right] \tag{19}$$

Remark that (19) is the potential distribution due to a current *I* injected in the origin, $x = y = 0$.

When a current *I* is injected in *A* and extracted from *D*, one obtains the following potential distribution:

$$\emptyset(\mathrm{x},\mathrm{y}) = -\frac{\mathrm{I}}{2\pi}\sqrt{\mathrm{R_{xx,\square}R_{yy,\square}}}\left[\ln\sqrt{\mathrm{x}^2 + \frac{\mathrm{R_{yy,\square}}}{\mathrm{R_{xx,\square}}}\left(\mathrm{y} - \frac{3\mathrm{a}}{2}\right)^2} - \ln\sqrt{\mathrm{x}^2 + \frac{\mathrm{R_{yy,\square}}}{\mathrm{R_{xx,\square}}}\left(\mathrm{y} + \frac{3\mathrm{a}}{2}\right)^2}\right] \tag{20}$$

The potential drop between the voltage sensing contacts *B* and *C* is then obviously:

$$\mathrm{V} = \emptyset\left(0,\frac{a}{2}\right) - \emptyset\left(0,-\frac{a}{2}\right) = \frac{I}{\pi}\ln 2\sqrt{R_{yy,\square}R_{xx,\square}} \tag{21}$$

With the four-point probe method one will measure the value of $\sqrt{R_{yy,\square}R_{xx,\square}}$ notwithstanding the fact that the four contacts are aligned along the *y* axis or any other direction.

If the four contacts are aligned along the *x* axis or any other direction, one can easily calculate that the same voltage drop (21) will be obtained. Hence, the conclusion is that it is not possible to detect electrical anisotropy with the four-point probe method. This statement has only been proved if the four are collinear, which is the most common configuration in practice.

Even when the contacts are not equidistant but still collinear, the voltage drop *V* remains proportional to $\sqrt{R_{yy,\square}R_{xx,\square}}$ irrespective of the orientation of the probe.

The conclusion is that the four-point probe method can only be used to measure the geometric mean $\sqrt{R_{yy,\square}R_{xx,\square}}$ of the two resistance values $R_{xx,\square}$ and $R_{yy,\square}$.

4.4 Square resistance measured with both methods

For the experimental part of this work, electric conducting inks have been screen-printed on several textile substrates. Two silver inks from SunChemical are applied in this study on textile materials such as Cotton/Polyester 2, Cotton 3, Viscose 2 and Polyester 3 (Table 4.1).

Table 4.1 Properties of applied woven textiles

Textile materials	The type of weave	Warp (threads/cm)	Weft (threads/cm)
Cotton/Polyester 2	twill 3/1	42	29
Cotton 3	twill 4/1	47	26
Viscose 2	plain 1/1	20	19
Polyester 3	twill 2/1	57	46

The conducting layers deposited on the fabrics were all square shaped with dimension 6 x 6 cm^2 (Figure 4.3). The samples were cured in the oven, since the curing process is essential to remove the organic solvents from the deposited ink and to guarantee a stable conducting layer on the substrate.

Four electroconductive contacts *P, Q, R* and *S* in the corners were provided for the resistivity measurements according to the Van Der Pauw method [8] and [11].

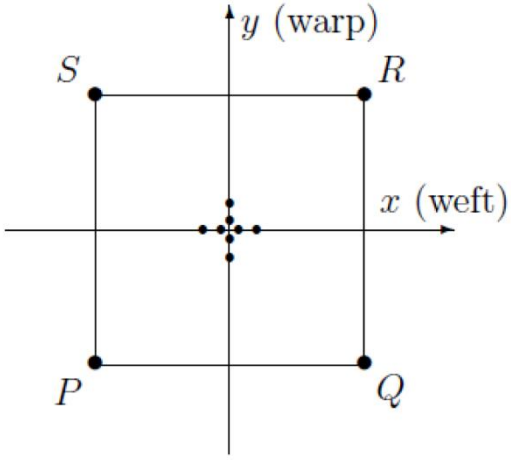

Figure 4.3 Square resistance measured in *x* and the *y* directions.

First of all, a current I_{PQ} was supplied through the contacts *P* and *Q* and the voltage drop V_{RS} was measured. Secondly, a current I_{PS} was fed through *P* and *S* and the resulting voltage drop V_{QR} between *Q* and *R* was recorded. From the relations V_{RS} / I_{PQ} and V_{QR} / I_{PS} the sheet resistivities $R_{xx,\square}$ and $R_{yy,\square}$ can be found [11]. In case of anisotropic conductivity one will get that $V_{RS} / I_{PQ} \neq V_{QR} / I_{PS}$ for a square shaped sample. For the four-point probe measurements the probe was placed in the middle of the sample, once along the weft and once along the warp direction.

The measurements are listed in Table 4.2. Cotton/Polyester 1 and 2 means the textiles with label Cotton/Polyester with the conductive ink 3 and 4 screen-printed on them.

Table 4.2 Measured values $R_{xx,\square}$ and $R_{yy,\square}$

Textile materials	Van Der Pauw method			four-point method	
	$R_{xx,\square}$	$R_{yy,\square}$	$\sqrt{R_{xx,\square}R_{yy,\square}}$	$R_{xx,\square}$	$R_{yy,\square}$
	(Ω)	(Ω)	(Ω)	(Ω)	(Ω)
Cotton/Polyester 1	*0.014	0.018	0.0158	0.01640	0.01691
Cotton/Polyester 2	*0.035	0.015	0.0229	0.01066	0.01117
Cotton 1	*0.007	0.023	0.0127	0.01436	0.01326
Cotton 2	*0.028	0.036	0.0317	0.02669	0.02718
Viscose 1	*0.019	0.014	0.0163	0.01649	0.01708
Viscose 2	0.007	0.009	0.0079	0.01062	0.01003
Polyester 1	*0.026	0.015	0.0197	0.01984	0.02010
Polyester 2	0.009	0.007	0.0079	0.00833	0.00858

The results clearly show electric anisotropy especially for those samples that are marked with asterisk (*).

On the same samples, four-point probe measurements were carried out as well. The probe was oriented in the *x* (weft) and the *y* (warp) directions. These results are also listed in Table 4.2 and it is clear that there is almost no difference at all for most of the samples. First of all the four-point probe results give the same value (within 5%) in the x and y direction. Moreover the values are quite close to the value $\sqrt{R_{xx,\square}R_{yy,\square}}$ obtained from the Van Der Pauw measurements. These experimental results are in full agreement with the theoretical analysis outlined in the foregoing section.

Kanagawa et. al. obtained values of 4.4 kΩ and 5.4 kΩ with the collinear probe arrangement [13]. With the square probe arrangement, the anisotropy could be detected, giving the values of 0.17 kΩ and 10.9 kΩ (anisotropy ratio of 60). The numerical value of $\sqrt{R_{xx,\square}R_{yy,\square}} = \sqrt{0.17 \times 10.9} = 1.32\ \mathrm{k\Omega}$ which is quite different from 4.4 kΩ or 5.4 kΩ. A possible explanation might be that the structure of In atom chains on a Si substrate cannot be modelled by a two dimensional conducting sheet because the Si is conducting as well.

4.5 Conclusions

In this chapter a theoretical and experimental investigation of measuring the square resistance on anisotropic electroconductive textiles is presented. Two methods are introduced the one of collinear four-point probe and the second, used as a reference value, the VDP method. It was proved, theoretically and verified experimentally, that no anisotropy can be detected with the collinear four-point probe method.

4.6 References

1. http://www.astm.org/Standards/F390.htm

2. *Magnetoconductive correction factors for an isotropic Hall plate with point sources.* **M. Buehler and G. Pearson.** 1966, Solid State Electronics, Vol. 9, pp. 395-407.

3. *Measurement of the resistivity of a thin square sample with a square four probe array.* **M. Buehler and R. Thurber.** 1977, Solid State Electronics, Vol. 20, pp. 403-406.

4. *A method of measuring specific resistivity and Hall effect of disc of arbitrary shape.* **L. J. Van Der Pauw.** 1958, Philips Research Reports, Vol. 13, pp. 1-9.

5. *Electrical and galvanomagnetic measurements on thin films and epilayers.* **H.H. Wieder.** 1976, Thin Solid Films, Vol. 31, pp. 123-138.

6. *Note on four point resistivity measurements on anisotropic conductors.* **J. D, Wasscher.** 1961, Philips Research Reports, Vol. 16, pp. 301-306.

7. *Extension of Van Der Pauw´s theorem for measuring specific resistivity in discs of arbitrary shape to anisotropic media.* **W. L. V. Price.** 1972, J. Phys. D: Appl. Phys., Vol. 5, pp. 1127-1132.

8. *The Van Der Pauw method for sheet resistance measurements of polypyrrole coated woven fabrics.* **J. Banaszczyk, G. De Mey, A. Schwarz, L. Van Langenhove.** 2010, Journal of Applied Polymer Science, Vol. 117, pp. 2553-2558.

9. *Current distribution modelling in electroconductive fabrics.* **J. Banaszczyk, G. De Mey, A. Schwarz and L. Van Langenhove.** 2009, Fibres and Textiles in Eastern Europe, Vol. 17, pp. 28-33.

10. *Electronically modified single wall carbon nanohorns with iodine absorption.* **F. Khoerunnisa, T. Fujimori, T. Itoh, H. Kamok, T. Ohba, H. Yudasaska, S. Lijima and K. Kaneko.** 2011, Chemical Physics Letters, Vol. 501, pp. 485-490.

11. *Van Der Pauw method for measuring resistivities of anisotropic layers printed on textile substrates.* **I. Kazani, G. De Mey, C. Hertleer, J.**

Banaszczyk, A. Schwarz, G. Guxho and L. Van Langenhove. 2011, Textile Research Journal, Vol.81 (20), pp. 2117-2124.

12. *Use of probes for measuring the electrical conductivity of anisotropic plate.* **V. M. Tatarnikov**. 1970, Measurement Techniques, Vol. 13, pp. 877-881.

13. *Anisotropy in conductance of a square one dimensional metallic surface state measured by a square micro four point probe method.* **T. Kanagawa, R. Hobana, I Matsuda, T. Tanikawa, A. Natori and S. Hasegawa.** 2003, Physical Review Letters, 91: 036805-1-4.

14. Bilinear approximation of anisotropic stress-strain properties of woven fabrics. **Ng. Sun-pui, Ng. Roger, Yu. Winnie.** 4, 2005, RJTA, Vol. 9, pp. 50-56.

15. *Prediction of surface uniformity in woven fabrics through 2-D anisotropic measures. Part I: Definition and theoretical model.* **M. W. Suh, M. Günay, W. P. Jasper.** 2007, Journal of the Textile Institute, Vol. 98, pp. 109-116.

16. *Anisotropy of woven fabric deformation after stretching.* **R. Klvaityle, V. Masteikaite.** 2008, Fibres and Textiles in Eastern Europe, Vol. 16, pp. 52-56.

17. *Anisotropic light transmission properties of plain woven fabrics.* **Y. Yazaki, M. Takatera, Y. Shimizu.** 10, 2004, Sen'I Gakkaishi, Vol. 60, pp. 281-286.

18. *Experimental and numerical analyses of fabric off-axes tensile test.* **R. Zouari, S. B. Amar, A. Dogui.** 2008, Journal of Textile Institute, Vol. 101, pp. 58-68.

19. *Effect of woven fabric anisotropy on drape behaviour.* **V. Sidabraitė, V. Masteikaitė.** 1, 2003, Material science (Medziagotyra), Vol. 9, pp. 111-115. 1392-1320.

20. *Measuring method of multidirectional force distribution in a woven fabric.* **I. Frontczak-Wasiak, M. Snycerski, Z. Stempien, H. Suszek.** 2004, Fibres and Textiles in Eastern Europe, Vol. 12, pp. 48-51.

21. *Anisotropy in electric properties of fabrics containing new conductive fibers.* **J. Azoulay.** 1988, IEEE Transactions on Electrical Insulation, Vol. 23, pp. 383-386.

22. *Accurate geometry factor estimation for the four point probe method using COMSOL multiphysics.* **A. Kalavagunta, R. A.Weller.** 2005, Excerpt from the proceedings of the COSMOL multiphysics user´s conference.

5

Anisotropic behaviour of printed textile substrates

This chapter is about the anisotropic behaviour of electroconductive textiles printed with silver-based ink. Using the Van Der Pauw method for electrical resistivity measurements in thin layers, it was observed that the screen-printed layers showed anisotropic behaviour. In order to be able to interpret the measurements correctly, a mathematical analysis of the measuring method has been established.

This chapter is based on the publication
Van Der Pauw method for measuring resistivities of anisotropic layers printed on textile substrates
In Textile Research Journal, Volume 81(20), p 2117-2124, 2011

TABLE OF CONTENTS

5.1 Introduction

The Van Der Pauw (VDP) method was established a long time ago as a special technique to measure the resistivity of thin conducting layers, in the direct current (DC) regime [1]. The basic idea is that four contacts can be placed arbitrarily on the boundary of the sample: two contacts are used for the current supply, while the remaining contacts are used for voltage sensing only, so that the parasitic contact resistance will have no influence. A major advantage is that, in addition, arbitrary shapes of the sample can be used. There is not a priori a need to make a sample with a well-defined shape and positioning of the contacts.

Recently, the VDP method has been extended to measure the sheet resistivity of electroconductive textile samples [2]. Strictly speaking, the VDP method can only be used for homogeneous and uniform resistive layers. Textiles are not perfectly uniform electrically conducting layers due to their structure (such as woven or knitted) and also due to the contact resistance between neighboring yarns and their numerous contact points at the crossing between warp and weft ones. Nevertheless, it was observed that the VDP method could be used successfully in many cases to measure the sheet resistance of textile fabrics [3]. Different properties, such as the distance between neighbouring yarns in the weft and warp directions give rise to an anisotropic behaviour.

In this contribution, conducting silver-based inks were screen-printed on textile fabrics and the electrical properties were investigated. Typically, textiles are characterised by tensile tests, bending and shearing. An anisotropic effect has been observed at several occasions. Theoretical analyses started with Peirce [4], who developed a geometrical model to analyse the weave structure. Weissenberg [5] observed the Poisson's effect in all directions. Then Kilby [6] determined the Young's modulus in all directions and measured the tensile properties of the woven textile substrates using Weissenberg's method. Several papers have been published about the experimental verification of the theoretical solution of the anisotropic tensile properties [7]. Textiles clearly show different mechanical properties in different directions or, in other words, they are anisotropic.

It has been assumed that the properties of a fabric are affected by the properties of the fibres and the yarns it is made of, giving rise to a notable anisotropic behaviour [8-14].

To our knowledge only one paper could be found dealing with anisotropic effects in the electrical properties of woven textile substrates with conductive fibres for electrostatic protection [15]. The anisotropy was caused by the selection of the yarns: the electroconductive yarns were only inserted in the weft direction.

In this chapter the VDP method is extended to the measurements of anisotropic layers on woven textile substrates, yielding different resistances in the *x*- and *y*-directions. Woven textiles used as substrates easily give rise to anisotropy due to the different properties in weft and warp direction (e.g. number of threads/cm)

The mathematical theory of this method will be outlined in the next section.

5.2 The Van Der Pauw (VDP) method for anisotropic layers

The deposition of conducting layers on a substrate is a well-established technology in electronics and microelectronics.

A popular technique is screen printing of electrically conducting pastes or inks on a ceramic substrate. These layers are usually characterised by the so called square resistance which is defined by:

$$R_{\square} = \varrho / t_s \qquad (1)$$

where ϱ is the resistivity of the material and t_s the thickness of the deposited layer. The name ´square resistance´ originates from the fact that if one deposits a layer in a square-shaped geometry provided with two contacts on two opposite sides, one will measure a resistance between these contacts that is exactly equal to the square resistance. Due to the fact that deposited layers have a very uniform thickness, it is more convenient to characterize a screen-printed layer by the square resistance than by the resistivity and the thickness, which are not so easy to measure.

If textiles are used as a substrate one has to face the problem that these substrates are not uniform in all directions. Due to the different threads in the weft (*x*) and warp (*y*) directions, these substrates have different properties in different directions or, in other words they are anisotropic [8-14]. As a consequence, electrically conducting layers screen-printed on them will show anisotropic properties as well. Different bulk resistivities ϱ_{xx} and ϱ_{yy} will be observed then. The corresponding square resistances are:

$$R_{xx\square} = \varrho_{xx} / t_s \quad \text{and} \quad R_{yy\square} = \varrho_{yy} / t_s \qquad (2)$$

The physical interpretation of $R_{xx,\square}$ and $R_{yy,\square}$ is the same. If a square-shaped layer is deposited with all sides parallel to the *x*- or *y*-axes, one will measure $R_{xx,\square}$ between two contacts on the sides parallel to the *y*-axis. Similarly, $R_{yy,\square}$ will be measured if the contacts are located on the other sides.

First of all it must be pointed out clearly that it is not possible to extend the VDP method for anisotropic layers still using an arbitrary geometry and arbitrarily placed contacts along the boundary. A theoretical analysis of the VDP method for anisotropic layers has been published by W. Price [16]. It was proved in this article that for arbitrary shapes only, the geometric mean of the resistivities, $\sqrt{R_{xx,\square} R_{yy,\square}}$, along the main axes could be measured. However, it will be shown in this contribution that for a rectangular-shaped sample with contacts situated in the four corners and with yarns being woven in the *x* (weft)- and *y* (warp)-direction, the VDP method can still be used, taking some modifications into account, which will be outlined in this chapter.

We consider a rectangular sample, as shown in Figure 5.1 (a), provided with four contacts *A*, *B*, *C* and *D*, in the corners.

For our analysis it is requested that the main axes of the resistivity tensor are the *x*- and *y*-axes.

This is quite straightforward to understand. The main axis of a tensorial quantity is also an axis of symmetry. Due to differences in weft and warp yarns and in types of weave, symmetry axes can only be found in the weft or warp directions.

For the analysis of thin layers it is more convenient to use the so-called square resistances $R_{xx,\square}$ and $R_{yy,\square}$ defined by Banaszczyk *et al*. [17]:

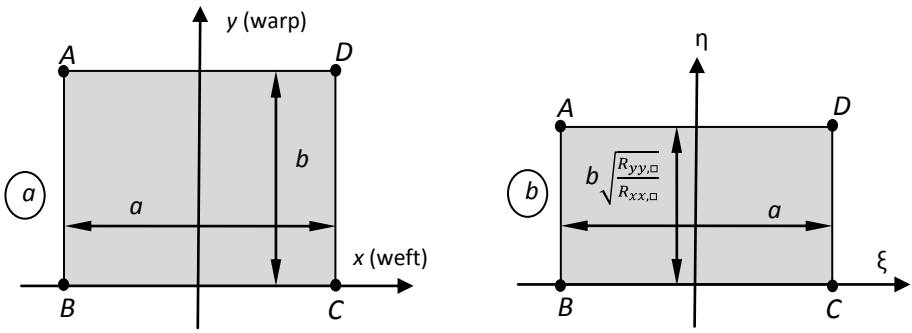

Figure 5.1 Affine transformations to convert an anisotropic layer (a) into an isotropic one (b).

The potential equation in an anisotropic layer is given by [18-19]:

$$\frac{1}{R_{xx,\square}}\frac{\partial^2 \emptyset}{\partial x^2}+\frac{1}{R_{yy,\square}}\frac{\partial^2 \emptyset}{\partial y^2}=0 \quad (3)$$

where Ø (x, y) denotes the potential distribution in the conducting layer.

In order to solve the equation (3), an affine transformation from the (*x*, *y*)-plane (Figure 5.1 (a)) into the (ξ, η)-plane (Figure 1b) has to be performed:

$$\xi = x$$

and

$$\eta = y\sqrt{\frac{R_{yy,\square}}{R_{xx,\square}}} \quad (4)$$

$R_{yy,\square}/R_{xx,\square}$ will henceforth be called *the anisotropy ratio*.

The most obvious way to measure the anisotropic properties is shown in Figure 5.2.

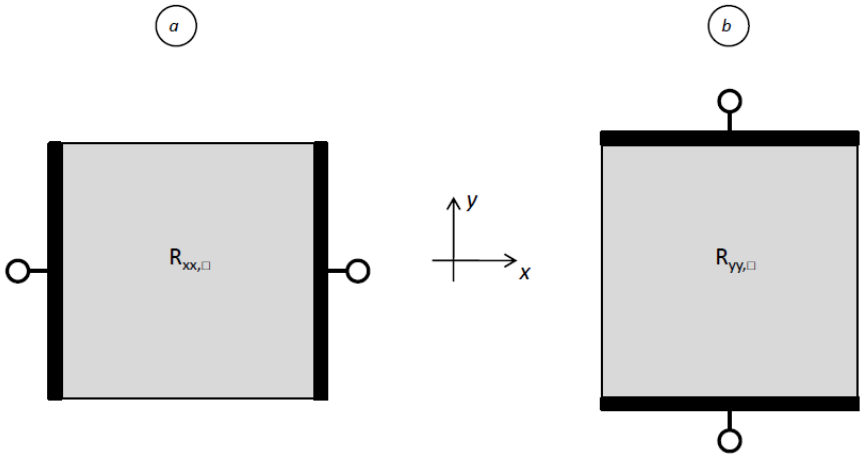

Figure 5.2 Square resistance measured in x- and y-directions.

Consider a square-shaped sample and put two metal bars along two opposite sides and measure the resistance between them. For the configuration of Figure 5.2 (a) one obtains $R_{xx,\square}$whereas $R_{yy,\square}$ will be obtained for other case (Figure 5.2 (b)). However, this simple approach has many shortcomings, making it impossible to use in practice. There is always a parasitic contact resistance between the metal bars and the underlying sample. These unknown resistances will disturb the measurements. With the Van Der Pauw method, the parasitic contact resistances will have no influence on the measurements, because four contacts are used, two for the current supply and two for the voltage sensing, although the parasitic contact resistances still exist.

In Figure 5.1 the particular situation has been drawn where $R_{yy,\square} < R_{xx,\square}$. Due to the affine transformation (4), the potential equation (3) is then replaced by:

$$\frac{\partial^2 \emptyset}{\partial \xi^2} + \frac{\partial^2 \emptyset}{\partial \eta^2} = 0 \qquad (5)$$

Equation (5) is nothing else than the Laplace equation, describing the potential in a homogeneous, isotropic and uniform conducting layer. These are exactly the conditions required to apply the VDP technique. Due to (4), the square resistance in the (ξ, η)-plane is just the square resistance $R_{xx,\square}$.

For the Laplace equation in a geometry, such as the rectangle in Figure 5.1(b), the potential distribution can be exactly determined using conformal mapping techniques described in several textbooks [20-21]. If ζ = ξ + j η is a complex variable, then any function w = u + j v = f (ζ) will be a complex variable too. Complex numbers are normally represented in a two-dimensional (2D) plane with the real and imaginary part on both axes.
If one has an arbitrary geometry in the ζ-plane one can calculate the function w = f (ζ) for every point zeta on the boundary. In such a way one creates another geometry in the w-plane, which is called a conformal mapping from the ζ- plane to the w-plane. One particular application of conformal mapping is that the Laplace equation is invariant for conformal mapping. If one can solve the Equation (5) in the ζ-plane, the equation has also been solved in the w-plane. If one finds that Ø = 1 in a point ζ, one has also that Ø = 1 in the corresponding w-plane. Sometimes the solution of the Laplace equation is rather straightforward in a particular geometry, such as a circle or a half-

infinite plane. By conformal mapping of this geometry into other ones, one has immediately the solution in other geometries, even when they look quite complicated at first sight. The geometry of Figure 5.1 (b) can be mapped into the half-infinite (*u, v*)-plane as shown in Figure 5.3 (a) and Figure 5.3 (b). The conformal transformation reads:

$$w = sn(\zeta, k) \tag{6}$$

where $\zeta = \xi + j\eta$ and $w = u + j v$ are the complex coordinates, sn denotes the elliptic sine function and k is the modulus [22]. In the complex w-plane the contact points A, B, C and D have the coordinates u = -1/k, u = -1, u = + 1 and u = +1/k respectively.

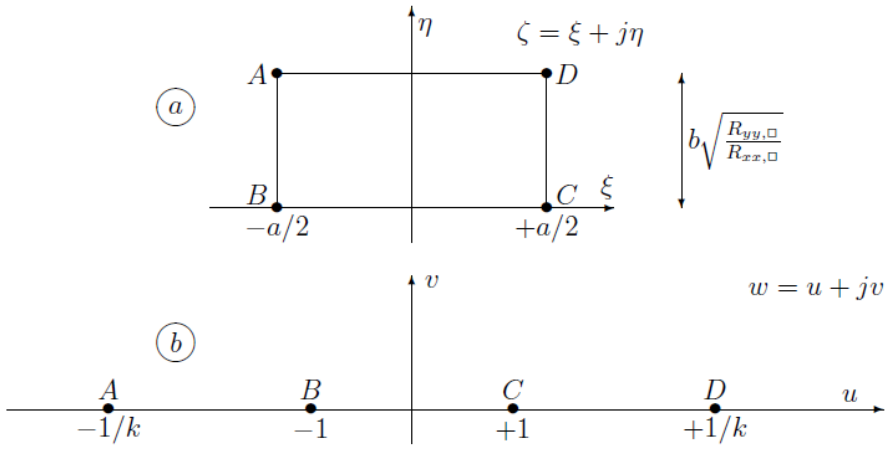

Figure 5.3 Conformal mapping from a rectangle (a) to a half- infinite plane (b).

The relation between the modulus *k* and the dimensions *a* and *b* of the rectangle in the ζ-plane is given by (Figure 5.3 (a)):

$$\frac{a/2}{b\sqrt{R_{yy,\square}/R_{xx,\square}}} = \frac{K(k)}{K(k')} = \frac{K(k)}{K(\sqrt{1-k^2})} \tag{7}$$

where $k' = \sqrt{1-k^2}$ is the complementary modulus. K(k) is the complete elliptic integral of the first kind defined by [23]:

$$K(k) = \int_0^{\pi/2} \frac{d\varphi}{\sqrt{1-k^2\sin^2\varphi}} \tag{8}$$

A plot of (7) is represented in Figure 5.4.

During the VDP measurements, first of all a current I_{AB} is supplied through the contacts *A* and *B* and the voltage drop V_{DC} across the contacts *D* and *C* is then measured. Similarly, a voltage drop V_{BC} is observed due to a current I_{AD}. Potentials, and hence voltage drops and, being invariant for conformal transformations, one can evaluate V_{DC} and V_{BC} from Figure 5.3 (b) only. One gets then:

$$V_{DC} = \frac{I_{AB}}{\pi} R_{xx,\square} \ln \frac{4/k}{(1/k+1)^2} \tag{9}$$

$$V_{BC} = \frac{I_{AD}}{\pi} R_{xx,\square} \ln \frac{(1/k-1)^2}{(1/k+1)^2} \tag{10}$$

From (9) and (10) one easily gets:

$$\alpha = \frac{V_{DC} / I_{AB}}{V_{BC} / I_{AD}} = \frac{\ln \dfrac{4/k}{(1/k+1)^2}}{\ln \dfrac{(1/k-1)^2}{(1/k+1)^2}} \tag{11}$$

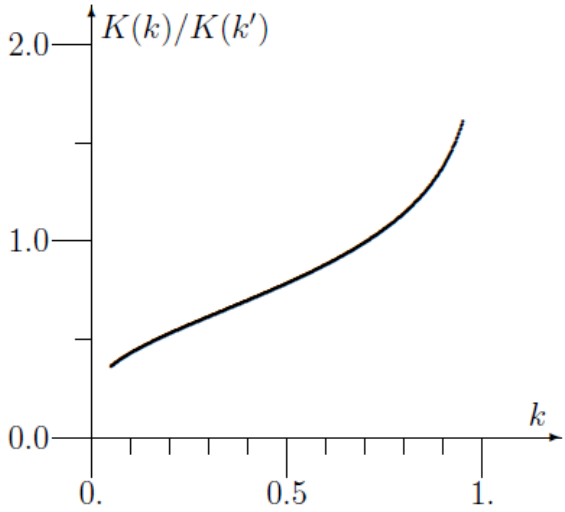

Figure 5.4 Plot of K (k)/K (k´) as a function of k.

or:

$$\frac{(1/k-1)^{2\alpha}}{(1/k+1)^{2\alpha}} = \frac{4/k}{(1/k+1)^2} \tag{12}$$

Equation (12) is a transcendental equation for the unknown *k*. It can be remarked that *α* is calculated from the experimental measurements. Once *k* has been determined, by numerically solving the equation (12), the anisotropy ratio $R_{yy,\square}/R_{xx,\square}$ can be found from (7).

By using the following transformation:

$$\lambda = (\frac{1-k}{1+k})^2$$

or

$$k = \frac{1-\sqrt{\lambda}}{1+\sqrt{\lambda}} \tag{13}$$

The transcendental equation (12) is then transformed into:

$$\lambda^{\alpha} + \lambda - 1 = 0 \tag{14}$$

Equation (14) can be easily solved numerically using the Newton-Raphson iteration method. The results are shown in Figure 5.5

If one replaces $\alpha \rightarrow 1/\alpha$ and $\lambda \rightarrow 1-\lambda$, the same equation as (14) is obtained. Hence, if $\lambda = 0.8349$ is the solution of (14) for $\alpha = 10$, the solution for $\alpha = 1/10$ will be given by $\lambda = 1 - 0.8349 = 0.1651$. Hence, only results for $\alpha > 1$ are displayed in Figure 5.5.

It was found that the results in Figure 5.5 can be very well approximated by the following function:

$$\lambda_{appr} = \frac{\alpha^{0.70416}}{\alpha^{0.70416}+1} \tag{15}$$

The function (15) is also shown in Figure 5.5. The relative error was found to be less than 0.5 % for the range $1<\alpha < 1000$.

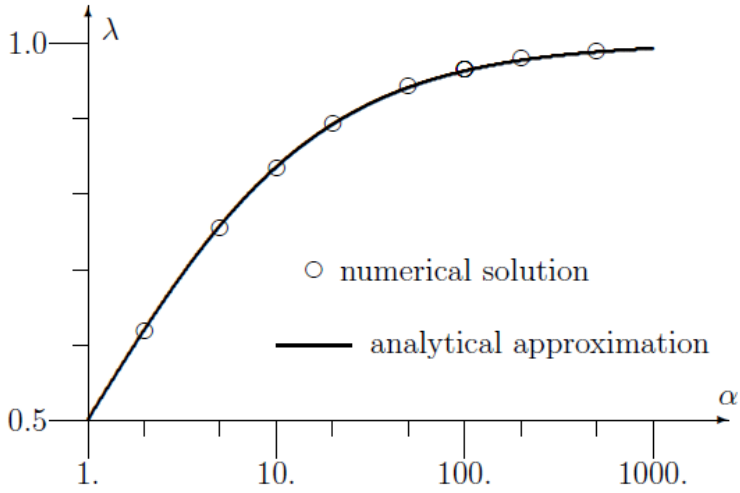

Figure 5.5 Numerical solution of the transcendental equation (14). The curve represents the analytical approximation (15).

The theoretical analysis presented so far can be repeated for other placements of the four contacts. As a consequence the formulae all have to be adjusted.

5.3 Square Resistance measured with the Van Der Pauw method

In our experiments silver-based ink 4 has been deposited by screen printing on different textile substrates (Table 2.2, Chapter 2). These silver-based inks are well known as polymer thick films in the field of hybrid microelectronics. When deposited on a ceramic substrate an isotropic conducting sheet is obtained.

The pattern of the screen-printed layer was a square with dimensions 6 x 6 cm^2. After printing the samples were cured in the oven at 120°C for 15 minutes, as given in the datasheet from the producer.

The materials of textile substrate used are polyamide, polyester, aramid and blended, as listed in Table 5.1

Table 5.1 Properties of different textile materials used

Woven textile material	Yarn Density		Warp yarn (Tex)	Weft yarn (Tex)	Type of weave	Thickness (mm)	Silver-based ink (g)
	Warp (threads/cm)	Weft (threads/cm)					
Polyamide	45	32	8.1	15.6	Twill 2/2	0.198	1.479
Polyester 4	21	22	35.5	35.6	Plain 1/1	0.478	1.827
Aramid	32	20	17.7 x 2	17.3 x 2	Plain 1/1	0.378	2.121
Cotton/Polyester 1	46	26	16.4	13.7	Twill 3/1	0.296	1.638
Cotton/Polyester 2	42	29	19.5	48.6	Twill 3/1	0.414	1.673
Polyester/Viscose	45	25	16.6	11.5	Twill 3/1	0.246	1.681

The difference in yarn density is in weft and warp directions, together with the type of weave, introduces an anisotropic textile structure, which can also be seen in Figure 5.6.

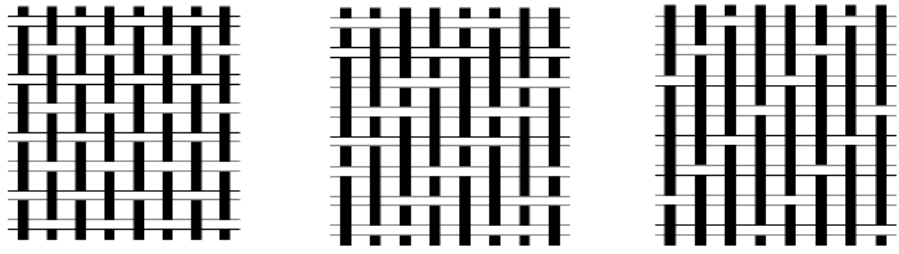

Figure 5.6 Layout of a plain 1/1 (a), twill 2/2 (b) and twill 3/1 (c) weave types.

All samples were provided with four contacts located in the corners of the conducting layers (Figure 5.7) in order to carry out the VDP measurements [16].

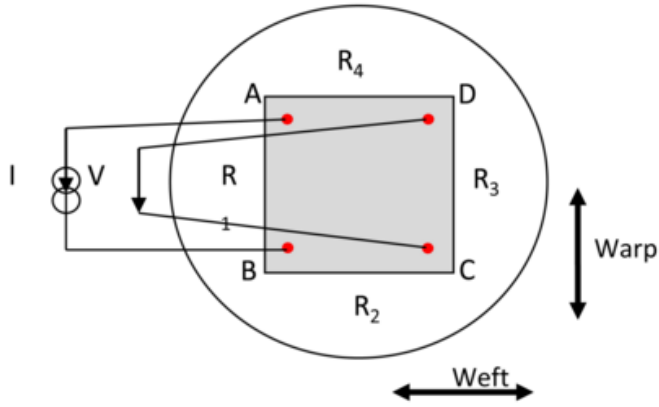

Figure 5.7 Scheme of Van Der Pauw measurement at the vertices.

The contacts are labelled *A*, *B*, *C* and *D* as indicated in Figure 5.1(a). First of all, a current I_{AB} was supplied through the contacts *A* and *B* and the resulting voltage drop V_{DC} across *D* and *C* was measured. Secondly, a current was fed through *A* and *D* and the voltage across the remaining contacts *B* and *C* was recorded. The resulting values of V_{DC}/I_{AB} and V_{BC}/I_{AD} are listed in Table 5.2.

By using (11) the value of α can be calculated.

The corresponding value for λ is calculated from (15) and the *k*-value from (13). From (7) it is then possible to find the anisotropic ratio $R_{yy,\square}/R_{xx,\square}$ which is listed in Table 5.2. An anisotropy ratio larger than 1 means that the resistivity in *y*-direction is larger than in *x*-direction; however, an anisotropy ratio lower than 1 indicates an anisotropy in the other direction. To compare the different textiles samples to find out which is most or least anisotropic, this should be taken into account.

Table 5.2 Measured values of V_{DC}/I_{AB} and V_{BC}/I_{AD} and calculated values for α and $R_{yy,\square}/R_{xx,\square}$

Textile material	V_{DC}/I_{AB}	V_{BC}/I_{AD}	α	$R_{yy,\square}/R_{xx,\square}$
Polyamide	0.009	0.005	1.800	**1.207**
Polyester	0.012	0.007	1.714	**1.187**
Aramid	0.005	0.003	1.667	**1.178**
Cotton/Polyester 1	0.016	0.005	3.200	**1.448**
Cotton/Polyester 2	0.008	0.005	1.600	**1.163**
Polyester/Viscose	0.007	0.006	1.167	**1.042**

The results of Table 5.2 indicate clearly that one should be careful with the interpretation of anisotropic effects. Let us have a closer look at the results obtained from the cotton/polyester 1 (twill 3/1) fabric. The two resistivity measurements V_{DC}/I_{AB} and V_{BC}/I_{AD} indicate a much higher voltage drop in the *y*-direction (for the same input current) giving rise to a value $\alpha = 3.2$. At first sight one would then have the impression that the layer is 3.2 times more resistive in the *y*-direction as compared to the *x*-direction. However, after a careful analysis as outlined in this chapter, the square resistance in the *y*-direction $R_{yy,\square}$ turns out to be only 1.448 times the value in the *x*-direction.

The polyester/viscose fabric (twill 3/1) shows the lowest anisotropy with a value of α=1.167. This means that this conductive layer seems 1.167 more resistive in *y*-direction than in *x*-direction, but an anisotropy ratio of only 1.042 reveals a much lower difference in square resistance.

These differences prove that the mathematical analysis is mandatory in order to get a correct interpretation of the experimental results.

Furthermore, Table 5.2 also discloses a systematic higher resistivity in warp direction (V_{DC}/I_{AB}) than in weft direction (V_{BC}/I_{AD}).

According to the one-way ANOVA results, the difference between the mean anisotropy ratio of the three textiles are statistically significant. The Duncan post-hoc test (Table 5.3), $p<0.05$, reveals that for the group of textile substrates with the twill 3/1 weave (Cotton/Polyester 1, Cotton/Polyester 2 and Polyester/Viscose), the Cotton/Polyester 1 has the highest anisotropy ratio of 1.448 and Polyester/Viscose has the lowest of 1.042. These three

textiles are very similar in type of weave and yarn density; however, the quantity of ink that forms the conductive layer differs. It seems that an increased amount of ink results in a lower anisotropy ratio.

Table 5.3 ANOVA table of means for groups in homogeneous subset

Ducan[a]

Textile materials	N	Subset for alpha = 0.05		
		1	2	3
Polyester/Viscose	3	1,042		
Cotton/Polyester 2	3		1,163	
Cotton/Polyester 1	3			1,1448
Sig.		1,000	1,000	1,000

According to the T test results, for the group of plain weave 1/1, the difference between the anisotropy ratio and the textiles are not statistically significant, $p>0.05$.

5.4 Conclusions

In this chapter an analysis of the potential distribution of anisotropic conducting layers has been presented in the case where the square resistance is measured using the VDP method. The method has been applied experimentally to investigate the electrical anisotropic effect in conducting layers screen-printed on various kinds of woven textile substrates. It was found that the mathematical analysis is mandatory to interpret the measurements correctly. This anisotropic behaviour is caused by the inherent anisotropic structure of the woven textile itself, on account of the warp and weft structure. Furthermore, the amount of ink deposited on the surface of woven textiles also influences the electrical properties.

5.5 References

1. *A method of measuring specific resistivity and Hall effect of disc of arbitrary shape.* **L. J. Van Der Pauw.** 1958, Philips Research Reports., Vol.13, pp.1-9

2. *The Van Der Pauw method for sheet resistance measurements of polypyrrole coated para aramide woven fabrics.* **J. Banaszczyk, G. De Mey, A. Schwarz, L. Van Langehove.** 2010, Journal of Applied Polymer Science, Vol.117, pp. 2553-2558

3. *Electronically modified single wall carbon nanohorns with iodine adsorption.* **F. Khoerunnisaa, T. Fujimorib, T. Itohb, H. Kanoha, T. Ohbaa, M. Yudasakac, S. Iijimac, K. Kaneko.** 2011, Chemical Physics Letters, 501, 4-6, pp. 485-490

4. *The geometry of cloth structure.* **F. T. Pierce.** 1937, Journal of the Textile Institute, 28, T45-96

5. *The use of a trellis model in the mechanics of homogenous materials***. K. Weissenberg.** 1949, Journal of the Textile Institute, 40, T89-110

6. *Planar stress-strain relationship in woven fabrics.* **W. F. Kilby.** 1963, Journal of the Textile Institute, 33, T9-27

7. *Bilinear approximation of anisotropic stress strain properties of woven fabrics.* **Ng. Sun-Pui, Ng. Roger, Yu Winnie.** 2005, Research Journal of Textile and Apparel, Vol. 9, pp. 50-56

8. Prediction of surface uniformity in woven fabrics through 2-D anisotropic measures. Part I: Definition and theoretical model. **M. W. Suh, M. Günay, W. P. Jasper.** 2007, Journal of the Textile Institute, Vol. 98, pp. 109-116

9. *Measuring technology of the anisotropic tensile properties of woven fabrics.* **JM. Zheng, M. Takatera, S. Inui, Y Shimizu.** 2008, Textile Research Journal, Vol. 78 (12), pp. 1116-1123

10. *Anisotropy of woven fabric deformation after stretching.* **R. Klvaityle, V. Masteikaite.** 2008, Fibres and Textiles in Eastern Europe, Vol. 16, pp. 52-56

11. *Anistropic light transmission properties of plain woven fabrics.* **Y. Yazaki, M. Takatera, M. Yoshio Shimizu.** 2004, Sen'I Gakkaishi, Vol. 60, pp. 41-46

12. *Experimental and numerical analyses of fabric off axes tensile test.* **R. Zouari, S. B. Amar, A. Dogui.** 2008, Journal of Textile Institute, Vol. 101, pp. 58-68

13. *Effect of woven fabric anisotropy on drape behaviour*. **V. Sidabraite, V. Masteikaite.** 2003, Materials Science, Vol. 9, pp. 111-115

14. *Measuring method of multidirectional force distribution in a woven fabric.* **I. Frontczak-Wasiak, M. Snycerski, Z. Stempien, H. Suszek.** 2004, Fibres and Textiles in Eastern Europe, Vol.12, pp. 48-51

15. *Anisotropy in electrical properties of fabrics containing new conductive fibers.* **J. Azoulay.** 1988, IEEE Transactions on Electrical Insulation, Vol. 23, pp. 383-386

16. *Extension of Van Der Pauw´s theorem for measuring specific resistivity in discs of arbitrary shape to anisotropic media.* **W. L. V, Price.** 1972, J. Phys. D: Appl. Phys, Vol. 5, pp. 1127-1132

17. *Current distribution modelling in electroconductive fabrics.* **J. Banaszczyk, G. De Mey, A. Schwarz, L. Van Langenhove.** 2009, Fibres and Textiles in Eastern Europe, Vol. 17, pp. 28-33

18. *Electrodynamique des milieux continus.* **L. Landau, E. Lifchitz.** 1969, MIR, Moscow, Vol. 87, pp. 336-344

19. *Analysis of transport phenomena.* **W. M. Deen.** 1998, Oxford University Press, pp.199-201

20. *Dictionary of conformal representations*. **H. Kober** 1957, NY : Dover, pp. 170-174

21. *Complex variables and applications*. **R. Churchill.** 1960, NY : Mc Graw Hill, pp. 189-240

22. *Handbook of mathematical functions*. **M. Abramowitz, I. Stegun.** 1970, NY: Dover, pp. 589-600

23. *Table of integrals, series and products. NY.* **I. Gradshteyn, I. Ryshik.** 1980, Academic Press, pp. 904-917

6

Temperature coefficient of resistance & Ageing

In this chapter, the square resistance change of screen-printed textiles as a function of temperature was investigated in order to evaluate temperature coefficient of resistance and ageing.

TABLE OF CONTENTS

6.1 Introduction

Electroconductive textiles through screen printing can find use in different applications. The technique combines electroconductive inks with textiles. In order to determine the influence of temperature on the electroconductive properties, the square resistance of these electroconductive textiles is measured at different temperatures varying between 23 – 60°C, in steps of about 10°C. During their operating life, the prepared samples are subjected to different electrical conditions. Thus, in this chapter we study the temperature coefficient of resistance (TCR) of the screen-printed samples, which is a very important electrical property. Furthermore, these samples are exposed to long-term thermal ageing, which will be discussed in the second part of this chapter. The variation of resistance with temperature and time is very important in electronics. Design engineers should take it into account. Therefore, as the conductive screen-printed materials will be used in wearable electronics, it is important to study this behaviour.

In electronics, the temperature coefficient of resistance (TCR) of printed thick films is generally specified in parts per million per degree Celsius (ppm/°C). In granular metal films one can distinct three structural regimes [1-2]:

- dielectric regime (where the TCR is negative)
- transition regime (where the TCR is nearly zero)
- metallic regime (where the TCR is positive)

A positive TCR is when the resistance increases with temperature and the TCR is negative when the resistance goes down with temperature. The ideal TCR should equal zero. However, in some applications a positive TCR is required for safety reasons (like in most household electronics).

Moreover, the metallic particle size affects the electrical properties. The larger the particle the more negative the TCR is [3 -4].

Jiang *et al.* [5] revealed that the thickness of the film can greatly influence its electrical properties. With increasing the thickness the TCR shifts from a negative value to a positive value.

The textile samples presented in this chapter are: Viscose 1, Polyamide, Polyester 3, Aramid, and blended (Cotton/Polyester and Polyester/Viscose) (Table 2.1, Chapter 2). The pattern of the screen-printed layers is a square of

6 cm by 6 cm and silver-based ink 2 from Acheson (Electrodag PF 410) has been used (Table 2.2, Chapter 2).

6.2 Temperature coefficient of resistance

The temperature coefficient of resistance expresses the effect of a changing temperature on the resistance of the screen-printed conductive layer. This is the amount of change of the square resistance in relation to the temperature difference, expressed in parts per million per degree Celsius [3, 6-7] and calculated as follows:

$$\mathrm{TCR} = \frac{R_{\square,max} - R_{\square,min}}{R_{\square,min}\,(T_{max} - T_{min})} \cdot 10^6$$

where $R_{\square,max}$ is the square resistance measured at T_{max} and $R_{\square,min}$ is the square resistance measured at T_{min}. In this experiment T_{max} is 60°C and T_{min} is 23°C.

The screen-printed conductive samples, prepared as in Figure 6.1 were placed on a heating plate manufactured by Temptronic Corporation; model TPO315A-2 (Figure 6.2) [6].

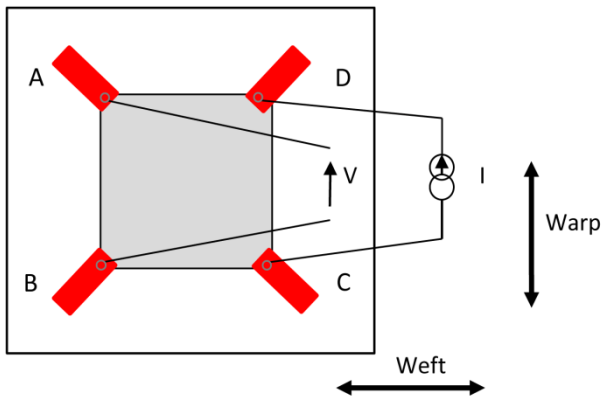

Figure 6.1 The screen-printed sample prepared with four contacts according to the Van Der Pauw measurements configuration

The heating plate was systematically heated up to 23°C, 30°C, 40°C, 50°C and 60°C. At each of these temperatures $R_{\square}$ is measured using the Van Der Pauw method (a current *I* was supplied and the resulting voltage drop *V* was measured). Subsequently, the plate cooled down and at 50, 40, 30 and 23°C, *V* and *I* were recorded and $R_{\square}$ was calculated. At the intermediate temperatures, the plate was allowed to stabilize for about ten minutes upon reaching the desired temperature [7].

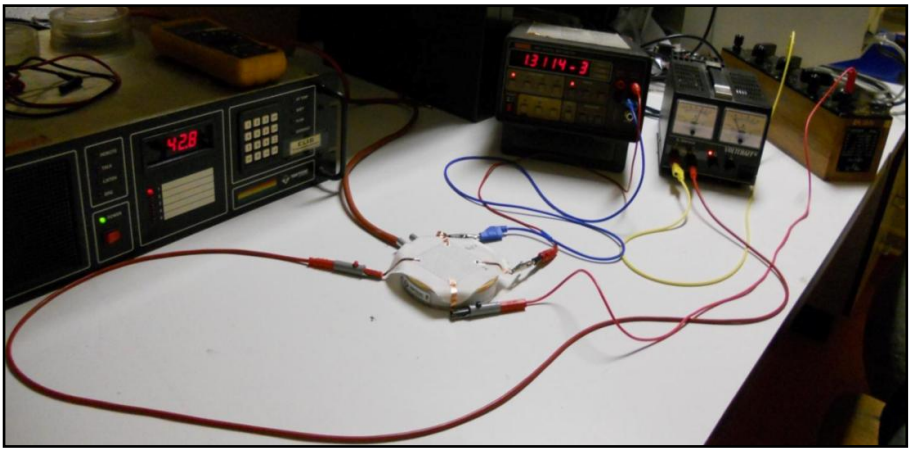

Figure 6.2 Measurements of $R_{\square}$ when the sample is on the heating plate

The calculated TCR values are shown in two tables, Table 6.1 showing the TCR values for the *weft direction* (*C-D*) and Table 6.2 for the *warp direction* (*A-D*). In each table, two series of TCR values are given: TCR_1 expresses the change when the temperature was *increased* and the TCR_2 when the temperature was *decreased*.

Table 6.1 Calculated values for $R_{\square}$ and TCR in C-D direction (***weft***)

	$R_{\square}$ *min* (Ω)	$R_{\square}$ *max* (Ω)	$R_{\square}$ *min* (Ω)	TCR_1 (ppm/°C)	TCR_2 (ppm/°C)
Viscose 1	0.0162	0.0175	0.0149	**2169**	**4716**
Polyamide	0.0122	0.0156	0.0131	**7532**	**5158**
Polyester 3	0.0238	0.0259	0.0239	**2385**	**2262**
Aramid	0.0215	0.0236	0.0209	**2640**	**3492**
Cotton/Polyester 1	0.0599	0.0608	0.0582	**406**	**1207**
Cotton/Polyester 2	0.0272	0.0296	0.0271	**2385**	**2493**
Polyester/Viscose	0.0266	0.0235	0.0239	**-3150**	**-452**

Table 6.2 Calculated values for $R_{\square}$ and TCR in A-D direction (***warp***)

	$R_{\square}$ *min* (Ω)	$R_{\square}$ *max* (Ω)	$R_{\square}$ *min* (Ω)	TCR_1 (ppm/°C)	TCR_2 (ppm/°C)
Viscose 1	0.0148	0.0161	0.0146	**2374**	**2777**
Polyamide	0.0122	0.0157	0.0129	**7754**	**5866**
Polyester 3	0.0240	0.0261	0.0239	**2365**	**2488**
Aramid	0.0202	0.0229	0.0208	**3613**	**2729**
Cotton/Polyester 1	0.0583	0.0596	0.0568	**603**	**1332**
Cotton/Polyester 2	0.0271	0.0295	0.0272	**2394**	**2285**
Polyester/Viscose	0.0258	0.0234	0.0257	**-2514**	**-2419**

Observation of the TCR values in Tables 6.1 and 6.2 shows that for all materials TCR_1 and TCR_2 are different, meaning that the values are not the same when the temperature is increased or decreased. This can be explained by the hysteresis shown in the graphs of Figures 6.4 to 6.10.

Furthermore, we also notice that the TCR value in weft direction differs from the TCR in warp direction, which indicates anisotropy of the screen-printed samples [6].

The negative TCRs of the screen-printed Polyester/Viscose can be explained through the thickness of the printed surface. Jiang *et al.* [5] showed that with an increase of the film thickness from 30 nm to 280 nm, the TCR of the samples shifted from a negative to a positive value.

One physical explanation can be that the electric conduction between two neighbouring particles is of the order of a few nanometers. For a larger gap, electrons can still be transferred from one particle to another by hopping between the so-called localised states (Figure 6.3).

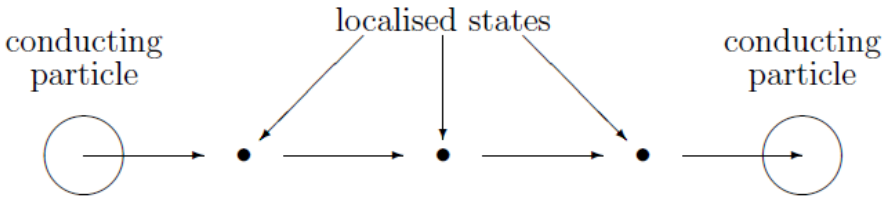

Figure 6.3 Electron transfer from one particle to another when the gap is larger

For this physical explanation a theory can be given for screen-printed conductors on ceramic substrates used in electronics. This theory gives that the resistance of such a material will be given by:

$$R(T) = R_0 \sqrt{\frac{T}{T_m}} \exp\left[2\left(\frac{T_m}{T}\right)^{1/4}\right]$$

Where R_0 is a constant and T the absolute temperature expressed in Kelvin. By solving dR/dT =0 one can easily prove that R(T) has a minimum for $T=T_m$.

T_m is the temperature which is theoretically given by:

$$T_m = \frac{\alpha^3}{k\,N}$$

Where α is the decay of the quantum wave function of an electron around a localised state,

k is the Boltzmann constant, 1.38066 x 10^{-23} J/K and *N* the density of localized states per unit volume and energy.

For $T>T_m$ the resistor will have a positive temperature coefficient and a negative one for $T<T_m$.

For our analysis α can be considered as a constant. Localised states usually exist as interfaces between crystallites. As a consequence, the preparation of the materials can affect the size of the crystallites and hence the value *N* of localised states. The only variable parameter here is *N*. For high values of *N*, T_m is small and the resistor has a positive temperature coefficient. For low values of *N* negative temperature coefficients can be expected. If *N* is reduced by 50 %, which means that the average distance between the localised states is increased by only $\sqrt[3]{2} = 1.259$ the value of T_m will be double, say from 200 K to 400 K or the resistor changes from a negative TCR to a positive one.

The slope of square resistance versus temperature determines the TCR. The figures below visualize the evolution of the square resistance with temperature for each textile substrate.

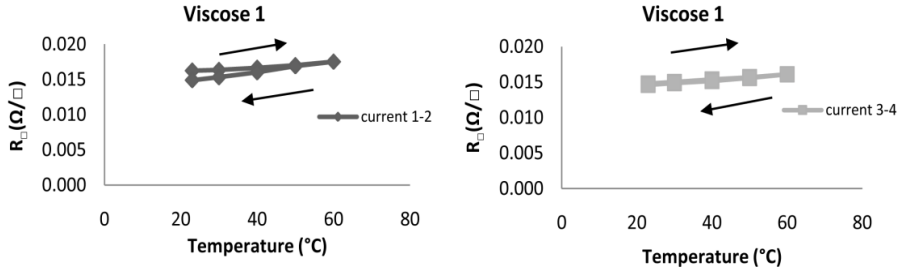

Figure 6.4 Resistance plots of screen-printed samples of Viscose

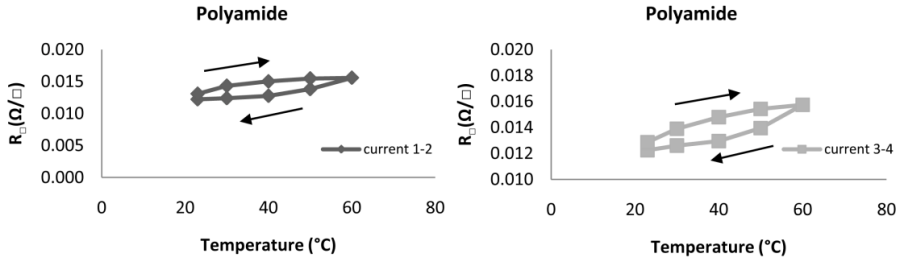

Figure 6.5 Resistance plots of screen-printed samples of Polyamide

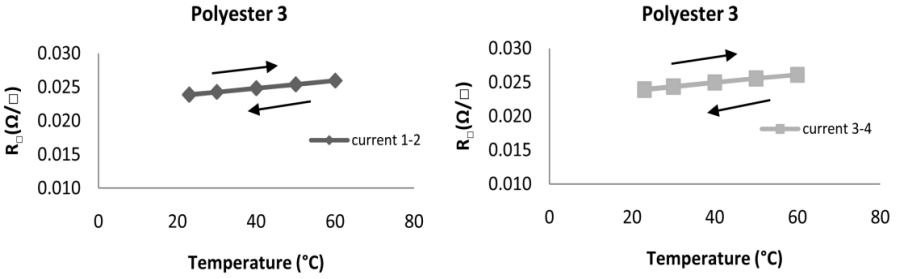

Figure 6.6 Resistance plots of screen-printed samples of Polyester

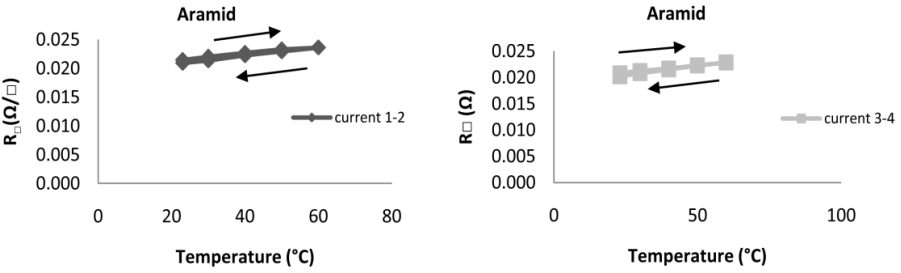

Figure 6.7 Resistance plots of screen-printed samples of Aramid

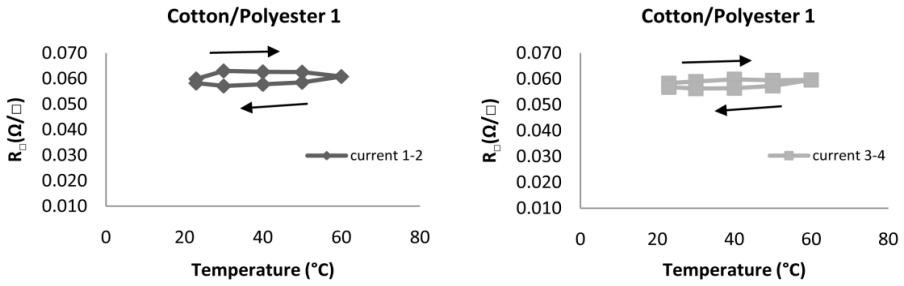

Figure 6.8 Resistance plots of screen-printed samples of Cotton/Polyester 1

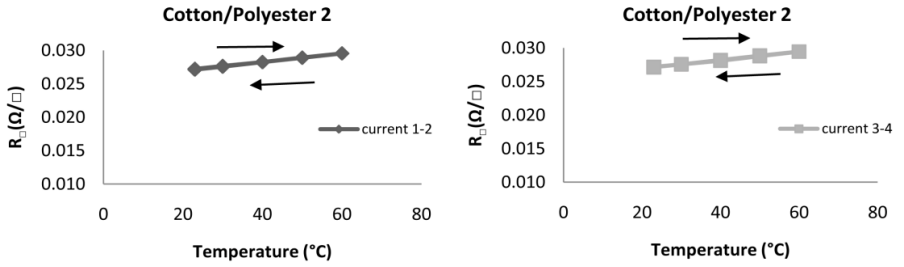

Figure 6.9 Resistance plots of screen-printed samples of Cotton/Polyester 2

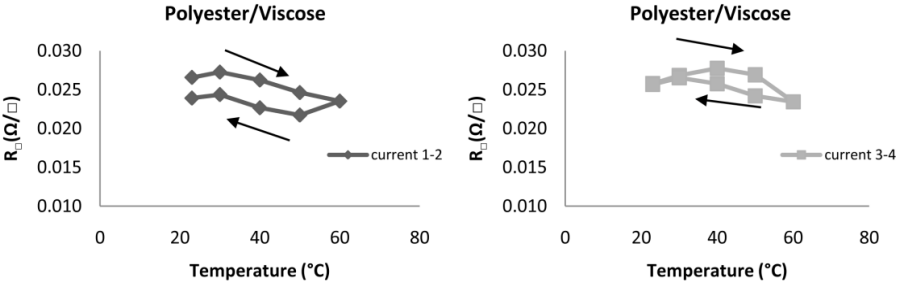

Figure 6.10 Resistance plots of screen-printed samples of Polyester/Viscose

As observed in Figures 6.4 to 6.10 the conductivity of most materials decreases as the temperature increases. Alternatively, the resistivity of most materials increases with increasing temperature. The reason the resistivity increases with increasing temperature may be the number of imperfections in the atomic lattice structure, that increases with temperature and this hampers electron movement. These imperfections include dislocations, vacancies, interstitial defects and impurity atoms.

From the slopes of the plots of Figures 6.4 - 6.10 and Tables 6.1, 6.2 it can be seen that the TCR is positive for Viscose, Polyamide, Polyester, Aramid, Cotton/Polyester 1 and 2, varying from 406 to 7754 ppm/°C however for Polyester/Viscose TCR is negative varying from -3150 to -452 ppm/°C.

The values of the TCRs for the screen-printed samples are high in sign but most of them are comparable with thick film materials [3, 7, 9-14] used in electronics.

Halder et al. [7] screen-printed thick film resistors of ruthenium oxide (RuO_2) on alumina substrates in order to determine the tunnelling and hopping parameters means by the values of TCR. The thick films showed to have positive and negative values from -663 to 222 ppm/°C.

Dziedzic et al. [3] have examined the electrical properties of iridium oxide (IrO_2), ruthenium oxide (RuO_2) and bismuth ruthenium oxide ($Bi_2Ru_2O_7$) compounds screen-printed on alumina substrates as thick-film resistors. The TCR measured for IrO_2, RuO_2 was highly positive and increasing with longer firing time from 1550 to 2150 ppm/°C. For $Bi_2Ru_2O_7$ it was negative and with the prolongation of firing time was becoming more negative from -131 to -980 ppm/°C.

Czarczynska et al. [9] have analyzed the electrical parameters of printed carbon/polyesterimide thick film resistors. The values of TCR varied from -100 to -1300 ppm/°C.

Morten et al. [10] have printed thick film of nickelate (NiCo) pastes on glazed alumina meant for sensor for linear displacement. The TCR measured for these sensors was approximately 2700 ppm/°C.

Scilingo et al. [11] have analyzed the thermal and ageing properties of polypyrrole (PPy) coated fabrics used as sensitive glove able to detect the position and the motion of fingers. This was the only paper found which was discussing the measurements of TCR and ageing of conductive textiles. The

TCR, measured here in varied temperature from 10 to 50°C, was -0.018°C^{-1} or -18000 ppm/°C. The value for this coated fabric is high and negative, more than in our case, but the author compare that with ceramic thermistors with a negative temperature coefficient from -0.03°C^{-1} to -0.05°C^{-1}. They also mention that in applications related to the monitoring of kinematics of human body segments, temperature variations typically encountered do not significantly affect the acquired data.

Prudenziati et al. [12] have studied the electrical properties of thermally sprayed nickel (Ni) and nickel-chromium alloy (Ni20Cr) resistors. The TCR was measured in the temperature range of 20-500°C and the results were varying from 180 to 2830 ppm/°C.

Sibinski et al. [13] have presented flexible temperature sensors on separate yarns for textronic applications. As a sensor core they used Polyvinylidene fluoride fiber in a monofilament structure. Polymer conductive pastes based on carbon nanotubes were placed on the fibers to create sensor structures. The TCR, measured in the range of temperatures from 20 to 160°C in 20 second cycles, were from 1010 to 7500 ppm/K. Strong hysteresis for all the samples, was noticed, which is similar to our case.

Sloma et al. [14] and [15] screen-printed thick-films of carbon nanotubes (different percentage) for application of transparent electrodes and temperature sensors. A significant hysteresis was observed and the TCR values were negative and varying from -350 to -2100 ppm/°C [14] and from - 680 ppm/K at T=300 K to -0.162 K^{-1} at T=5 K (14).

6.3 Ageing

In textile industry ageing tests are important, because the material properties can change when textiles are exposed to different atmospheric conditions such as ultra violet (UV) light (sunlight), heat or humidity [16, 17]. These conditions contribute to the degradation of the textile material during their service life. UV light has the biggest influence on the degradation of textile materials. It is important to carry out the ageing test in order to improve the time of the textile usefulness, especially for those textile materials destined for outdoor clothing, curtains, car seats, etc.

The reliability/ageing is also one of the major concerns of the electronics industry so it is important not only for textiles but also for electronics [18, 19]. Here, is important to know how the resistance value will change with time.

In this chapter we present the reliability/ageing of the electroconductive screen-printed textiles. Our samples are a combination of the textile and the electronic field so the resistance change over time is an important issue. The reliability/ageing is a measure of how much the resistance changes with time/days and it is defined as the slope of the change in resistance versus time/days as illustrated in Figures 6.14 - 6.20.

Lezak et al. [17] have drawn conclusions about the measurements of anti-electrostatic properties for textiles destined for protective clothing, before and after 1200 h of light exposure in natural conditions. In their case the textile fabrics with a net arrangement of carbon conductive thread did not show any significant influence, while those with a coppered thread showed an increase in the surface resistance. In their research they also made experiments regarding the strength of textile materials before and after 1200 h of exposure to light and atmospheric factors, where an anisotropy of the textiles was observed from the data in weft and warp direction but not mention by the author.

Scilingo et al. [11] used two samples of polypyrrole (PPy) coated fabrics, for the ageing test, where one fabric sample was put inside a sealed container and the second in a tray in open air. The resistance of the two fabric samples in a period of 60 days changed from 0.9 kΩ/cm at the beginning to 8.8 kΩ/cm for the sample in contact with the open air and 2.3 kΩ/cm for the other sample.

The screen-printed conductive samples for this research were prepared in the same way as for the TCR measurements. They were placed in an oven heated at 60°C for 24 hours. During the following 24 hours the samples where cooled down and the square resistance was measured. This cycle was repeated for duration of 15 days.

In Figure 6.13, the average of resistance versus time of the screen-printed textile samples is presented, and reveals that this average value does not really change. However, when having a closer look at the values of the measurements in warp and weft directions (Figures 6.11 and 6.12) one can see that the square resistance is increasing in one direction and decreasing in the other one. That is why the *average* of the square resistance has not changed and shows to be significantly less sensitive to ageing. The square resistance for Polyester 3 in warp direction is very stable during ageing test for all the time compared with the other textiles and other directions, which have shown increase and decrease throughout the period. For Polyamide, the square resistance is decreasing in weft direction (Figure 6.11) and increasing in warp direction (Figure 6.12).

Here, the square resistance was measured, similar to TCR, in *weft* and *warp* direction. Although the same conductive ink was used for all the screen-printed samples, the ageing tests revealed that the ageing behaviour is quite different for the different textile materials. This can only be explained by the differences between the textile materials, not by the ink. Furthermore, when having a closer look at Figures 6.14 - 6.20 the influence of ageing on the square resistance is not the same in *weft and warp* direction thus also showing an anisotropic behaviour [6].

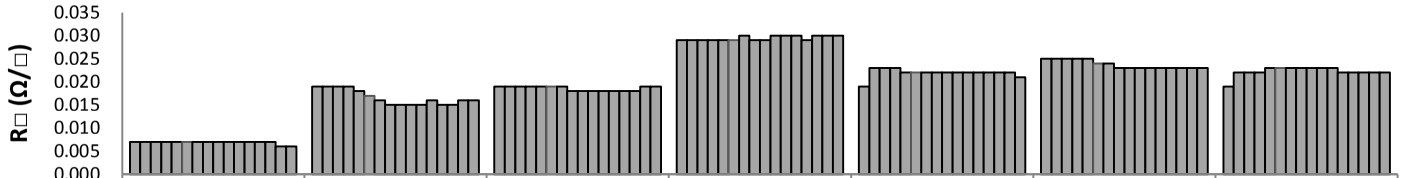

	Viscose 1	Polyamide	Polyester 3	Aramid	Cotton/Polyester 1	Cotton/Polyester 2	Polyester/Viscose
Before aging	0.007	0.019	0.019	0.029	0.019	0.025	0.019
after 1 day	0.007	0.019	0.019	0.029	0.023	0.025	0.022
after 2 days	0.007	0.019	0.019	0.029	0.023	0.025	0.022
after 3 days	0.007	0.019	0.019	0.029	0.023	0.025	0.022
after 4 days	0.007	0.018	0.019	0.029	0.022	0.025	0.023
after 5 days	0.007	0.017	0.019	0.029	0.022	0.024	0.023
after 6 days	0.007	0.016	0.019	0.030	0.022	0.024	0.023
after 7 days	0.007	0.015	0.018	0.029	0.022	0.023	0.023
after 8 days	0.007	0.015	0.018	0.029	0.022	0.023	0.023
after 9 days	0.007	0.015	0.018	0.030	0.022	0.023	0.023
after 10 days	0.007	0.015	0.018	0.030	0.022	0.023	0.023
after 11 days	0.007	0.016	0.018	0.030	0.022	0.023	0.022
after 12 days	0.007	0.015	0.018	0.029	0.022	0.023	0.022
after 13 days	0.007	0.015	0.018	0.030	0.022	0.023	0.022
after 14 days	0.006	0.016	0.019	0.030	0.022	0.023	0.022
after 15 days	0.006	0.016	0.019	0.030	0.021	0.023	0.022

Figure 6.11 Resistance versus time of screen-printed textile samples in ***weft*** direction

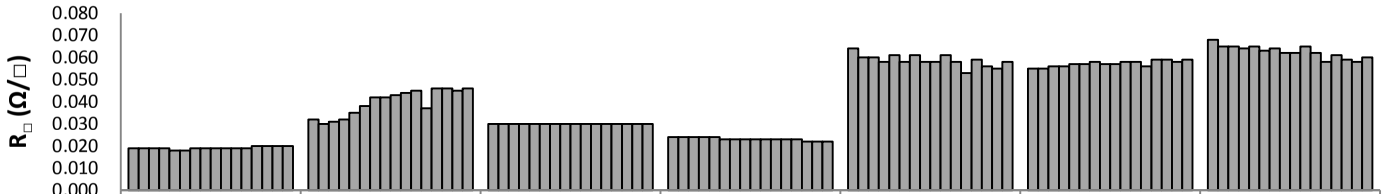

	Viscose 1	Polyamide	Polyester 3	Aramid	Cotton/Polyester 1	Cotton/Polyester 2	Polyester/Viscose
Before aging	0.019	0.032	0.030	0.024	0.064	0.055	0.068
after 1 day	0.019	0.030	0.030	0.024	0.060	0.055	0.065
after 2 days	0.019	0.031	0.030	0.024	0.060	0.056	0.065
after 3 days	0.019	0.032	0.030	0.024	0.058	0.056	0.064
after 4 days	0.018	0.035	0.030	0.024	0.061	0.057	0.065
after 5 days	0.018	0.038	0.030	0.023	0.058	0.057	0.063
after 6 days	0.019	0.042	0.030	0.023	0.061	0.058	0.064
after 7 days	0.019	0.042	0.030	0.023	0.058	0.057	0.062
after 8 days	0.019	0.043	0.030	0.023	0.058	0.057	0.062
after 9 days	0.019	0.044	0.030	0.023	0.061	0.058	0.065
after 10 days	0.019	0.045	0.030	0.023	0.058	0.058	0.062
after 11 days	0.019	0.037	0.030	0.023	0.053	0.056	0.058
after 12 days	0.020	0.046	0.030	0.023	0.059	0.059	0.061
after 13 days	0.020	0.046	0.030	0.022	0.056	0.059	0.059
after 14 days	0.020	0.045	0.030	0.022	0.055	0.058	0.058
after 15 days	0.020	0.046	0.030	0.022	0.058	0.059	0.060

Figure 6.12 Resistance versus time of screen-printed textile samples in ***warp*** direction

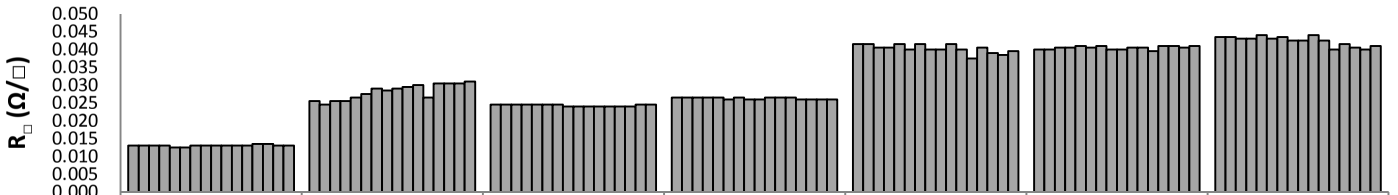

	Viscose 1	Polyamide	Polyester 3	Aramid	Cotton/Polyester 1	Cotton/Polyester 2	Polyester/Viscose
Before aging	0.013	0.026	0.025	0.027	0.042	0.040	0.044
after 1 day	0.013	0.025	0.025	0.027	0.042	0.040	0.044
after 2 days	0.013	0.026	0.025	0.027	0.041	0.041	0.043
after 3 days	0.013	0.026	0.025	0.027	0.041	0.041	0.043
after 4 days	0.013	0.027	0.025	0.027	0.042	0.041	0.044
after 5 days	0.013	0.028	0.025	0.026	0.040	0.041	0.043
after 6 days	0.013	0.029	0.025	0.027	0.042	0.041	0.044
after 7 days	0.013	0.029	0.024	0.026	0.040	0.040	0.043
after 8 days	0.013	0.029	0.024	0.026	0.040	0.040	0.043
after 9 days	0.013	0.030	0.024	0.027	0.042	0.041	0.044
after 10 days	0.013	0.030	0.024	0.027	0.040	0.041	0.043
after 11 days	0.013	0.027	0.024	0.027	0.038	0.040	0.040
after 12 days	0.014	0.031	0.024	0.026	0.041	0.041	0.042
after 13 days	0.014	0.031	0.024	0.026	0.039	0.041	0.041
after 14 days	0.013	0.031	0.025	0.026	0.039	0.041	0.040
after 15 days	0.013	0.031	0.025	0.026	0.040	0.041	0.041

Figure 6.13 The average of resistance versus time of screen-printed textile samples

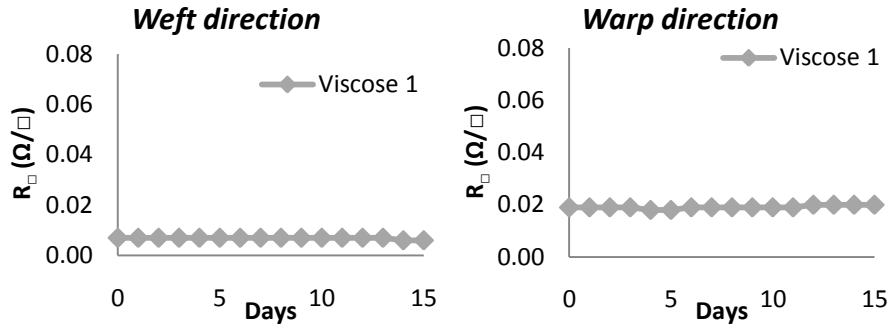

Figure 6.14 Resistance versus time of screen-printed Viscose textile in both directions

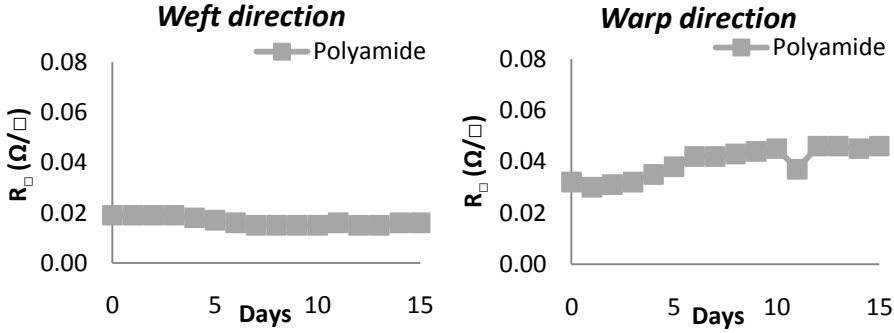

Figure 6.15 Resistance versus time of screen-printed Polyamide textile in both directions

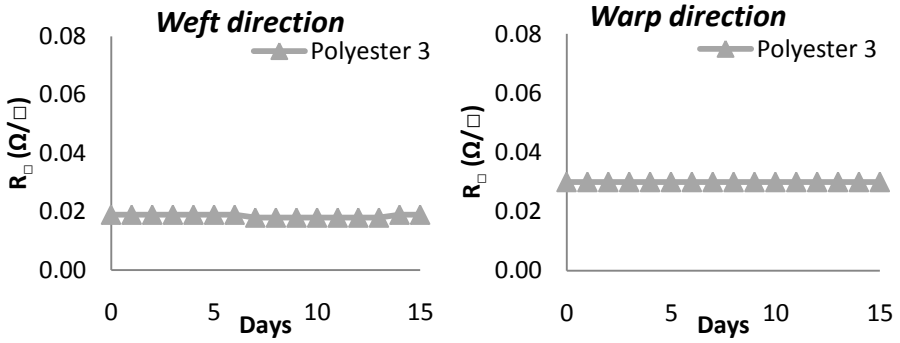

Figure 6.16 Resistance versus time of screen-printed Polyester 3 textile in both directions

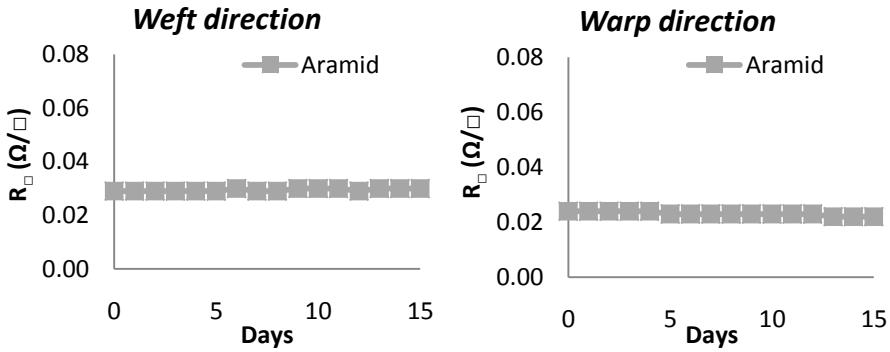

Figure 6.17 Resistance versus time of screen-printed Aramid textile in both directions

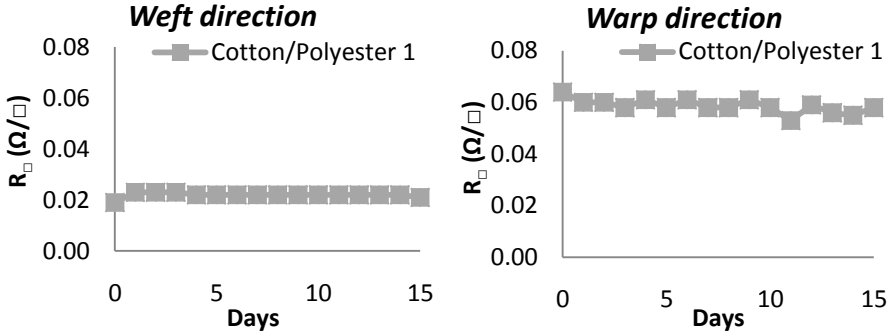

Figure 6.18 Resistance versus time of screen-printed Cotton/Polyester 1 textile in both directions

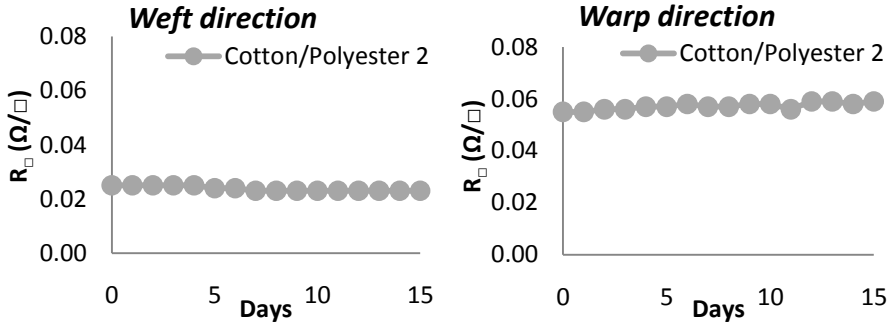

Figure 6.19 Resistance versus time of screen-printed Cotton/Polyester 2 textile in both directions

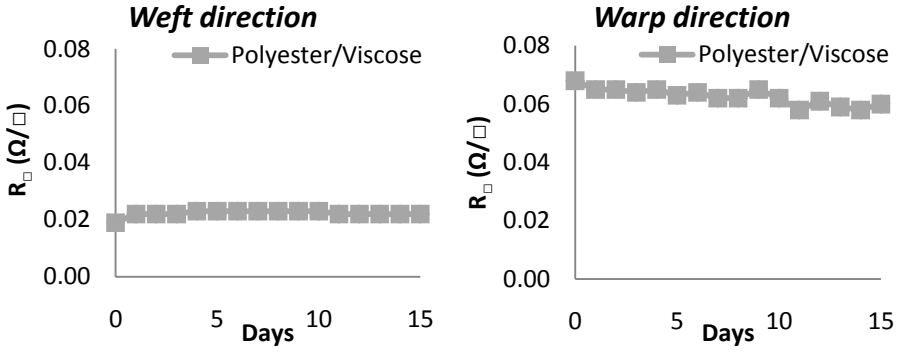

Figure 6.20 Resistance versus time of screen-printed Polyester/Viscose textile in both directions

6.4 Conclusions

In this chapter an analysis of temperature coefficient of resistance and ageing of the screen-printed textiles was made. For both, TCR and ageing, an anisotropic behaviour according to weft and warp direction of the fabrics was observed.

From the TCR measurements positive and negative TCR values were obtained, comparable with TCR measurements in the field of electronics where they are commonly measured. Additionally, hysteresis was also observed for most of the samples in weft and warp directions.

The results indicate that the effects of ageing upon the printed textiles are negligible for a period of 15 days at 60°C.

6.5 References

1. *Electric conduction in thin metalic films.* **T. J. Coutts.** s.l. : Elsevier, 1974.

2. *Electric conduction in metallic Ag particles—Cs2O semiconductor thin films.* **Q-D. Wu, X-Q. Liu.** 2, 1983, Journal of Vacuum Science & Technology A, Vol. 1, pp. 371-375.

3. *Electrical properties of conductive materials used in thick-film resistors.* **A. Dziedzic and L. Golonka.** 1988, Journal of Materials Science, Vol. 23, pp. 3151-3155.

4. *The effect of particles size on the temperature coefficient of the resistance of the thick film resistors.* **A. H. Boonstra, C. A. H. A. Mutsaers.** 1980, Thin Solid Films, Vol. 67, pp. 13-20.

5. *Influences of Film Thickness on the Electrical Properties of TaNx Thin Films Deposited by Reactive DC Magnetron Sputtering.* **H. Jiang, C. Wang, W. Zhang, X. Si, Y. Li.** 7, 2010, Journal of Materials Science & Technology, Vol. 26, pp. 597-600.

6. *"Van Der Pauw method for measuring resistivities of anisotropic layers printed on textile substrates".* **I. Kazani, G. De Mey, C. Hertleer, J. Banaszczyk, A. Schwarz, G. Guxho and L. Van Langenhove.** 2011, Textile Research Journal, Vol. 81 (20), pp. 2117-2124.

7. *Measurement of the tunneling and hopping parameters in RuO2 thick films.* **N. C. Halder, R. J. Snyder.** 1984, Electrocomponent Science and Technology, Vol. 11, pp. 123-136.

8. *Processing, microstructure, and electric properties of buried resistors in low-temperature co-fired ceramics.* **P. Yang, M. A. Rodriguez, P. Kotula, B. K. Miera, D. Dimos.** 7, 2001, Journal of Applied Physics, Vol. 89, pp. 4175 - 4182.

9. *Some properties of carbon black/polyestermide and electrode carbon/polyesterimide thick films.* **H. Czarczynska, A. Dziedzic, B. W. Licznerski.** Warsaw : s.n., 1990. 14-th Conference of the ISHM Poland. pp. 35-38.

10. *Magnetoresistive thick film sensor for linear displacements.* **B. Morten, G. De Cicco, M. Prodenziati, A. Masoero, G. Mihai.** 1995, Sensors and Actuators A, Vols. 46-47, pp. 261-265.

11. *Strain-sensing fabric for wereable kinaesthetic-like systems.* **E. P. Scilingo.** 2003, IEEE SENSORS JOURNAL, Vol. 3, pp. 460-467.

12. *Electrical Properties of Thermally Sprayed Ni- and Ni20Cr-Based Resistors.* **M. Prudenziati, M. L. Gualtieri.** 3, 2008, Journal of Thermal Spray Technology, Vol. 17, pp. 385-394.

13. *Flexible temperature sensors on Fibres.* **M. Sibinski, M. Jakubowska, M. Sloma.** 2010, Sensors, Vol. 10, pp. 7934-7946. 1424-8220.

14. *Polymer composites with carbon nanotubes for printed electronics application.* **M. Sloma.** 2010. XII International PhD Workshop.

15. *Investigations on printed elastic resistors containing carbon nanotubes.* **M. Sloma, M. Jakubowska, A. Kolek, K. Mleczko, P. Ptak, A. W. Stadler, Z. Zawislak, A. Mlozniak.** 9, 2011, Journal of Materials Science: Materials in Electronics, Vol. 22, pp. 1321-1329.

16. *Effect of outdoor exposure and accelerated aging on textile materials used in aerostat and aircraft arrester barrier nets.* **S.K. Pal, V. B. Thakare, G. Singh, M. K. Verma.** 2011, Indian Journal of Fibre & Textile Research, Vol. 36, pp 145-151.

17. *Ageing simulation of fabrics destined for protective clothing.* **K. Lezak, I. Frydrych.** 2, 2011, Fibres and Textiles in Eastern Europe, Vol. 19, pp. 54-60.

18. *Ageing in electronic systems.* **J. P. Rooney, M. A. Foxboro Co,** 1999, Reliability and Maintainability Symposium, pp. 293-299. 0-7803-5143-6

19. *Study of thermal interfaces aging for power electronics applications.* **J. P. Ousten, Z. Khatir,** 2011, Power Electronics and applications, pp. 1-10. 987-1-61284-167-3

7

Applications

This chapter introduces potential applications of screen-printed textiles such as electrodes or textile antennas for off-body communication.
The electrodes are studied through electrochemical impedance spectroscopy and the performance of the antennas is studied after five washing cycles.

TABLE OF CONTENTS

7.1 Screen-printed textiles electrodes

7.1.1 Introduction

Textiles with electroconductive characteristics have found use in different applications as they combine functionality with high wearing comfort. Electroconductive textiles can have various functions such as electromagnetic shielding, infrared absorption and as electronic component. One of the main applications of these conductive textiles is in the medical field for sensors and electrodes [1 - 5] (Figure 7.1.1).

The conductivity of traditional textiles can be achieved by means of conductive polymers, metals and metallised fibres, coating and printing, thus adding conductive particles [6].

As mentioned above there are many techniques to obtain electroconductive textiles but sometimes the conductivity is not good or they become very expensive so we have chosen to screen print with silver conductive inks. With this method we can have a flexible and low cost material, diversity of patterns, which cannot easily be achieved with other methods.

These conductive materials can be used as electrodes for health care and many groups have investigated the integration of textile electrodes in garments. Catrysse *et al.* [7] have integrated knitted electrodes into a belt for the recording of electrocardiogram (ECG) and respiration rate for children in the hospital. Linz *et al.*, in the framework of the ConText project, [8] have embroidered sensors, integrating them into garments, for monitoring health parameters on the human body. Schwarz *et al.* [9] have integrated electrodes in socks for electro stimulation, based on conductive silicones and elastic conductive yarns in order to prevent or heal the decubitus wounds and support patients with Parkinson disease. Merritt *et al.* [10] have screen-printed on nonwoven textile substrates electrodes for potential use in health monitoring garments. Other groups have developed woven or knitted electrodes [3, 11 and 12].

When using screen-printed fabrics as electrodes it is important to investigate their behaviour in combination with sweat because the textile electrodes will be in close contact with the human body. Electrochemical Impedance Spectroscopy (EIS) is the appropriate method to investigate and analyze

these screen-printed textile electrodes combined with (artificial) sweat. Since these electroconductive textiles with two silver-inks used show to have good conductivity after 20 washing cycles, confirming that these electrodes can be easily maintain, here will be investigate more about the resistivity when they will be in contact with the human sweat. These textile electrodes may be used for measuring biomedical parameters or for giving therapeutic treatments.

Figure 7.1.1 Textile electrode prototypes from UGent: ECG garment prototypes like baby suit and Mickey Mouse band and textile electrodes integrated in socks for electro stimulation

7.1.2 Electroconductive textiles

In this study eight textile substrates were used: Viscose 2, Aramid, Polyamide, Polyester 3 and 4, Cotton/Polyester 1 and 2 and Polyester/Viscose (Table 2.1, Chapter 2). They were screen-printed with two silver conductive inks, ink 3 and 4 provided by Sun Chemical Company. These inks were chosen because of the very good conductivity they had shown after washing them 20 times (Figure 7.1.2) compared with ink 1 and 2 (Chapter 2).

Merritt *et al.* [10] have washed the screen-printed electrodes 5 times and washing tests revealed problems because of the cracks but in our experiments as it can be seen from Figure 7.1.3 that all the printed samples show very good conductivity after 20 washing cycles.

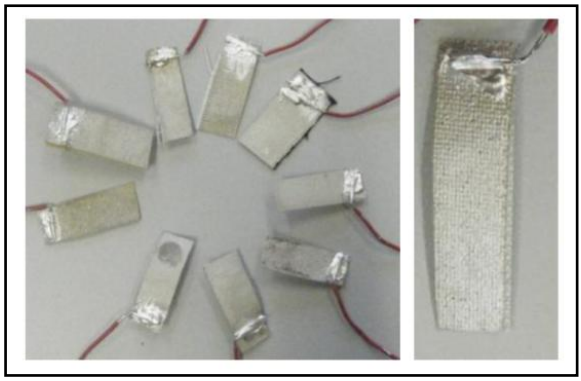

Figure 7.1.2 Electroconductive screen-printed textiles

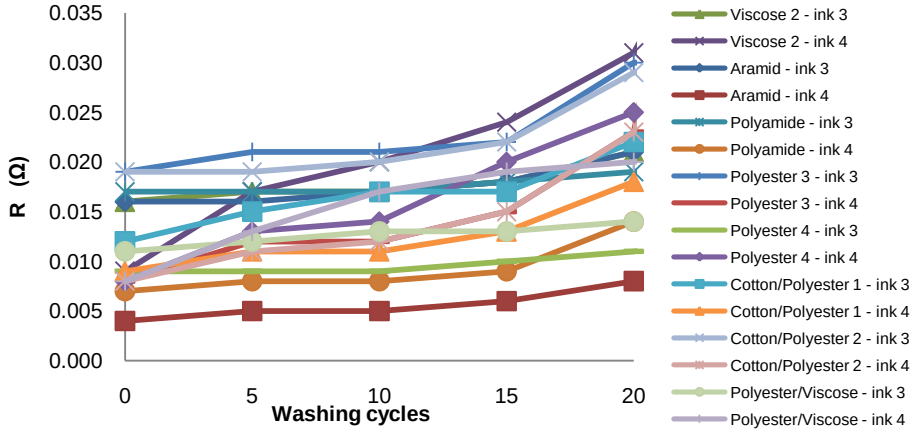

Figure 7.1.3 Square resistance of printed samples after every 5th washing cycle

7.1.3 Impedance measurement

Up to now the conductivity of the screen-printed electroconductive textiles has only been evaluated by applying direct current (DC). However, when using these textiles as textile electrodes, we are also interested in evaluating their alternating current (AC) behaviour. Here, the impedance of the complex system textile-human skin is required as it is evident that the electroconductive textile will be in contact with the skin. So with EIS it is possible to study the properties of electroconductive textiles for medical application. Electrochemical impedance is measured by applying an AC potential to an electrochemical cell and then measuring the current through the cell. The EIS measures the total opposition to an altering current in the circuit. The impedance can then be calculated using Ohm´s law (1) [13]:

$$Z(\omega) = \frac{\Delta E\,(\omega)}{\Delta I(\omega)} \qquad (1)$$

This is limited to only one circuit element, the ideal resistor, which has several simplifying properties such as:

- It follows Ohm´s Law at all current and voltage levels.

- Its resistance value is independent of frequency.
- AC current and voltage signals though a resistor are in phase with each other.

The impedance of the electrodes can be described as a resistance in series with a capacitance C, where R_{ct} is the charge transfer resistance and R_e is the electrolyte resistance (Figure 7.1.4).

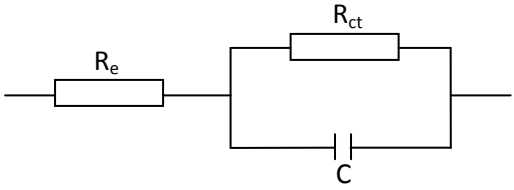

Figure 7.1.4 Electric equivalent circuit model of an electrode-sweat interface

The resistance R and the capacitance C have the following impedance functions:

$$Z_R = R \text{ and } Z_C = \frac{1}{j\omega C} \quad (2)$$

The impedance itself $Z(\omega)$ is a complex quantity, which can be represented in Cartesian (3) and in polar co-ordinates (4).

$$Z(\omega) = Z_r(\omega) + jZ_j(\omega) \quad (3)$$

where Z_r is the real part of the impedance and Z_j is the imaginary part. The plot of real part of impedance against the imaginary part gives ***the Nyquist Plot*** (Figure 7.1.10).

$$Z(\omega) = |Z(\omega)|e^{-j\emptyset} \quad (4)$$

where |Z| is magnitude of the impedance and ∅ is the phase shift. The plot of absolute value of impedance and the phase shift as a function of frequency in two different plots gives ***the Bode Plot*** (Figure 7.1.11).

7.1.3 Measurement set-up

The measurement set-up comprises two main components:

- An electrochemical cell
- A potentiostat

which are described more in detail in the following section.

To study the impedance of the textile electrode–skin interface, ***an electrochemical cell*** was built to simulate the human body [14]. This cell is shown in Figures 7.1.5 and 7.1.6.

The cylinder (3) is a PVC tube filled with artificial sweat to resemble the human body. The tube was filled with an electrolyte that imitates human sweat. The artificial sweat recipe used as electrolyte solution contained: 900 ml of distilled water, 5.00 $\pm$ 0.01 g of sodium chloride, 1.00 $\pm$ 0.01 g of urea, 940 $\pm$ 20 µL of lactic acid and ammonia to adjust the pH to 6.50 $\pm$ 0.10, as defined by EN 1811.

The diameter of the tube is 18 mm and the length is 58 mm. In each open side of the tube PVC plates were placed (1).

On the one side of the cell a reference electrode is placed, the conductive printed textile electrode is placed on the other side. Both electrodes are kept in place through rubber rings fittings. The reference electrode is a metal sheet of 99.995% pure palladium with a thickness of 0.25 mm from Goodfellow. The printed textile electrodes were prepared through screen printing with two types of silver-based inks on different textile materials (Table 2.1, Chapter 2). The diameter for the printed textile electrodes is 10 mm and for the palladium electrode 15 mm. The rubber ring fingers (2) were used to prevent the cell from leaking. Screws were used to keep the cell together.

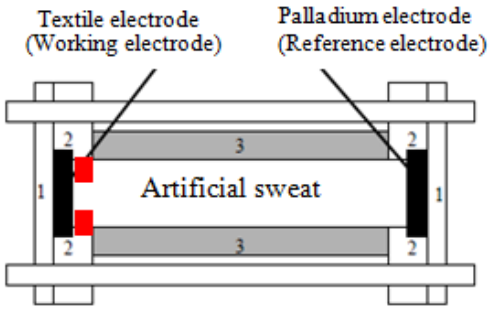

Figure 7.1.5 Scheme of the electrochemical cell

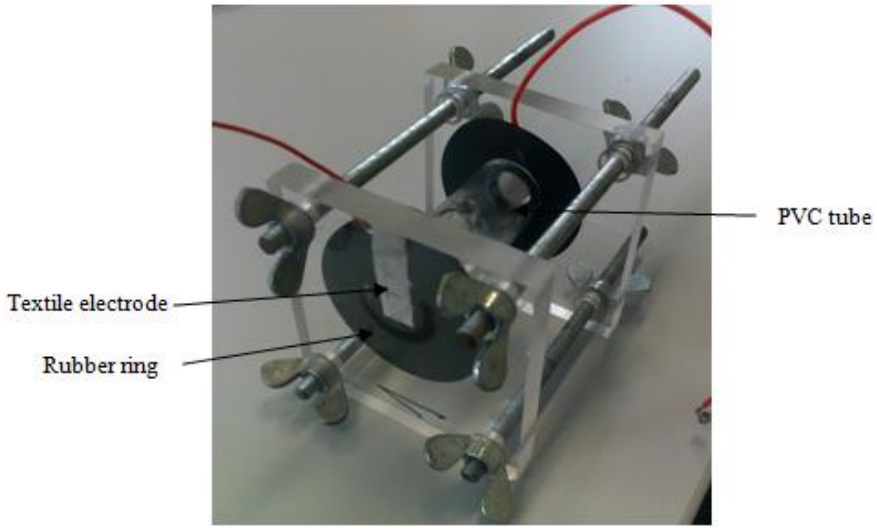

Figure 7.1.6 Electrochemical cell build

The electrochemical cell was put in an oven at a temperature of 30°C which mimics the average skin temperature.

The overall impedance of this cell consists of following blocks:

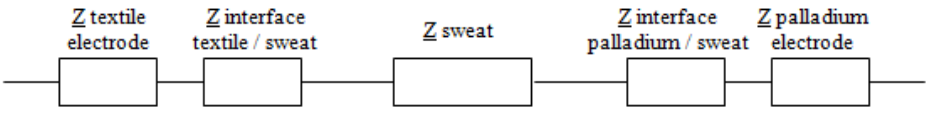

Figure 7.1.7 Equivalent electrical circuit of the electrochemical cell

The surface area of the reference electrode (palladium, 176.7 mm^2) is larger than the one of the working electrode (textile, 78.5 mm^2) because the kinetics of the working electrode are slower than the one of the counter electrode. The slowest reaction will determine the overall reaction rate and it is the overall reaction rate that is measured by a potentiostat. With this procedure the potentiostat only measures the signals from the working electrode. Consequently the equivalent electrical circuit measured becomes:

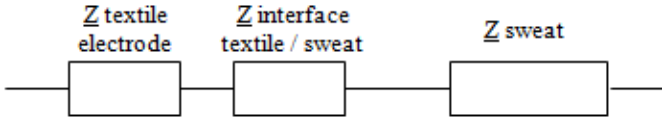

Figure 7.1.8 Impedance measured by the potentiostat

For measuring the impedance ***a potentiostat PARSTAT 2273*** of ECO chemie was used extended with a Frequency Response Analyser (FRA) (version 4.9) module in order to be able to perform impedance measurements (Figure 7.1.9) [15]. The frequency of the alternating potential applied was ranging from 0.5 Hz to 500 kHz with maximum amplitude of 10 mV in order to cover a large number of potential applications.

Figure 7.1.9 Impedance meter

7.1.4 Electrochemical characterisation of the textile electrodes

7.1.4.1 Different textiles printed with silver conductive inks

In this paragraph the Nyquist and Bode plots of all textiles printed with ink 3 and with ink 4 are shown.

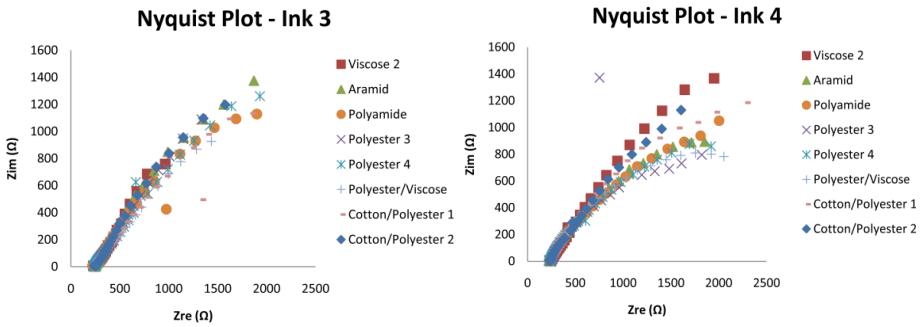

Figure 7.1.10 Nyquist plot of impedance for printed samples with conductive inks 3 and 4

Figure 7.1.10 also reveals that the maximum impedance varies between 1250 and 2500 Ω. Rattfält *et al.* [3] reported that the impedance of an electrode is

acceptable when it is lower than 50 kΩ at 50 Hz. Our results show that the impedance of the printed electrodes (both with ink 3 and ink 4) remains under 2500 Ω for frequencies between 0.5 Hz and 500 kHz. The impedance frequency dependency is shown in Figure 7.1.11.

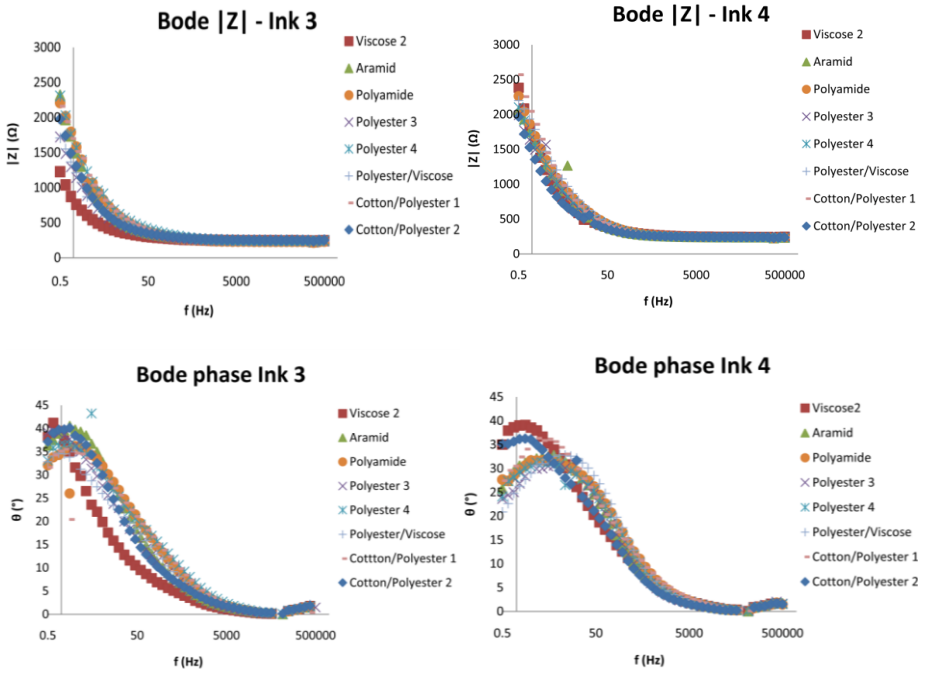

Figure 7.1.11 Bode plot showing the magnitude of impedance and the phase-angle shift as a function of applied frequency

Observing the Bode plot (Figure 7.1.11), the impedance decreased with increasing frequency. In the Bode plot, for textile printed with ink 3, Viscose 2 has the lowest impedance for the lowest frequencies (< 50 Hz) while for high frequencies (> 50 Hz) Cotton/Polyester 2 has the lowest impedance. The Bode plot for ink 4 shows that Cotton/Polyester 2 has the lowest impedance over the entire frequency range.

7.1.4.2 Every textile printed with two silver conductive ink

After we have compared the impedance of the printed textiles with the same ink, we have a closer look at the impedance of the same textile material with both conductive inks.

From the Nyquist plot (Figure 7.1.12) we observe that printing with a different ink results in a change of impedance, as could be expected because also the DC resistance varied when applying a different ink. Every textile printed with ink 4 shows to have lower impedance compared with ink 3 except for the substrate Viscose 2 which shows to have similar impedance with both inks. The same result was obtained when measuring the square resistance with a four-point probe using DC (direct current). As can be seen from the table below (Table 7.1.1) the samples printed with ink 4 show to have lower square resistances than those with ink 3.

Table 7.1.1 Square resistance of the samples before washing

	Square resistance $R_{\square}$ (Ω/□)	
Screen-printed textile	**Ink 3**	**Ink 4**
Viscose 2	0.016	0.009
Aramid	0.016	0.004
Polyamide	0.017	0.007
Polyester 3	0.019	0.008
Polyester 4	0.009	0.008
Cotton/Polyester 1	0.012	0.009
Cotton/Polyester 2	0.019	0.008
Polyester/Viscose	0.011	0.008

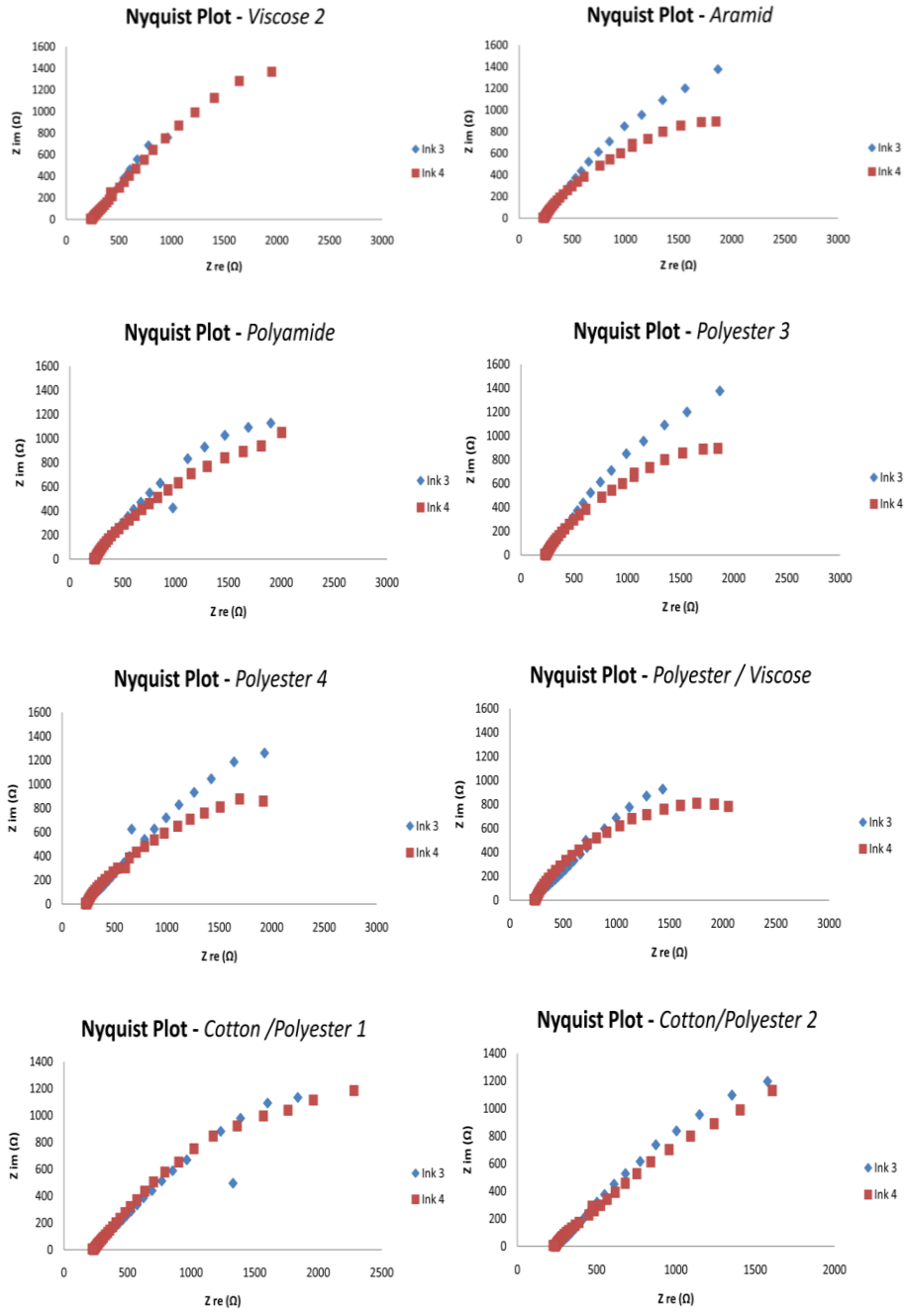

Figure 7.1.12 Nyquist plot of impedance for each printed sample with both inks

7.1.5 Conclusion

A lot of research was done in textile electrodes for biomedical monitoring. Here it was introduce another type of electroconductive textile by means of screen printing.

The results of electrochemical impedance spectroscopy have shown to be promising as the impedance of the electrodes are acceptable up to 50 kΩ at 50 Hz and in our case they results to be lower than that value.

7.2 Screen-printed textile antennas for off-body communication

Wireless communication has become commonly used in a variety of applications such as computers, mobile phones, satellites and antennas for off-body communication for wearables. For the latter, rigid antennas are preferably substituted by flexible textile-based antennas, which have been under research for the last decade. Since textiles for clothing are normally maintained through washing, this chapter describes the influence of five washing cycles on the antenna performance. In order to protect the antennas against the mechanical and chemical action in the washing machine, they are covered with a thermoplastic polyurethane layer.

7.2.1 Introduction

In the last decade research has started into the development of flexible textile antennas to be integrated into garments in order to have a wearable textile system that can wirelessly communicate with a nearby base-station. A lot of research effort has been put in obtaining antennas with smaller dimensions and with better performance [16]. The textile antennas can find use in the medical and military sector or in personal protective clothing e.g. to monitor first responders [17 - 19]. The antenna patch is made out of conductive material, for which in the case of a textile antenna, commercially available conductive coated textile materials, conductive threads for embroidery or conductive inks can be used [17, 20 - 24].

Many papers have been published on design, fabrication and applications of textile antennas. Hertleer *et al.* [25] proposed a truncated corner microstrip patch antenna on a flexible pad foam substrate; in [22] she describes a rectangular ring microstrip patch antenna. In [26] Kennedy presented an eight-element microstrip patch antenna and Subramaniam *et al*. [27] have developed a circular microstrip patch antenna, all made out of textile materials.

When using conductive coated textile it is necessary to cut the patch in the desired pattern by means of a simple cutting tool which sometimes is not very precise and accurate. Therefore, in this chapter we will describe one

application of electroconductive textiles through screen-printing. It was decided to continue what was started by Hertleer *et al*. [28]. They screen-printed silver-based ink on aramid fabric and concluded that the screen printing with conductive inks has powerful potential and fulfils the requirements. However, the properties of the antenna were not tested after a washing process, which is inevitable when the garment with incorporated antenna is cleaned. In our research we wanted to explore other textile substrates and another antenna type, a microstrip inset-fed patch antenna. It was decided to use two different nonconductive substrate materials: Polyester and Cotton/Polyester and three different conductive materials: two silver-based inks for screen-printing and a metallic plated fabric (*FlecTron*®*). FlecTron*® is a thin copper plated nylon ripstop fabric.

7.2.2 Antenna design and performance

The planar textile antennas used in this research consist of several layers (Figure 7.2.1): a patch, a substrate and a ground plane. Two of the layers, the patch and the ground plane, consist of conductive materials, whereas the substrate is nonconductive.

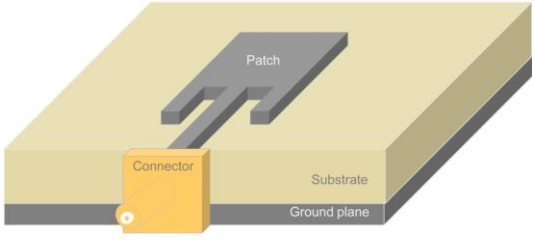

Figure 7.2.1 A microstrip inset-fed patch antenna

The antenna was designed by means of a 2.5-D EM field simulator Momentum of Agilent's Advanced Design System (ADS). Because of the thickness of textile substrates (Table 7.2.1) used and the frequency band to be covered by the antenna (2.45 GHz ISM band), it was decided to have a

multiple layer antenna, meaning that several layers of nonconductive textile material are used to form the substrate layer. So each antenna is assembled by applying 4 or 6 layers, where the antenna patch was screen-printed on the top layer and the ground plane on the bottom layer (Figure 7.2.2).

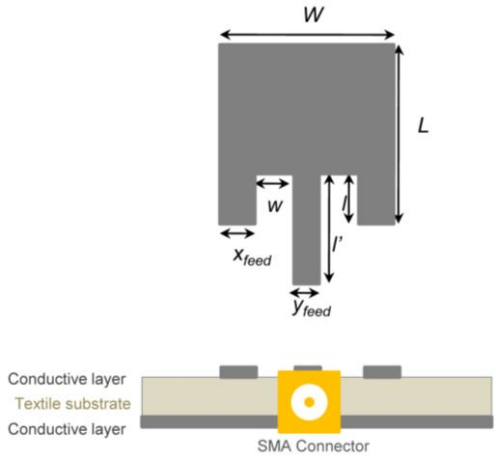

Patch for PES (mm)						Substrate	
W	43,5	*w*	6.25			*h (mm)*	2.808 (6 layers)
L	50.3	*l*	12.3	*l'*	*30*	ε_r	1.5
x_{feed}	10.5	y_{feed}	10			*tanδ*	0.02

Patch for CO/PES (mm)						Substrate	
W	42.5	*w*	6.25			*h (mm)*	2.808 (4 layers)
L	48.5	*l*	12.3	*l'*	*30*	*εr*	1.6
x_{feed}	10.5	y_{feed}	9			*tanδ*	0.02

Figure 7.2.2 Microstrip inset-fed patch antenna printed with conductive inks

As mentioned above, the antenna is expected to operate in the 2.45 GHz ISM band. This corresponds to a bandwidth of 83.5 MHz between 2.4 and 2.4835 GHz.

During the designing process some parameters should be considered, such as the thickness of the substrate layer (h), the electrical permittivity (ε_r) and the loss tangent ($tan\delta$) of the substrate material. The thickness can be determined according to ISO 5084 standard [29]. The permittivity (ε_r) determines the response of the material to an applied electrical field. The loss tangent characterizes conduction losses inside the substrate. Both parameters can be determined as described in [30].

The dimensions of the two microstrips inset-fed patch antennas, one with a Polyester substrate and one with a Cotton/Polyester substrate, are given in Figure 7.2.2, together with the properties of the substrate material.

7.2.3 Antenna materials

Screen printing with conductive silver-based inks was selected to construct the conductive patch and ground plane of the antennas because with this technique it is possible to accurately produce any kind of pattern [22], is a fast and cost-effective method.

The screen printing was performed with the semiautomatic machine, Johannes Zimmer Klagenfurt - type Mini MDF 482, and the diameter of the squeegee used was 15 mm.

Two silver-based inks are used, Ink 1 (D) from DuPont (5025) and ink 2 (E) from Acheson (Electrodag PF 410) (Table 2.2, Chapter 2). In the third group of antennas the metalized plated textile named *FlecTron*® was used for the patch and the ground plane.

Different textile materials have been used by different research groups as antenna substrate material: Flannel of 100% cotton [17], Polyester/Cotton (65:35) [27], Polyurethane foam and Aramid fabric [31], felt [32], Jeans Cotton and Polycot [33].

In this research two textile substrates were chosen: Polyester (100%) and blended Cotton/Polyester (20%/80%). These two materials were selected because they have a high thickness and low moisture regain (MR) (Table 7.2.1). Hertleer *et.al* [28, 34] recommend to select textile substrate materials with moisture regain that is not higher than 3 % to make the antenna performance more stable in varying relative humidity conditions. The textiles used in this study have a MR of 0.2% and 2.5%, respectively (Table 7.2.1). The physical and mechanical properties (e.g. density, structure and thickness) were determined according to ISO standards and are listed in Table 7.2.1 ([1]ISO/TR 6741-4:1987, [2]ISO 5084, [3]ISO 3801, [4]ISO 7211-2, [5]ISO 7211-1).

Table 7.2.1 Properties of applied woven textiles

Woven textile substrate	Moisture regain[1] (%)	Thickness[2] (mm)	Basis weight[3] (g/m²)	Yarn density[4]		The type of textile weave[5]
				Warp (threads/cm)	Weft (threads/cm)	
Cotton/Polyester 3	2.5	0.702	252.47	39	18	Twill 4/1
Polyester 4	0.2	0.478	177.3	21	22	Plain 1/1

In total 36 antennas were prepared, of which 24 antennas were screen-printed (six for each textile substrate material printed with each conductive silver-based ink) and 12 antennas were made with FlecTron® conductive textile (also six per substrate material). Two antennas of each group were covered with a TPU layer (Section 1.5.2, Chapter 1) to be protected during the washing process (Figure 7.2.3), while the other four stayed unprotected.

After manufacturing the antennas, they were kept in a climatic test cabinet at 20°C and humidity of 65% for duration of 24 hours. Then, measurements of the reflection coefficient were performed with an Agilent RF Network Analyzer and the radiation efficiency of the antennas was characterized.

Based on these measurement results, 16 antennas of the 24 printed ones were withdrawn for use in the further research (shown in Table 7.2.2).

Table 7.2.2 Number of the used textile antennas

Conductive materials	Textile materials	Reference antenna	Antenna without TPU	Antenna with TPU
FlecTron®	Cotton/Polyester	1	4	3-5
	Polyester	2	5	4-6
Ink 1 (D)	Cotton/Polyester	1	2	4-6
	Polyester	1	2	5-6
Ink 2 (E)	Cotton/Polyester	5	2	4-6
	Polyester	5	2	4-6

7.2.4 The maintenance of antennas

In this study, the domestic washing behaviour of the printed textile antennas was done according to the international standard, ISO 6330:2000 [29] as explained in Section 2.3.2.2, Chapter 2.

There are not many research groups working on the washability of antennas. Zhu *et al.* [32] have used a textile antenna where the conductive material was a nylon fabric plated with copper and tin. She washed the antenna during a number of *hand washing* cycles and the performance of antenna did not change. However, since different textile materials have different properties she suggests the best solution is to protect the antennas with a waterproof layer.

In our research the printed antennas were subjected to five washing cycles. In order to be sure that the antennas were completely dried (as they were made up of 4 and 6 layers of textiles) we decided to put them in a room with a temperature of 23 ± 2°C and a humidity of 50 ± 4%, according to standard ISO 139 [29]. The antennas were weighed at intervals of 2 hours after reposing in that room for 24 hours. They were considered dried when successive weighings at intervals of 2 hours showed a change in mass not

greater than 0.25%. Following the drying process the samples were put in the climatic test cabinet for 24 h in 20°C and 65% humidity.

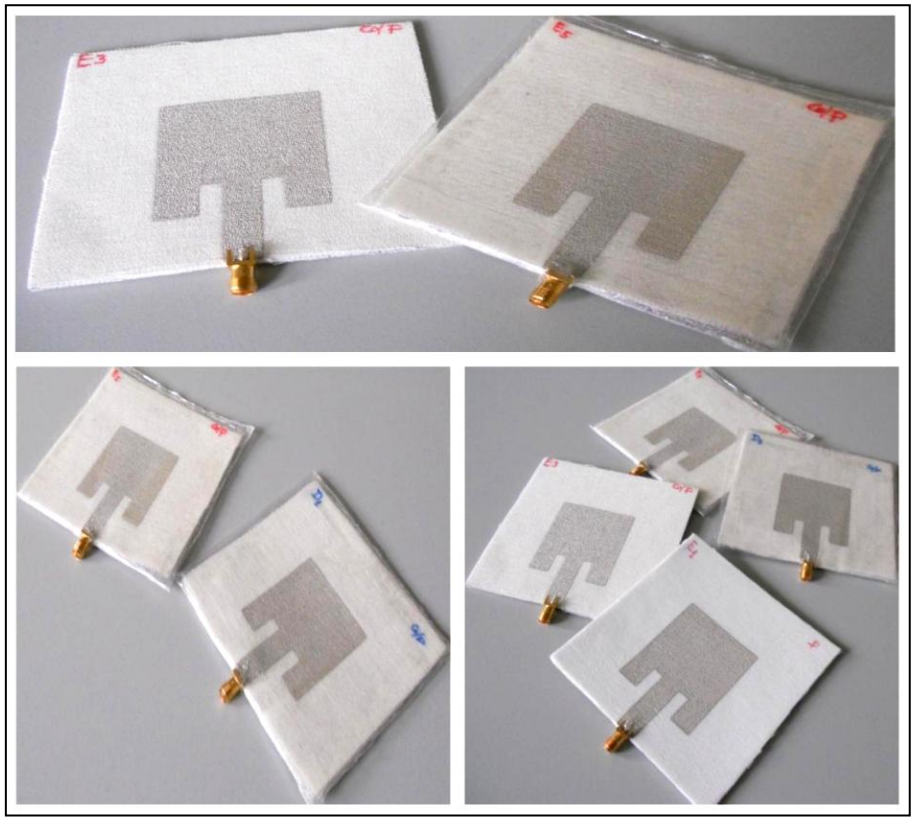

Figure 7.2.3 Printed antennas with conductive ink, covered and not covered with TPU

7.2.5 Measurements results before and after washing

The antenna characteristics such as the reflection coefficient ($|S_{11}|$) and the radiation efficiency (η) were measured and calculated before and after washing. In total 5 washing cycles were completed and the measurements were done after each washing cycle. After being dried the antennas were put in the climatic test cabinet for 24 h. In order to calculate the radiation efficiency, the Generalized Wheeler cap method with Matlab was used [35].

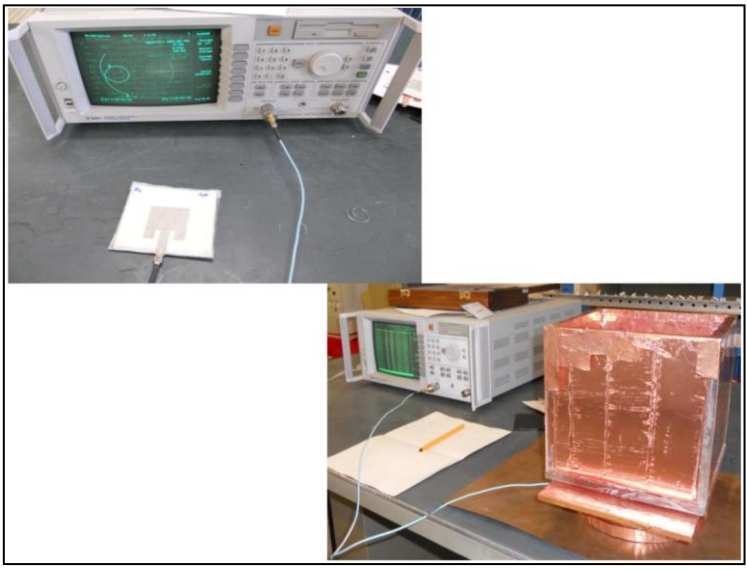

Figure 7.2.4 The measurements of reflection coefficient and radiation efficiency on printed antennas performed with Agilent RF Network Analyzer

In Figures 7.2.5, 7.2.6, 7.2.7 and 7.2.8 the plots of Cotton/Polyester and Polyester antennas are shown. In each figure the reflection coefficient is plotted of the antennas made with Ink 1 (D), Ink 2 (E) and (FlecTron® (F), before and after washing (*WC* – washing cycles and *NO WC* – no washing cycles). Figures 7.2.5 and 7.2.7 show uncovered antennas and Figures 7.2.6 and 7.2.8 show the antennas covered with TPU.

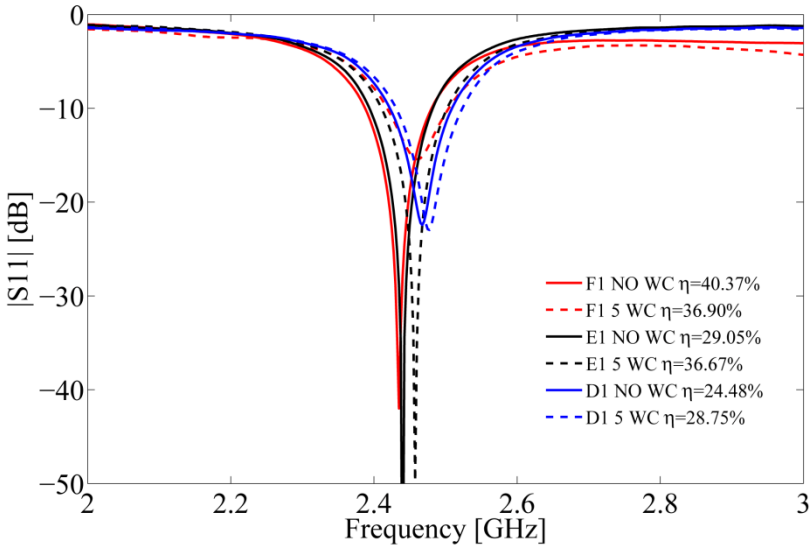

Figure 7.2.5 Antennas with Cotton/Polyester ***without TPU***; F1 (FlecTron® electroconductive textile), E1 (Electrodag, ink 2), D1 (DuPont, ink 1)

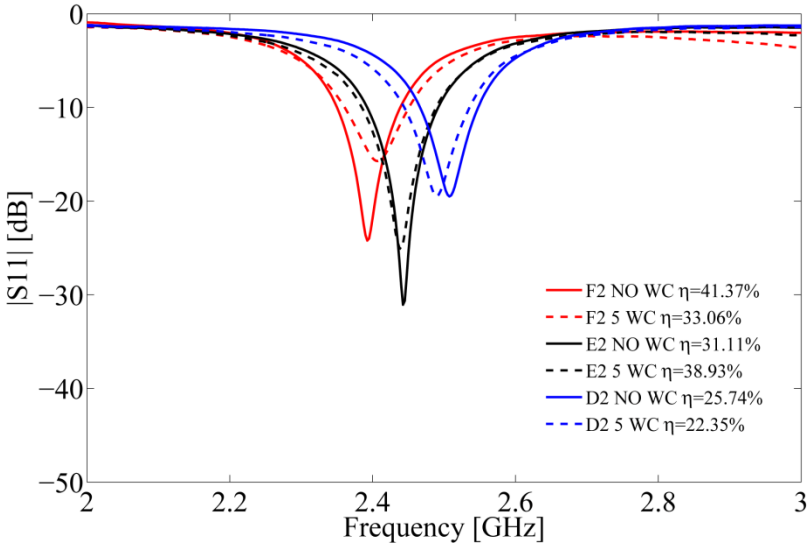

Figure 7.2.6 Antennas with Cotton/Polyester ***with TPU***; F2 (FlecTron® electroconductive textile), E2 (Electrodag, ink 2), D2 (DuPont, ink 1)

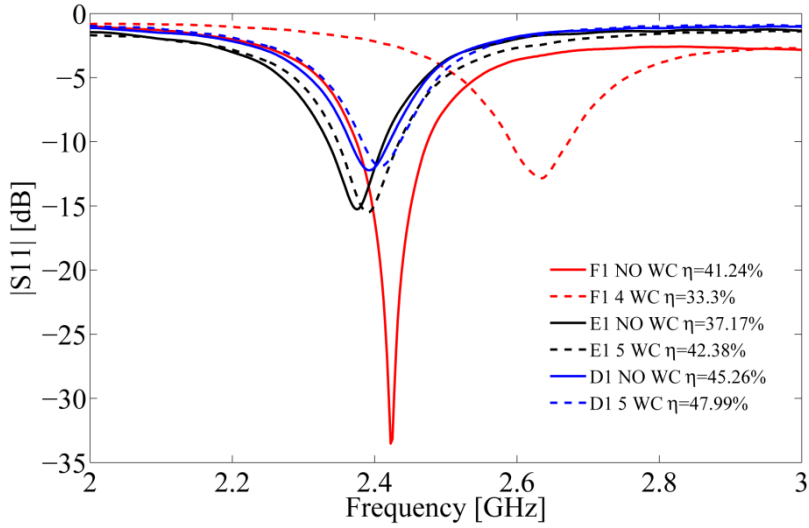

Figure 7.2.7 Antennas with Polyester ***without TPU***; F1 (FlecTron® electroconductive textile), E1 (Electrodag, ink 2), D1 (DuPont, ink 1)

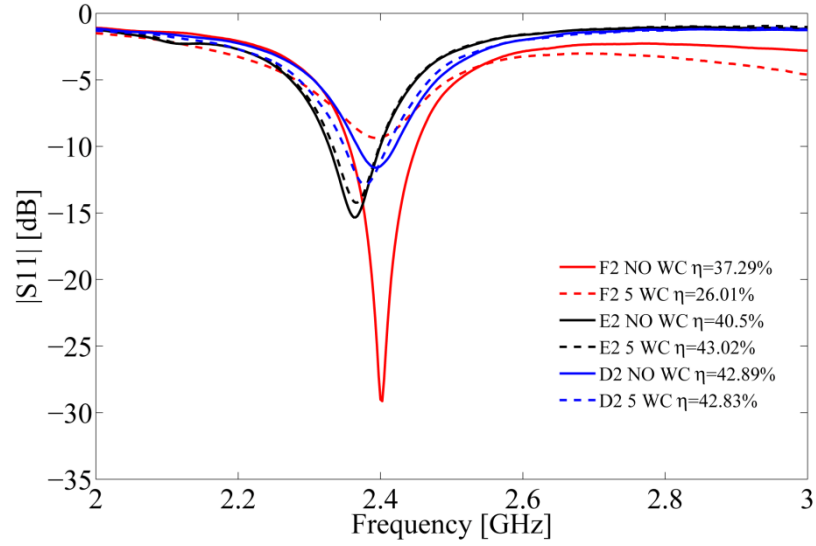

Figure 7.2.8 Antennas with Polyester ***with TPU***; F2 (FlecTron® electroconductive textile), E2 (Electrodag, ink 2), D2 (DuPont, ink 1)

The peak for the ***reflection coefficient*** (**$|S_{11}|$**) of all the antennas (Figures 7.2.5 - 7.2.8) is less deep when the antennas are covered with TPU: for Cotton /Polyester S_{11} changes from -50 dB to -32 dB and for Polyester from -34 dB to -29 dB). Here we can also mention that for FlecTron®, with both substrates, the peak of S_{11} is less deep after washing. However, the influence of washing for both screen-printed antennas on the reflection coefficient is very small.

The ***radiation efficiency*** (***η***), indicated as a number in (%) in the legend, after five cycles of washings decreases in the case of the FlecTron® antennas (with or without TPU) and increases for the antennas printed with conductive ink. Here we can also mention that the radiation efficiency for the Cotton/Polyester antennas printed with ink 1 (D) (24.48 % *without* and 25.74 % *with TPU*) is lower compared to those printed with ink 2 (E) (29.05 % *without* and 31.11 % *with TPU*). In case of Polyester antennas with ink 1 (D), the radiation efficiency is higher or almost equal (45.26 % *without* and 42.89 % *with TPU*) compared to those with ink 2 (E) (37.17 % *without* and 40.5 % *with TPU*).

The figures also reveal that covering the FlecTron® antennas with TPU results in a shift of the ***resonance frequency*** towards lower frequencies. This can happen because the patch of FlecTron®, which is a metallic plated textile, was cut by using a simple cutting tool (hand-cut) and sometimes are not very precise and accurate. The shift in resonance frequency of FlecTron® Polyester antenna, without TPU, after four washing cycles is very large and this is because the antenna was damaged and could not even resist to the fifth washing cycle. The plot of the fourth washing cycle for this antenna was put in Figure 7.2.7 to show the behaviour of the antenna, and as it can be seen the difference is quite obvious.

The reflection coefficient and the radiation efficiency for screen-printed antennas with and without TPU are more stable. The washing process has no influence in their performance.

The Polyester screen-printed antennas with both inks, with and without TPU, show to have a shift in resonance frequencies to lower frequencies (from 2.37 to 2.4 GHz) compared to the FlecTron-based antennas. This is caused by the spread of the ink in the textile surface.

However, the antennas with conductive inks are more stable over the washing process compared to FlecTron® antennas.

7.2.6 Conclusions

In this chapter the influence of washing on textile-based microstrip inset-fed patch antennas is studied. The antennas were based on two different textile substrate materials: Cotton/Polyester and Polyester. As conductive material for the antenna patch and the ground plane two silver inks and a metalized plated textile material, named FlecTron®, were used. The performance of antennas was determined before and after covering with TPU layer, and after five washing cycles, by measuring the reflection coefficient and radiation efficiency. The antennas were covered with TPU to be protected against the mechanical and chemical action in the washing machine.

The printed antennas covered and not covered with TPU, after five washing cycles were more stable than the FlecTron® antennas. This makes the screen printing with conductive inks on textiles substrates a very valuable technique to be used in the future for the textiles antennas.

7.2.7 References

1. *The Challenge of the Skin-Electrode Contact in Textile-enabled Electrical Bioimpedance, Measurements for Personalized Healthcare Monitoring Applications.* **F. Seoane, J. C. Marquez, J. Ferreira, R. Buendia and K. Lindecrantz.** InTech, 2011. pp. 541-546. 978-953-307-513-6.

2. *A comparison study of electrodes for neonate electrical impedance tomography.* **M. Rahal, J. M. Khor, A. Demosthenous, A. Tizzard and R. Bayford.** 2009, Physiological Measurement, Vol. 30, pp. 73-84.

3. *Electrical characteristics of conductive yarns and textile electrodes for medical application.* **L. Rattfält, M. Lindén, P. Hult, L. Berglin, P. Ask.** 12, 2007, Medical and Biological Engineering and Computing, Vol. 45, pp. 1251-1257.

4. *Characterization of textile electrodes and conductors using standardized measurement setups.* **L. Beckmann, C. Neuhaus, G. Medrano, N. Jungbecker, M. Walter, T. Gries and S. Leonhardt.** 2010, Physicological Measurment, Vol. 31, pp. 233–247.

5. *Textile-structured electrodes for electrocardiogram.* **P. J. Xu, H. Zhang, X. M. Tao.** 4, 2008, Textile Progress, Vol. 40, pp. 183-213.

6. *Electrochemical polymerisation of aniline on conducting textiles of polyester covered with polypyrrole/AQSA.* **J. Molina, A. I. Del Rio, J. Bonastre, F. Cases.** 4, 2009, European Polymer Journal, Vol. 45, pp. 1302-1315.

7. *Fabric sensors for the measurement of physiological parameters.* **M. Catrysse, R. Puers, C. Hertleer, L. Van Langenhove, H. Van Egmond, D.Matthys.** s.l. : IEEE, 2003. Vol. 1 AND 2 , pp. 1758-1761, 0-7803-7731-1.

8. *Contactless EMG Sensors Embroidered into Textile.* **T. Linz, L. Gourmelon, G. Langereis.** 2007. Vol. 13, pp. 29-34. 9783540709947.

9. *Electrotherapeutic socks.* **A. Schwarz, J. Banaszczyk, P. Moerkens, I. Soliani, G. De Mey, L. Van Langenhove.** s.l. : Smart Textiles Salon, 2009. Vol. 1, pp. 56-57.

10. *Textile-Based Capacitive Sensors for Respiration Monitoring.* **C. R. Merritt, H.T. Nagle, E. Grant.** 1, s.l. : IEEE Sensors Jornal, 2009, Vol. 9, pp. 71-78.

11. *Woven Electrodes for Flexible Organic Photovoltaic Cells.* **W. Kylberg, F. A. de Castro, P. Chabrecek, U. Sonderegger, B. T-T. Chu , F. Nüesch , R. Hany.** 8, 2011, Advanced Materials, Vol. 23, pp. 1015–1019.

12. *Textile electrodes of jacquard woven fabrics for biosignal measurement.* **H.-Y. Song a, J.-H. Lee, D. Kang, H. Cho, H.-S. Cho, J.-W. Lee, Y.-J. Lee.** 8, 2010, Journal of the Textile Institute, Vol. 101, pp. 758–770.

13. *Analytical electrochemistry in textiles.* **P. Westbroek, G. Priniotakis, P. Kiekens** 2005. 0-8493-3485-3.

14. *Electro-conductive yarns: Their development, characterization and applications.* **A. Schwarz.** 2010-2011, UGent : PhD disertation, 98-90-8578-430-2.

15. *An experimental simulation of human body behaviour during sweat production measured at textile electrodes.* **G. Priniotakis, P. Westbroek, L. Van Langenhove and P. Kiekens.** 3-4, 2005, International Journal of Clothing Science and Technology, Vol. 17, pp. 232-241. 0955-6222 .

16. *E-Textile Conductors and Polymer Composites for Conformal Lightweight Antennas.* **Y. Bayram, Y. Zhou, B. S. Shim, Sh. Xu, J. Zhu, N. A. Kotov, J. L. Volakis.** 8, 2010, IEEE Transactions on Antennas and Propagation, Vol. 58, pp. 2732-2736.

17. *Embroidered fully textile wereable antenna for medical monitoring applications.* **M. A. R. Osman, M. K. A. Rahim, N. A. Samsuri, H. A. M. Salim, M. F. Ali.** 2011, Progress in Electromagnetics Research, Vol. 117, pp. 321-337.

18. *A Textile Antenna for Off-Body Communication Integrated Into Protective Clothing for Firefighters.* **C. Hertleer, H. Rogier, L. Vallozzi, and L. Van Langenhove.** 4, 2009, IEEE Transactions on Antennas and Propagation, Vol. 57, pp. 919-925.

19. *Wireless communication for firefighters using dual-polarized textile antennas integrated in their garment.* **L. Vallozzi, P. Van Torre, C. Hertleer, H. Rogier, M. Moeneclaey, J. Verhaevert.** s.l. : IEEE Transactions on Antennas and Propagation, 2010, Vol. 58 (4). 1357-1368.

20. *Textile material characterization for soft wear antennas.* **J. Lilja, P. Salonen.** 2009. IEEE Conference on Military Communications. pp. 628-634. 978-1-4244-5238-5.

21. *The use of textile materials to design wearable microstrip patch antennas.* **C. Hertleer, A.Tronquo, H. Rogier, L. Van Langenhove.** s.l. : Textile Research Journal, 2008, Vol. 78(8). 651-658.

22. *Printed Textile Antennas for Off-Body Communication.* **C. Hertleer, L. V. Langenhove, H. Rogier.** 2008, Advances in Science and Technology, Vol. 60, pp. 64-66.

23. *Development and performance study of michrostrip patch textile antenna.* **G-H.Wang, Zhu, C-H. and Xu, C-Y.** 2011. Silk: Inheritance and Innovation - Modern Silk Road. Vols. 175-176, pp. 450-453. 978-3-03785-011-4.

24. *Exposing textile antennas for harsh environment.* **T.Kaija, J. Lilja, P. Salonen.** s.l. : IEEE, 2010. The 2010 Military Communications Conference. pp. 737-742. 978-1-4244-8179-8.

25. *A Textile Antenna for Off-Body Communication Integrated Into Protective Clothing for Firefighters.* **C. Hertleer, H. Rogier, L. Vallozzi, and L. Van Langenhove.** 4, 2009, IEEE Transactions on Antennas and Propagation, Vol. 57, pp. 919-925.

26. *Body-Worn E-Textile Antennas: The Good, the Low-Mass, and the Conformal.* **T.F. Kennedy, P.W. Fink, A.W. Chu, N.J. Champagne, G. Y. Lin, M.A. Khayat.** 4, 2009, IEEE Transactions on Antennas and Propagation, Vol. 57, pp. 910-918.

27. *Design and development of flexible fabric antenna for body-worn application and its performance study under flat and bent positions.* **S. Subramaniam, B. Gupta.** 9, 2011, Microwave and Optical Technology Letters, Vol. 53, pp. 2004-2011.

28. *Design of planar antennas based on textile materials.* **C. Hertleer.** 2008-2009. UGent : PhD disertation, 987-90-8578-297-1.

29. www.iso.org. [Online]

30. *Permittivity and Loss Tangent Characterization for Garment Antennas Based on a New Matrix-Pencil Two-Line Method.* **F. Declercq, H. Rogier and C. Hertleer.** 8, 2008, IEEE Transactions on Antennas and Propagation, Vol. 56, pp. 2548-2554.

31. *Active Integrated Wearable Textile Antenna With Optimized Noise Characteristics.* **F. Declercq, H. Rogier.** 9, 2010, IEEE Transactions on Antennas and Propagation, Vol. 58, pp. 3050-3054.

32. *Dual-Band Wearable Textile Antenna on an EBG Substrate.* **Sh. Zhu, R. Langley.** 4, 2009, IEEE Transactions on Antennas and Propagation, Vol. 57, pp. 926-935.

33. *Determination of dielectric constant of fabric materials and their use as substrates for design and development of antennas for wereable applications.* **S. Subramaniam, B. Gupta.** 12, 2010, IEEE Transactions on Instrumentation and Measurment, Vol. 59, pp. 3122-3130.

34. *Influence of Relative Humidity on Textile Antenna Performance.* **C. Hertleer, A. V. Laere, H. Rogier, L. Van Langenhove.** 2, 2009, Textile Research Journal, Vol. 80, pp. 177-183.

35. *An improved small antenna radiation-efficiency measurement method.* **R. H. Johnston, J. G. McRory.** 5, 1998, IEEE Antennas and Propagation Magazine, Vol. 40, pp. 40-48.

General conclusions and future work

Over the last years, the combination of textiles with electronics has introduced the so called smart/intelligent textiles or wearable electronics. The challenge for textile researchers is to make as many components as possible out of textile materials. Since smart textiles are becoming popular as a concept, more and more conductive textiles are needed to manufacture the applications. Therefore, it is necessary to develop electroconductive textiles which have to be lightweight, flexible and washable.

In this dissertation we presented the screen printing method with silver-based inks to obtain electroconductive textiles which meet the requested properties. Through this technology, different substrates, either woven, nonwoven or foam were screen-printed. Moreover, four silver-based inks were applied: Ink 1 from DuPont (5025), ink 2 from Acheson (Electrodag PF 410), ink 3 and 4 from SunChemical.

The electroconductive properties of these conductive substrates were investigated.

Here the most important results reached are listed:

- The screen-printed woven textiles with silver-based ink 1 (DuPont) and ink 2 (Electrodag) show to have good electrical conductivities, after printing, with a square resistance ranging from 0.020 to 0.129 Ω/□;

- When screen printing with silver-based inks available in the market, on textile substrates, one should take into account that the conductivity will decrease after several washing cycles;

- After 20 washing cycles, nearly half of the samples tested in this dissertation lost their conductivity so to make them long-term washable it was necessary to protect the conductive layer e.g. with a thermoplastic polyurethane (TPU) layer;

- The square resistance of the screen-printed woven textiles, with all four inks after 5000 abrading cycles had considerably increased from 0.007 to 0.396 Ω/□;

- The screen-printed textiles with all four inks, used in the framework of this dissertation and covered with TPU show to have a square resistance varying from 0.003 to 0.061 Ω/□, which after 60 washing cycles varied from 0.008 to 0.308 Ω/□. Screen printing on Polyester 4 shows to have the best conductivity after 60 washing cycles with all four inks;

- When screen printing one should take into consideration that the electrical properties of the conductive textiles are influenced by the amount of ink, the solid content and the nominal sheet resistance of the ink;

- Besides cleaning through washing, the screen-printed substrates such as foam or nonwoven polyester can also be dry-cleaned, when dry-cleaning up to 60 times. The values of the square resistance increased from 0.001 to 0.014 Ω/□ before dry-cleaning to 0.025 to 2.263 Ω/□ after 60 times dry-cleaned;

- As the square resistance is changing with the washing cycles, we advise to take into account this change for the future applications;

- During the measurements of the square resistance it was found that the screen-printed textiles are anisotropic. The anisotropy cannot be detected with every measurement method: the four-point probe method will not reveal anisotropy, but the Van Der Pauw method will;

- When using the Van Der Pauw method, it was found that a mathematical analysis is mandatory to interpret the measurements correctly;

- The measurements of temperature coefficient of resistance (TCR) revealed hysteresis for most of the samples in both directions. The results indicate that the effects of aging upon the printed textiles are insignificant after 15 days at 60°C. During the measurements of TCR and ageing anisotropy was also found;

To finalize the summary, Table 8.1 gives an overview of the square resistance of the flexible substrate materials that were washed/dry-cleaned 60 times.

Table 8.1 Overview of the square resistance of screen-printed flexible substrate materials after 60 washing/dry-cleaning cycles

	Ink 1	Ink 2	Ink 3	Ink 4
	$R_{\square}$ (Ω/□)			
Woven Viscose 2	0.034	0.270	0.013	0.013
Woven Aramid	0.116	0.122	0.018	0.012
Woven Polyamide	0.103	0.208	0.010	0.021
Woven Polyester	0.076	0.308	0.016	0.009
Woven Polyester 4	0.013	0.037	0.009	0.009
Woven Cotton/Polyester 1	0.076	0.091	0.020	0.018
Woven Cotton/Polyester 2	0.118	0.140	0.026	0.020
Woven Polyester/Viscose	0.062	0.080	0.008	0.008
Urecom foam	-	2.263	0.308	0.129
Nonwoven Polyester	-	0.025	0.313	0.125

It is obvious, from Table 8.1, that ink 4 shows to have better conductivity on flexible substrate materials after 60 washing/dry-cleaning cycles compared with the other inks used.

The screen-printed textiles were investigated in different applications such as electrodes and textile antennas for off-body communication.

- The screen-printed woven textiles with silver-based ink 3 and 4 from Sun Chemical have shown very good electrical properties after 20 washing cycles. One possible application can be used as electrodes in contact with electrolytes. In this research the electrochemical impedance spectroscopy results are promising. A further study on testing these electrodes is recommended to be done in the future and to compare with different electrodes available in the market.

- For the second application, antennas for off-body communication, the screen-printed antennas, uncovered and covered with TPU, were more stable than the FlecTron® antennas.

- The spreading of the ink should be taken into consideration when printing the antennas or when a specific design is required. In our case the screen-printed antennas of Cotton/Polyester did not have any spread but the Polyester antennas did.

- This research showed that printed textile antennas can be washed. However, further work could be done to improve the antenna performance.

We believe that it is possible to use screen printing with conductive inks on textile substrates not only for the applications that were mentioned here but also for many others. The information given in this dissertation can be evaluated and exploited in those applications. Based on our experiments, covering the printed surface with a protective layer of TPU considerably increases the lifecycle of the smart textiles.

In the nearest future this technology might be used in another application such as the manufacturing of flexible textile batteries.

As a final concluding remark I hope that the work presented in this dissertation will contribute to the future of smart textiles.